NASA/TM—2001-210366

Structures and Acoustics Division Annual Report for 1997 to 1999

Cynthia S. Acquaviva
Glenn Research Center, Cleveland, Ohio

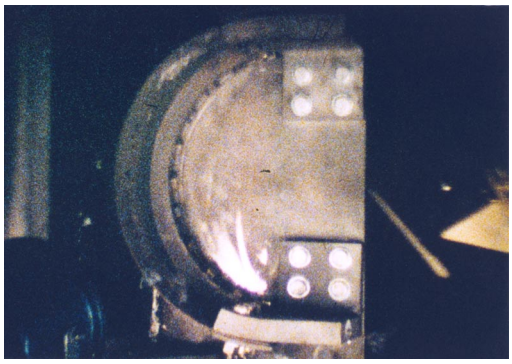

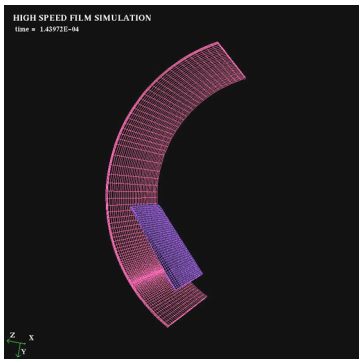

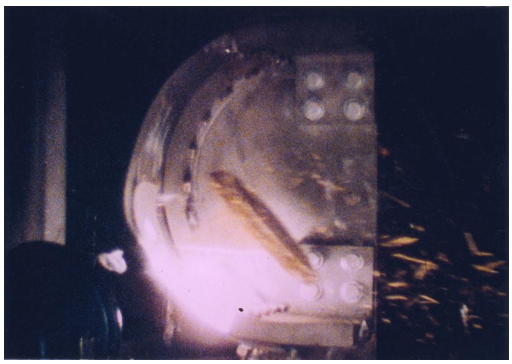

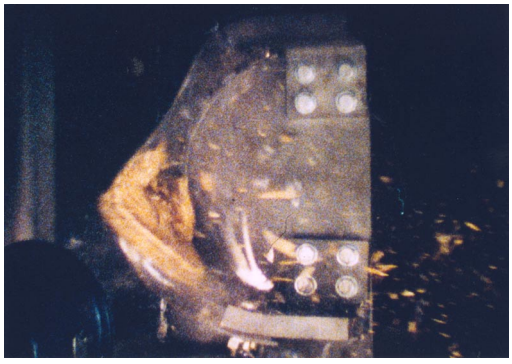

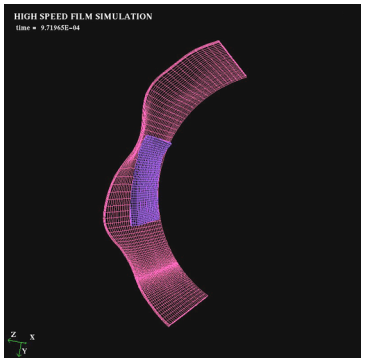

March 2001

The NASA STI Program Office . . . in Profile

Since its founding, NASA has been dedicated to the advancement of aeronautics and space science. The NASA Scientific and Technical Information (STI) Program Office plays a key part in helping NASA maintain this important role.

The NASA STI Program Office is operated by Langley Research Center, the Lead Center for NASA's scientific and technical information. The NASA STI Program Office provides access to the NASA STI Database, the largest collection of aeronautical and space science STI in the world. The Program Office is also NASA's institutional mechanism for disseminating the results of its research and development activities. These results are published by NASA in the NASA STI Report Series, which includes the following report types:

- TECHNICAL PUBLICATION. Reports of completed research or a major significant phase of research that present the results of NASA programs and include extensive data or theoretical analysis. Includes compilations of significant scientific and technical data and information deemed to be of continuing reference value. NASA's counterpart of peer-reviewed formal professional papers but has less stringent limitations on manuscript length and extent of graphic presentations.

- TECHNICAL MEMORANDUM. Scientific and technical findings that are preliminary or of specialized interest, e.g., quick release reports, working papers, and bibliographies that contain minimal annotation. Does not contain extensive analysis.

- CONTRACTOR REPORT. Scientific and technical findings by NASA-sponsored contractors and grantees.

- CONFERENCE PUBLICATION. Collected papers from scientific and technical conferences, symposia, seminars, or other meetings sponsored or cosponsored by NASA.

- SPECIAL PUBLICATION. Scientific, technical, or historical information from NASA programs, projects, and missions, often concerned with subjects having substantial public interest.

- TECHNICAL TRANSLATION. English-language translations of foreign scientific and technical material pertinent to NASA's mission.

Specialized services that complement the STI Program Office's diverse offerings include creating custom thesauri, building customized data bases, organizing and publishing research results . . . even providing videos.

For more information about the NASA STI Program Office, see the following:

- Access the NASA STI Program Home Page at ***http://www.sti.nasa.gov***

- E-mail your question via the Internet to help@sti.nasa.gov

- Fax your question to the NASA Access Help Desk at 301–621-0134

- Telephone the NASA Access Help Desk at 301–621-0390

- Write to:
  NASA Access Help Desk
  NASA Center for AeroSpace Information
  7121 Standard Drive
  Hanover, MD 21076

NASA/TM—2001-210366

Structures and Acoustics Division Annual Report for 1997 to 1999

Cynthia S. Acquaviva
Glenn Research Center, Cleveland, Ohio

National Aeronautics and
Space Administration

Glenn Research Center

March 2001

Note that some of these articles were written before NASA Lewis Research Center's name was changed to NASA John H. Glenn Research Center at Lewis Field. Those articles that were written before the name change (March 1, 1999) retain the original name.

Available from

NASA Center for Aerospace Information
7121 Standard Drive
Hanover, MD 21076
Price Code: A05

National Technical Information Service
5285 Port Royal Road
Springfield, VA 22100
Price Code: A05

Available electronically at http://gltrs.grc.nasa.gov/GLTRS

Introduction

The 1997, 1998, and 1999 Annual Report of the Structures and Acoustics Division reflects the work areas performed by the Division staff during the 1997, 1998, and 1999 calendar years. Its purpose is to give a brief, but comprehensive, review of the Division's technical accomplishments. As with the reports for the previous years, the report is organized topically. The descriptions of the research reflect work that has been reported in the open literature during the year.

The Structures and Acoustics Division comprises a staff of approximately 82 engineers and scientists plus administrative and support personnel. The work areas comprise composite mechanics, fatigue, fracture, and dynamics with emphasis on life and reliability, as well as mechanical system technologies and aeroacoustics. The Division works cooperatively with both industry and universities to develop the technology necessary for state-of-the-art advancement in aeronautical and space propulsion systems. In the future, propulsion systems will need to be lighter, to operate at higher temperatures, and to be more reliable in order to achieve higher performance. Achieving these goals is complex and challenging. If you need additional information, please do not hesitate to contact me or the staff contacts provided in this publication.

L. James Kiraly

Chief, Structures and Acoustics Division

Contents

Structures and Acoustics

Life Prediction

Structural Mechanics and Dynamics

Acoustics

Mechanical Components

Structures and Acoustics

Thermoelastic Stress Analysis: An NDE Tool for the Residual Stress Assessment of Metallic Alloys

During manufacturing, certain propulsion components that will be used in a cyclic fatigue environment are fabricated to contain compressive residual stresses on their surfaces because these stresses inhibit the nucleation of cracks. Overloads and elevated-temperature excursions cause the induced residual stresses to dissipate while the component is still in service, lowering its resistance to crack initiation. Research at the NASA Glenn Research Center at Lewis Field has focused on employing the Thermoelastic Stress Analysis technique (TSA, also recognized as SPATE: Stress Pattern Analysis by Thermal Emission) as a tool for monitoring the residual stress state of propulsion components.

TSA is based on the fact that materials experience small temperature changes when they are compressed or expanded. When a structure is cyclically loaded (i.e., cyclically compressed and expanded), the resulting surface-temperature profile correlates to the stress state of the structure's surface. The surface-temperature variations resulting from a cyclic load are measured with an infrared camera. Traditionally, the temperature amplitude of a TSA signal has been theoretically defined to be linearly dependent on the cyclic stress amplitude. As a result, the temperature amplitude resulting from an applied cyclic stress was assumed to be independent of the cyclic mean stress.

Recent studies established that the temperature response also depends on the cyclic mean stress or static stress. A study by the authors (Gyekenyesi and Baaklini, 1999) showed that static stresses significantly influenced the TSA results for titanium- and nickel-based alloys. A more in-depth analysis, which involved analyzing multiple harmonics of the temperature response, was also conducted (Gyekenyesi and Baaklini, 2000). This research showed that the thermoelastic response of a structure subjected to a pure sinusoidal mechanical load with frequency ω produced a TSA signal with frequency components at the primary frequency, ω, as well as at the second harmonic, 2ω. The first harmonic of the thermal response is a function of the cyclic stress amplitude and the mean stress, whereas the second harmonic is a function of the square of the stress amplitude. By obtaining the TSA amplitudes of the first and second harmonics, we are now able to obtain the stress amplitude and

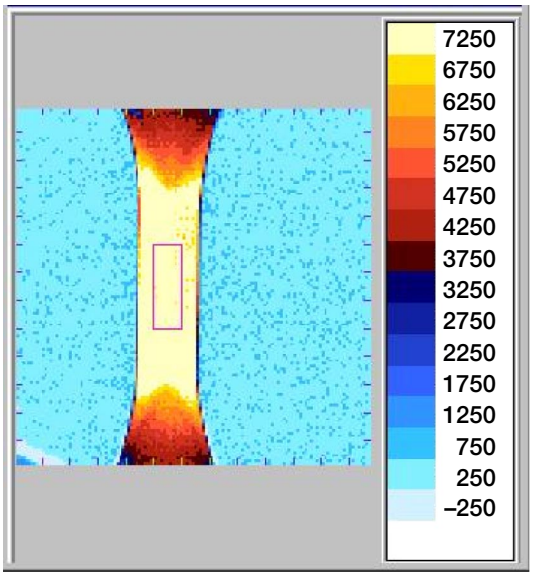

Typical infrared test image for a dogbone TIMETAL 21S specimen. The rectangular box within the specimen indicates the area where the average signal was obtained. The scale displays the dimensionless digital values of the infrared camera signal corresponding to the cyclic temperature amplitude.

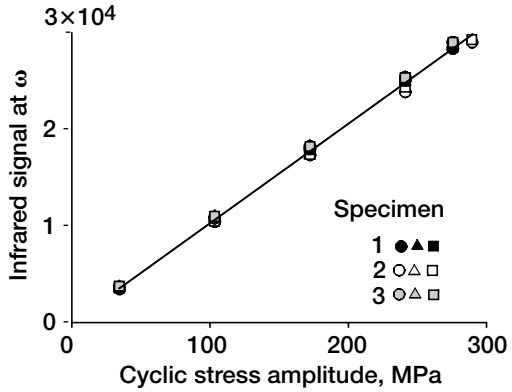

First harmonic (ω) infrared signal output at various stress amplitudes (σ_m = 0) for TIMETAL21S. Indicated is the linear relationship of the TSA signal to the cyclic stress amplitude for a fixed mean stress. Mean stress variations would affect the data by changing the slope of the line.

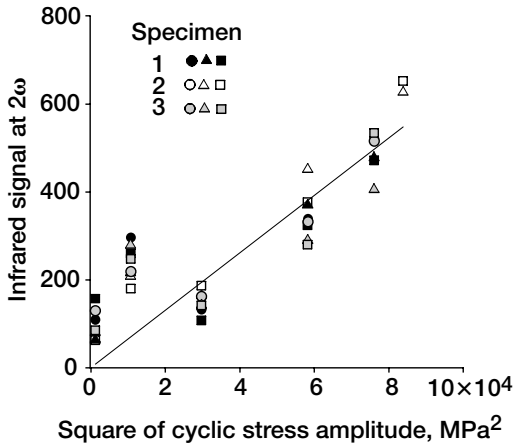

Second harmonic (2ω) infrared signal output at various stress amplitudes ($\sigma_m = 0$). Indicated is the linear relationship of the TSA signal to the square of the cyclic stress amplitude. The second harmonic TSA response is independent of the cyclic mean stresses.

the mean stress at a given point on a structure subjected to a cyclic load simultaneously. The rather complex analysis of the temperature response involved obtaining the first and second harmonic amplitudes for 16,384 infrared detectors (in a 128 by 128 focal plane array). In addition, comparisons were made between the experimental data and theoretical predictions that were based on a revised theory that takes into account the mean stress effect. Good agreement was achieved.

Since confidence was achieved concerning reliable TSA measurements of the mean stress effect (i.e., the static stress), research can focus on the application of the method to residual stress assessment. Such measurements will assist researchers in the characterization of materials in the laboratory as well as in the in situ monitoring of the current residual stress state in actual structural components during fabrication and service.

Ohio Aerospace Institute contact:
Dr. Andrew L. Gyekenyesi, 216–433–8155,
Andrew.L.Gyekenyesi@grc.nasa.gov

Glenn contact: Dr. George Y. Baaklini, 216–433–6016,
George.Y.Baaklini@grc.nasa.gov

Life Prediction

Time-Dependent Reversible-Irreversible Deformation Threshold Determined Explicitly by Experimental Technique

Structural materials for the design of advanced aeropropulsion components are usually subject to loading under elevated temperatures, where a material's viscosity (resistance to flow) is greatly reduced in comparison to its viscosity under low-temperature conditions. As a result, the propensity for the material to exhibit time-dependent deformation is significantly enhanced, even when loading is limited to a quasi-linear stress-strain regime as an effort to avoid permanent (irreversible) nonlinear deformation. An understanding and assessment of such time-dependent effects in the context of combined reversible and irreversible deformation is critical to the development of constitutive models that can accurately predict the general hereditary behavior of material deformation. To this end, researchers at the NASA Glenn Research Center at Lewis Field developed a unique experimental technique that identifies the existence of and explicitly determines a threshold stress κ, below which the time-dependent material deformation is wholly reversible, and above which irreversible deformation is incurred.

This technique is unique in the sense that it allows, for the first time, an objective, explicit, experimental measurement of κ. The underlying concept for the experiment is based on the assumption that the material's time-dependent reversible response is invariable, even in the presence of irreversible deformation. The first step is to conduct a test (preferably two) where the time-dependent deformation response is wholly reversible. Shown in the figure are two such tests on the titanium alloy TIMETAL 21S at 650 °C; one is a creep test (constant stress hold) at 0.5 ksi, and the other is a stress relaxation test (constant strain hold) at 60 $\mu\varepsilon$.

Both tests exhibit shutdown of the time-dependent response, which is generally best seen in a time-based plot. For example, after approximately 5 hours of creep at 0.5 ksi, the creep strain rate went to zero (i.e., all creep shut down), and it remained in that state for 7 more hours. Upon unloading to zero stress subsequent to 12 hours of stress hold, the data revealed that the creep strain was fully recovered in time. The viscoelastic creep shut down at a strain of approximately 140 $\mu\varepsilon$. The stress relaxation test behaved in a similar way, terminating at approximately 0.23 ksi with subsequent full strain recovery observed. The stress-strain slope E_s determined by the termination point(s) represents the time-independent stiffness at 650 °C and is indicative of an infinite limit stress for the spring within the standard solid viscoelastic model (see Saleeb and Arnold, 1997)

The value of κ is determined by loading a sample beyond κ (well into the irreversible range) and holding the load long enough to allow the viscoelastic (time-dependent reversible) response to be fully exhausted. This is termed the "overload" test in the figure. The minimum hold time for this test

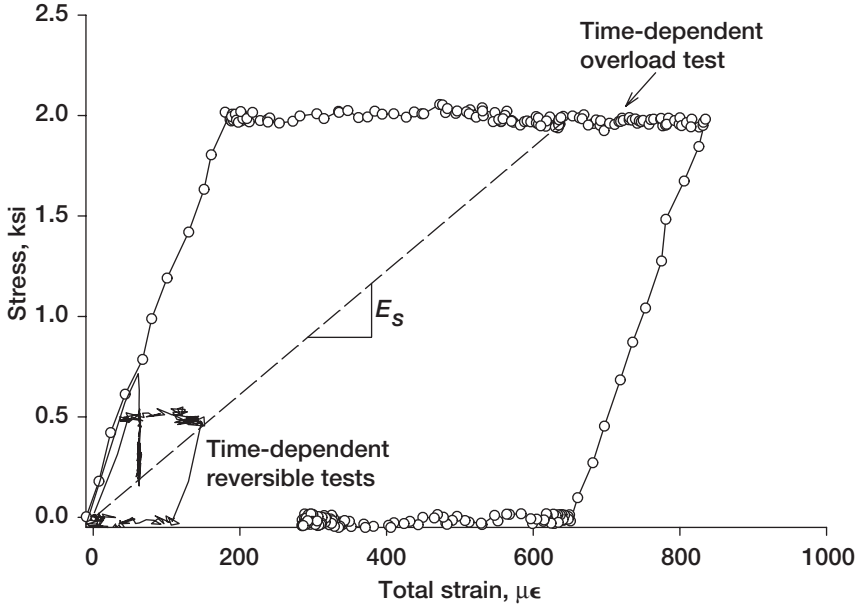

Time-dependent deformation tests provide explicit determination of the reversible-irreversible threshold stress ($\kappa = \sigma_{applied} - \varepsilon_{IR} E_s$) by using viscoelastic subtraction for a titanium alloy at 650 °C.

should correspond to the shutdown time required for the viscoelastic tests. Subsequent to this hold period, where the accumulated creep strain results from both time-dependent reversible and irreversible behavior, the specimen is unloaded and given sufficient time to allow for full recovery of the time-dependent reversible strains. From this data, the excess equilibrium stress corresponding to the irreversible portion of the induced strain is calculated ($\sigma_{\chi e} = \varepsilon^{IR} E_s$) and then simply subtracted from the stress level at which the test is performed to obtain κ ($\kappa = \sigma_{applied} - \sigma_{\chi e}$). This value effectively represents the upper bound of the viscoelastic regime and, thereby, represents the threshold of irreversible behavior. Appropriately, this technique has been termed "viscoelastic subtraction." Values of κ obtained from the viscoelastic subtraction technique were initially verified with more tedious, so-called probing experiments designed to establish the threshold of yield and extremely slow-rate proportional limit tests (Arnold, Saleeb, and Castelli, 1997).

Glenn contact: Dr. Steven M. Arnold, 216–433–3334, Steven.M.Arnold@grc.nasa.gov

Nondestructive Evaluation Correlated With Finite Element Analysis

Advanced materials are being developed for use in high-temperature gas turbine applications. For these new materials to be fully utilized, their deformation properties, their nondestructive evaluation (NDE) quality and material durability, and their creep and fatigue fracture characteristics need to be determined by suitable experiments. The experimental findings must be analyzed, characterized, modeled and translated into constitutive equations for stress analysis and life prediction. Only when these ingredients—together with the appropriate computational tools—are available, can durability analysis be performed in the design stage, long before the component is built.

For example, for NDE information to be useful in structural characterization and modeling, the NDE data format must be compatible with microstructural and structural models currently being developed (Baaklini et al., 1996 and 1997). In addition, qualitative and quantitative computer analysis tools based on NDE imaging modalities must be developed to enhance the usefulness of NDE applications. Qualitative tools include two- and three-dimensional visualization methods. Quantitative tools include segmentation methods that can send output to commercial finite element, micromechanical, and/or continuum damage model software (Wilt, Arnold, and Goldberg, 1997, and Arnold and Wilt, 1996) for evaluation of composite materials and components. Linking NDE data with engineering analysis methods will provide the engineering community the great ability to do a complete structural analysis on as-manufactured or as-inspected components rather than solely on as-designed components. With this capability, extensive effect-of-defect studies can be performed to determine the effect of manufacturing anomalies or in-service component degradation on part performance. This will provide an NDE capability for engineering structures and condition-based maintenance.

One of the many structural components being evaluated by the NDE group at the NASA Lewis Research Center is the flywheel system. It is being considered as an energy storage device for advanced space vehicles. Such devices offer advantages over electrochemical batteries in situations demanding high power delivery and high energy storage per unit weight. In addition, flywheels have potentially higher efficiency and longer lifetimes with proper motor-generator and rotor design (Ashley, 1993). Flywheels made of fiber-reinforced polymer composite material show great promise for energy applications because of the high energy and power densities that they can achieve (Olszewski et al., 1998) along with a burst failure mode that is relatively benign in comparison to those of flywheels made of metallic materials (Coppa, 1984).

However, the big challenge of developing materials for high-energy flywheel systems that can withstand the stresses caused by high rotational speeds remains eminent. For example, a typical 16-in. steel or titanium flywheel can shatter at 20 000 rpm. However, flywheels made out of composites show good promise since they can store 20 to 30 times more power per unit/weight than lead-acid batteries, can be recharged repeatedly, and can handle a wide range of temperature variations. They can also be respun thousands of times to regain their stored energy.

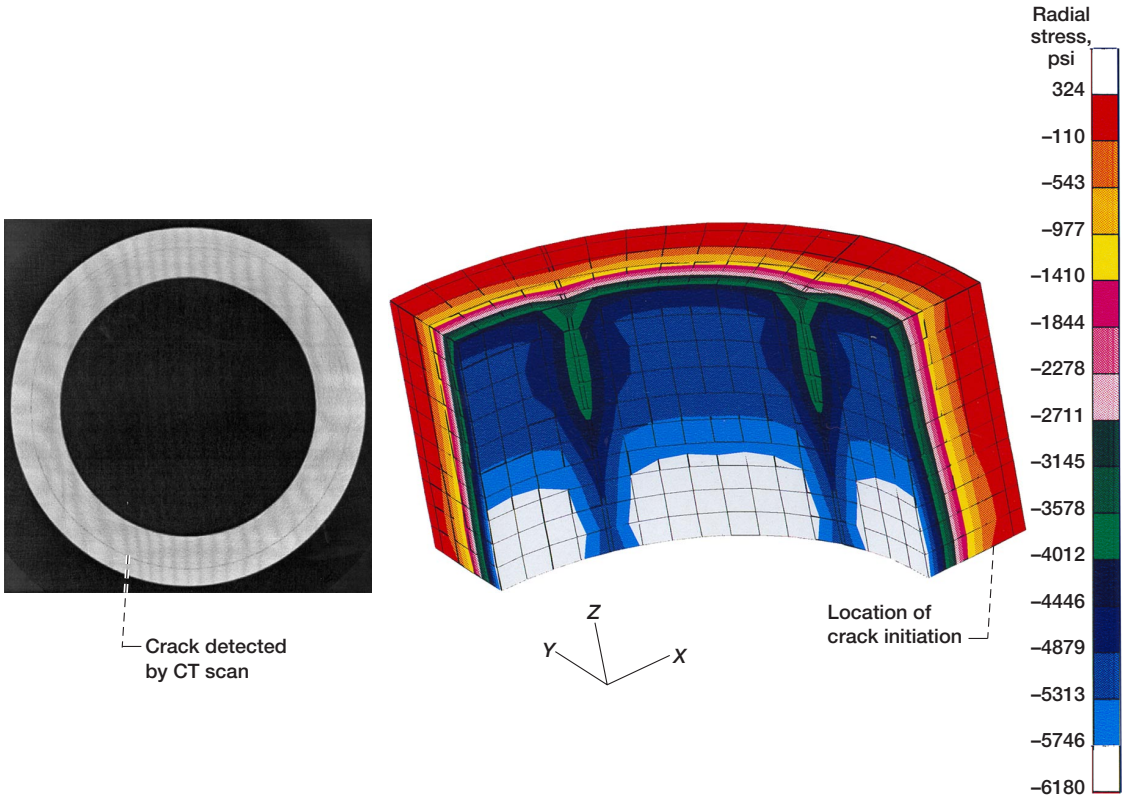

Left: Computer tomograph (CT) of a flywheel. Right: Radial stresses in a rotor.

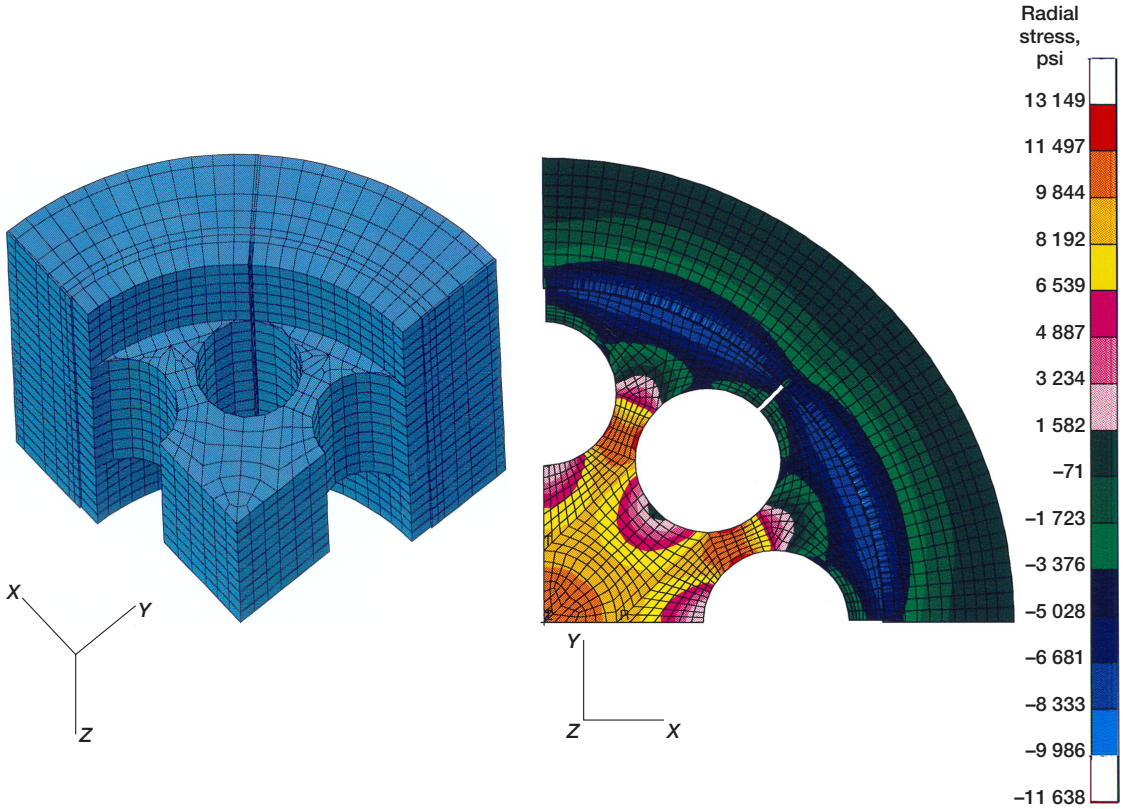

Left: Three-dimensional finite element model; 6747 nodes, 5424 hexagonal elements. Right: Radial stresses in a rotor-hub assembly. These figures are shown in color in the online version of this article (http://www.grc.nasa.gov/WWW/RT1998/5000/5920aziz.htm).

Therefore, to help improve durability and reduce structural uncertainties, we are developing a comprehensive analytical approach to predict the reliability and life of these components under these harsh loading conditions. The combination of NDE and two- and three-dimensional finite element analyses (e.g., stress analyses and fracture mechanics) is expected to set a standardized procedure to accurately assess the applicability of using various composite materials to design a suitable rotor/flywheel assembly. Following the figures is a brief description of some preliminary analytical results.

The figures represent typical NDE-finite element results. The top left figure shows a computed tomography (CT) scan for a rotor made of polymer matrix composite. This scan illustrates the defects in the rotor due to centrifugal loading (spun at 34 000 rpm); a crack along the circumferential direction is very obvious. The bottom left figure shows the finite element model for the rotor assembly. This assembly consists of the composite rotor (Hexel's IM–7 and AS4D) and an aluminum hub (7075–T6). Two and three-dimensional models were generated (The MacNeal-Schwendler Corporation, 1997) because of analysis requirements. Results obtained via finite element analyses (MARC Analysis Research Corporation, 1996) are shown in the figures on the right, where the stress levels depend on the applied loading. Furthermore, the bottom right figure illustrates the radial stress distribution in the rotor whereby the tensile stresses near the middle indicate the presence of the crack as detected by the computed tomography scanning shown in the top figure. Although these results are considered to be preliminary, they reflect a step forward in correlating NDE findings with finite element analysis.

For more information, visit Lewis' Life Prediction Branch on the World Wide Web:
http://www.grc.nasa.gov/WWW/LPB/

Glenn contact: Ali Abdul-Aziz, 216–433–6729, Ali.Abdul-Aziz@grc.nasa.gov

Composite Flywheels Assessed Analytically by NDE and FEA

As an alternative to expensive and short-lived lead-acid batteries, composite flywheels are being developed to provide an uninterruptible power supply for advanced aerospace and industrial applications. Flywheels can help prevent irregularities in voltage caused by power spikes, sags, surges, burnout, and blackouts. Other applications include load-leveling systems for wind and solar power facilities, where energy output fluctuates with weather. Advanced composite materials are being considered for these components because they are significantly lighter than typical metallic alloys and have high specific strength and stiffness. However, much more research is needed before these materials can be fully utilized, because there is insufficient data concerning their fatigue characteristics and nonlinear behavior, especially at elevated temperatures.

Moreover, these advanced types of structural composites pose greater challenges for nondestructive evaluation (NDE) techniques than are encountered with typical monolithic engineering metals (Achebach and Rajapakse, 1987; and Vary and Snyder, 1987). This is particularly true for ceramic polymer and metal matrix composites, where structural properties are tailored during the processing stages. In fully densified components, NDE techniques must detect and characterize various types of discrete defects like cracks, voids, and other overt discontinuities. It is also important to detect and characterize microstructural and diffuse flaw conditions that govern overall strength, fracture toughness, impact resistance, and resistance to thermal-mechanical-chemical degradation. These diffuse flaw states can reduce reliability and diminish service life just as much as discrete flaws (Vary and Klima, 1986).

In addition, the processing of innovative high-temperature materials requires the concurrent development of innovative NDE technologies. Sanders and Baaklini (1988) demonstrated that the nondestructive characterization of materials and proper feedback help optimize the processing procedures. Applying American Society for Testing and Materials (ASTM) standards in nondestructive quality inspection assures the reliability of selected materials. Vary (1991) suggested that new NDE standards and methodologies should mature

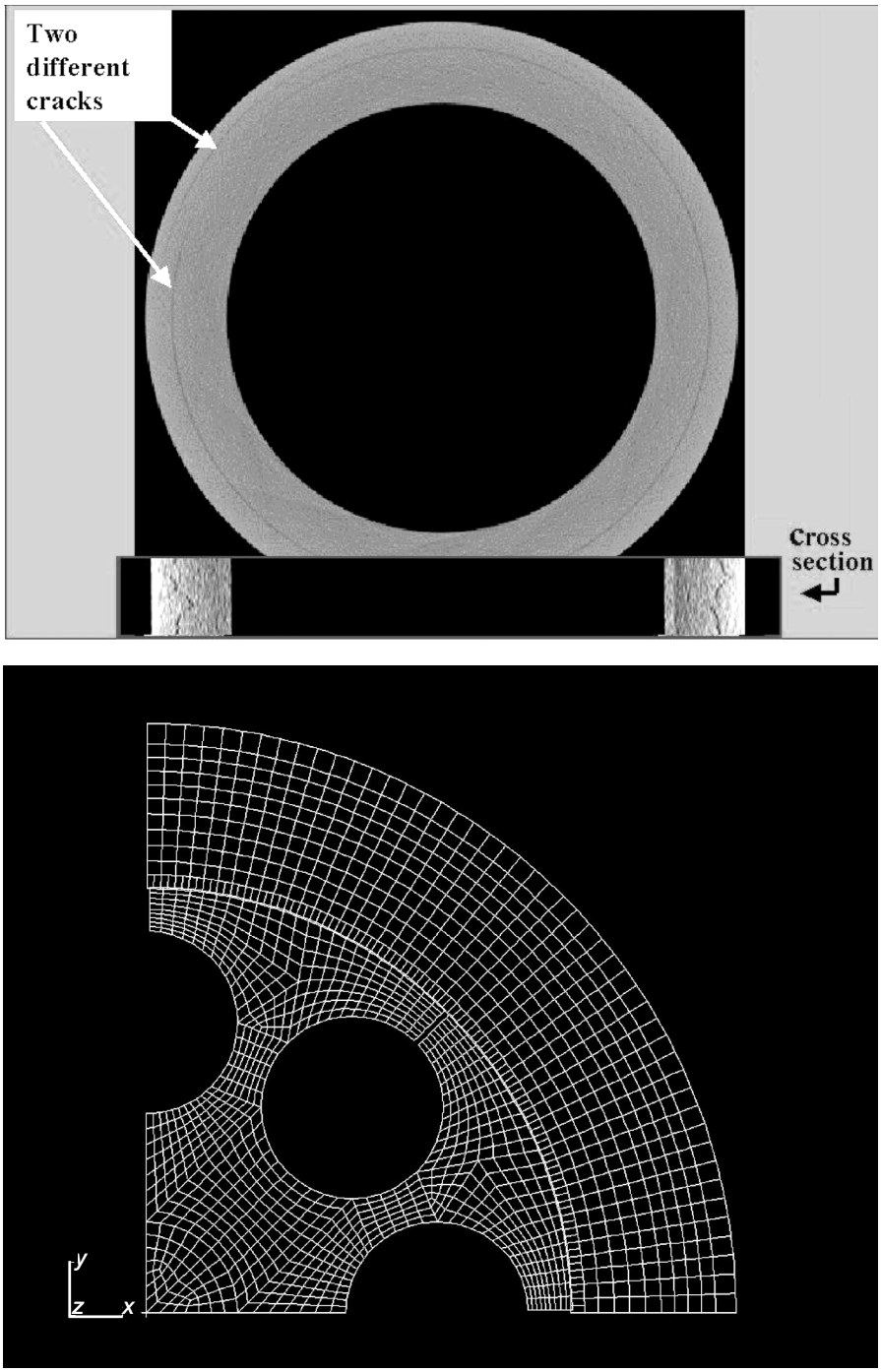

Top: CT cross section of a tested flywheel and cross section from a limited three-dimensional data set. Bottom: Finite element model of rotor-hub assembly.

simultaneously with advancements in materials development.

Current efforts involving the NDE group at the NASA Glenn Research Center at Lewis Field are focused on evaluating many important structural components, including the flywheel system. It has been shown that, with proper motor-generator and rotor design, flywheels have potentially higher efficiencies and longer lifetimes than other power systems, especially those made of fiber-reinforced polymer composite materials (Ashley, 1993). However, the challenge of designing high-energy flywheel systems that can withstand the stresses caused by high rotational speeds is still considerable. At certain centrifugal loads, steel or titanium flywheels have shattered and been destroyed, which has increased interest in investigating the use of composite materials for future flywheels.

Glenn's in-house analytical and experimental capabilities are being applied to analyze data produced by computed tomography (CT) scans to help assess the damage and defects of high-temperature structural composite materials. Finite element analysis (FEA) has been used extensively to model the effects of static and dynamic loading on aerospace propulsion components. This technique allows the use of complicated loading schemes by breaking the complex part geometry into many smaller, geometrically simple elements. In-house and commercial software packages are being used to construct three-dimensional models of images from CT scan slices. For example, Velocity^2 (image processing and three-dimensional reconstruction visualization software, Velocity^2 Technical Reference Manual Version 2.1, 1996–1999) is being used to construct the three-dimensional model and subsequently to generate a stereolithography file that will be suitable for computer-aided design applications. Tools developed in-house are being used to convert Velocity^2 stereolithography files to solid, three-dimensional FEA meshes. The entire process that outlines the link between the data extracted via NDE and FEA will be published soon.

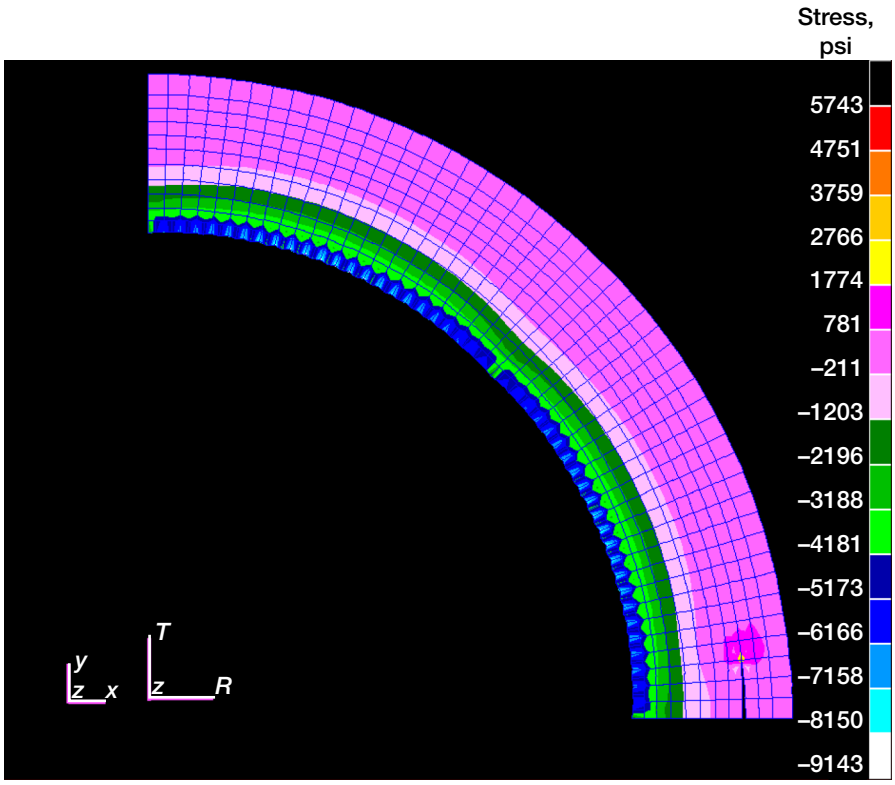

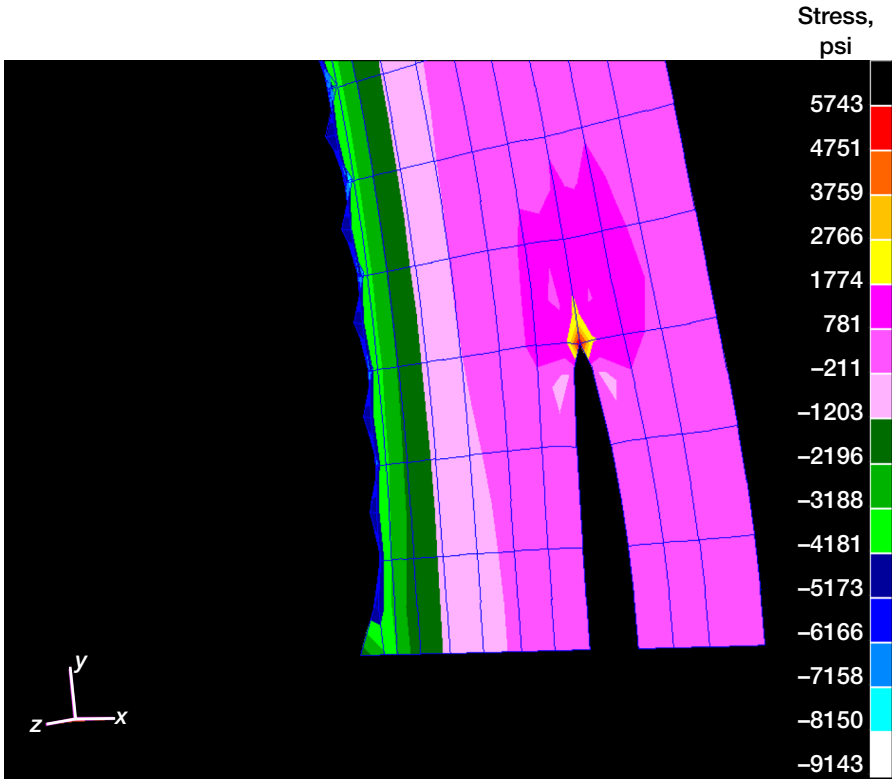

Top: Fracture mechanics analysis, radial stress distribution. Bottom: Fracture mechanics analysis, radial stress distribution, and closer view of crack propagation.

The figures presented in this article represent typical NDE–FEA results. The top figure on the facing page shows a computed tomography (CT) scan for a polymer matrix composite rotor. It illustrates the defects due to centrifugal loading extracted by the CT scan in the rotor (spun at 34,000 rpm); two cracks along the circumferential direction are clearly shown. In addition, a cross-sectional view of the crack that is parallel to the axis of rotation of the rotor is shown at the bottom of this figure. The bottom figure on the facing page is the FEA model of the rotor-hub assembly.

The figures to the left represent the FEA results obtained via fracture mechanic analyses; radial stress distribution is presented. Crack propagation is also documented in these figures. Stress levels due to the applied loading are noted. Tensile stresses at the crack tip reached nearly 6 ksi while the region where the rim contacts the hub remained compressive as anticipated. It can be concluded from the data that the finite element fracture mechanics closely simulated the CT scan findings. Furthermore, this work has established the preliminary grounds for an NDE–FEA–Fracture Mechanics interface methodology that can be used for the structural analysis of composite rotors.

Glenn contact:
Ali Abdul-Aziz, 216–433–6729,
Ali.Abdul-Aziz@grc.nasa.gov

Benchmark Testing of the Largest Titanium Aluminide Sheet Subelement Conducted

To evaluate wrought titanium aluminide (γTiAl) as a viable candidate material for the High-Speed Civil Transport (HSCT) exhaust nozzle, an international team led by the NASA Glenn Research Center at Lewis Field successfully fabricated and tested the largest γTiAl sheet structure ever manufactured. The γTiAl sheet structure, a 56-percent subscale divergent flap subelement, was fabricated for benchmark testing in three-point bending. Overall, the subelement was 84-cm (33-in.) long by 13-cm (5-in.) wide by 8-cm (3-in.) deep. Incorporated into the subelement were features that might be used in the fabrication of a full-scale divergent flap. These features include the use of (1) γTiAl shear clips to join together sections of corrugations, (2) multiple γTiAl face sheets, (3) double hot-formed γTiAl corrugations, and (4) brazed joints.

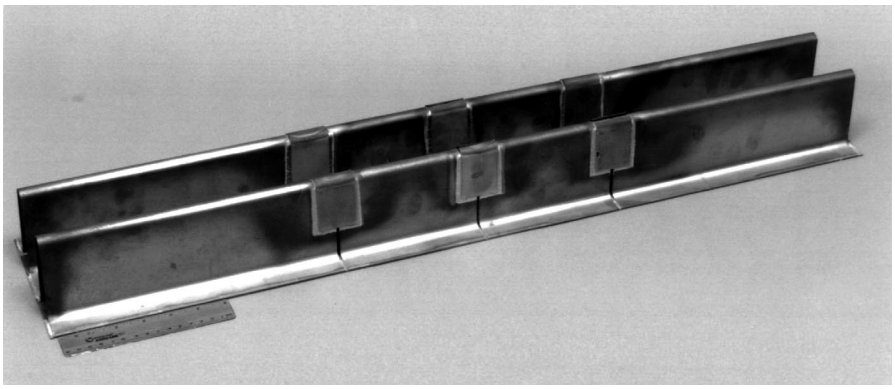

Double corrugated titanium aluminide divergent flap subelement.

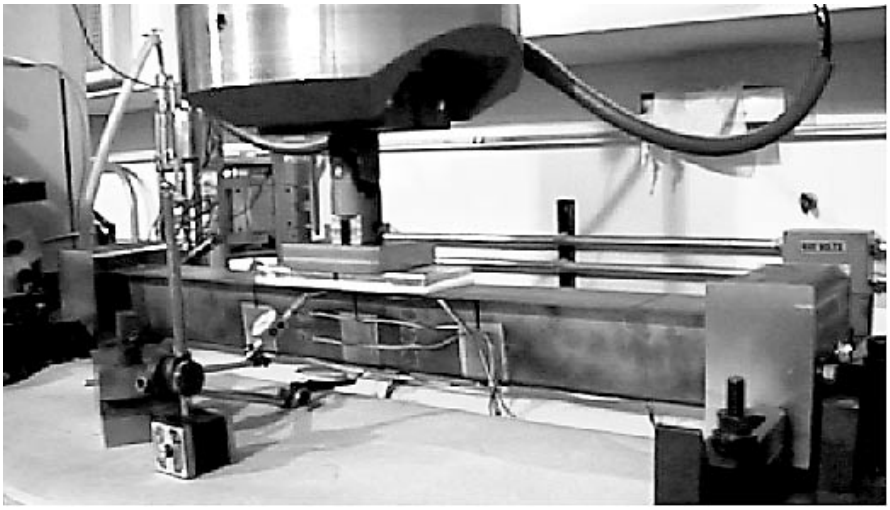

Benchmark test of titanium aluminide subelement (load at 340 kg).

The structural integrity of the γTiAl sheet subelement was evaluated by conducting a room-temperature three-point static bend test. The maximum beam deflection was approximately 2 mm (0.075 in.) at 340 kg (750 lb). Subelement failure occurred shortly after reaching 385 kg (850 lb). This is 93-percent higher than the predicted failure load.

The subelement failed at the center shear clip edge within the stress concentration area. Pretest finite element analysis (FEA) results accurately predicted the measured corrugation strains and stresses. Corrugation stresses were within 4 percent of predicted stresses. The pretest FEA results illustrated that the tools and methodology to design components with this new material were in hand. Posttest FEA using a failure load of 850 lb (385 kg) showed that the stress at the failure location was 520 MPa (75 ksi). Since this is within 5 percent of the γ-sheet's ultimate tensile strength of 550 MPa (80 ksi), it proved that the fabrication process of hot-forming and brazing did not affect the material's structural capability.

This successful effort showed the tremendous potential of the γTiAl sheet for advanced aerospace propulsion systems. Present interests in this material technology include a metallic thermal protection system for the VentureStar (Lockheed Martin Corporation) program, hot ducts and acoustic tiles for the Joint Strike Fighter program, and nozzle elements in the F119 propulsion system program.

Glenn contacts:
Dr. Paul A. Bartolotta, 216–433–3338, Paul.A.Bartolotta@grc.nasa.gov; and David L. Krause, 216–433–5465, David.L.Krause@grc.nasa.gov

Titanium Aluminide Technologies Successfully Transferred From HSR Program to RLV VentureStar Program

Through a cost-share contract, BFGoodrich Aerostructures group successfully fabricated three titanium aluminide (γTiAl) truss core structures using technologies pioneered in the High-Speed Research (HSR) program at the NASA Glenn Research Center at Lewis Field. The truss core subelement is approximately 60-cm (24-in.) long by 14-cm (5.5-in.) wide by 6-cm (2.5-in.) deep. To fabricate this subelement, BFGoodrich first obtained γTiAl sheets from Plansee (Austria) which produced the sheets using techniques developed collaboratively by Glenn, Pratt & Whitney, and Plansee. This new γTiAl production technology has significantly lowered the cost of γTiAl sheet (~75-percent decrease) and has made the production of larger γTiAl sheets possible (~60-percent increase).

BFGoodrich then hot-formed the γTiAl sheets into "hat" sections (individual internal stiffeners of the truss core that are shaped like the Greek letter omega) using a production hot press at near production rates as established by the HSR program. The γTiAl hat sections and γTiAl face sheets were then joined using HSR brazing technologies to produce the final truss core structure. NDE methods indicated that the truss core structures were sound, with over 98-percent coverage of all brazed joints.

The significance of this program is twofold. First, it demonstrated that HSR γTiAl sheet fabrication technologies could be transferred from the laboratory into the production house environment. Second, it was a vehicle to transfer the HSR γTiAl fabrication technologies to the Reusable Launch Vehicle (RLV)/ VentureStar (Lockheed Martin Corporation) program and other space transportation programs. According to BFGoodrich, this transfer has significantly aided their efforts in developing a metallic γTiAl thermal protection system for the RLV/VentureStar program. This technology transfer is a prime example of the synergy between technologies developed for aeronautic applications enabling space transportation programs to meet their goals.

Glenn contact:
Dr. Paul A. Bartolotta, 216–433–3338
Paul.A.Bartolotta@grc.nasa.gov

Titanium aluminide truss core subelement manufactured by BFGoodrich Aerostructures group using HSR technologies.

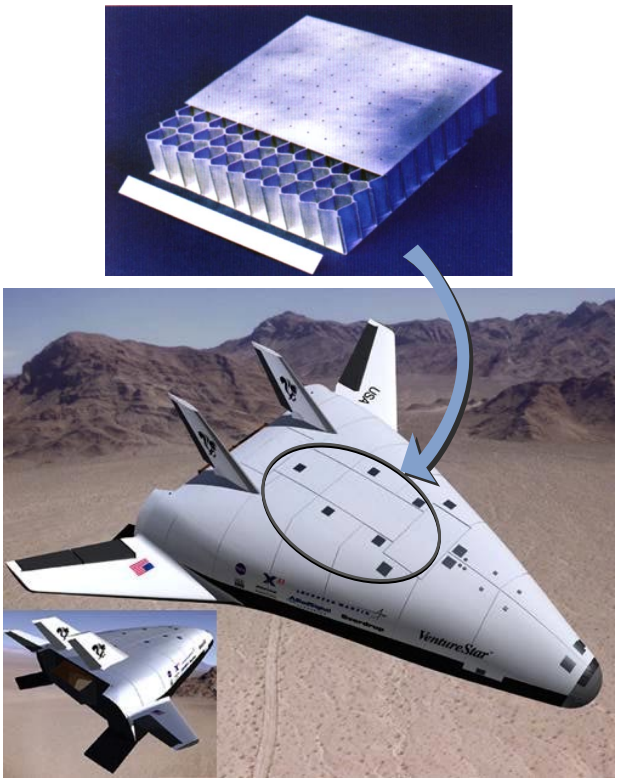

VentureStar reusable launch vehicle, showing where the titanium aluminide metallic thermal protection system will be used.

Mechanical Characterization of Thermomechanical Matrix Residual Stresses Incurred During MMC Processing

In recent years, much effort has been spent examining the residual stress-strain states of advanced composites. Such examinations are motivated by a number of significant concerns that affect composite development, processing, and analysis. The room-temperature residual stress states incurred in many advanced composite systems are often quite large and can introduce damage even prior to the first external mechanical loading of the material. These stresses, which are induced during the cooldown following high-temperature consolidation, result from the coefficient of thermal expansion mismatch between the fiber and matrix.

Experimental techniques commonly used to evaluate composite internal residual stress states are nonmechanical in nature and generally include forms of x-ray and neutron diffraction. Such approaches are usually complex, involving a number of assumptions and limitations associated with a wide range of issues, including the depth of penetration, the volume of material being assessed, and erroneous effects associated with oriented grains. Furthermore, and more important to the present research, these techniques can assess only "single time" stress in the composite. That is, little, if any, information is obtained that addresses the time-dependent point at which internal stresses begin to accumulate, the manner in which the accumulation occurs, and the presiding relationships between thermoelastic, thermoplastic, and thermoviscous behaviors. To address these critical issues, researchers at the NASA Lewis Research Center developed and implemented an innovative mechanical test technique to examine in real time, the time-dependent thermomechanical stress behavior of a matrix alloy as it went through a consolidation cycle.

In general, a standalone matrix material is subjected to the strain-temperature history experienced by the in situ matrix material during a uniaxially simulated hot isostatic pressing (HIP), or hot press cycle. First, the identical temperature time history experienced during the HIP cycle is imposed on the composite coupon while the composite cooldown thermal strain response is measured in a load-controlled environment. Employing the concept of fiber/matrix strain compatibility, we assume that

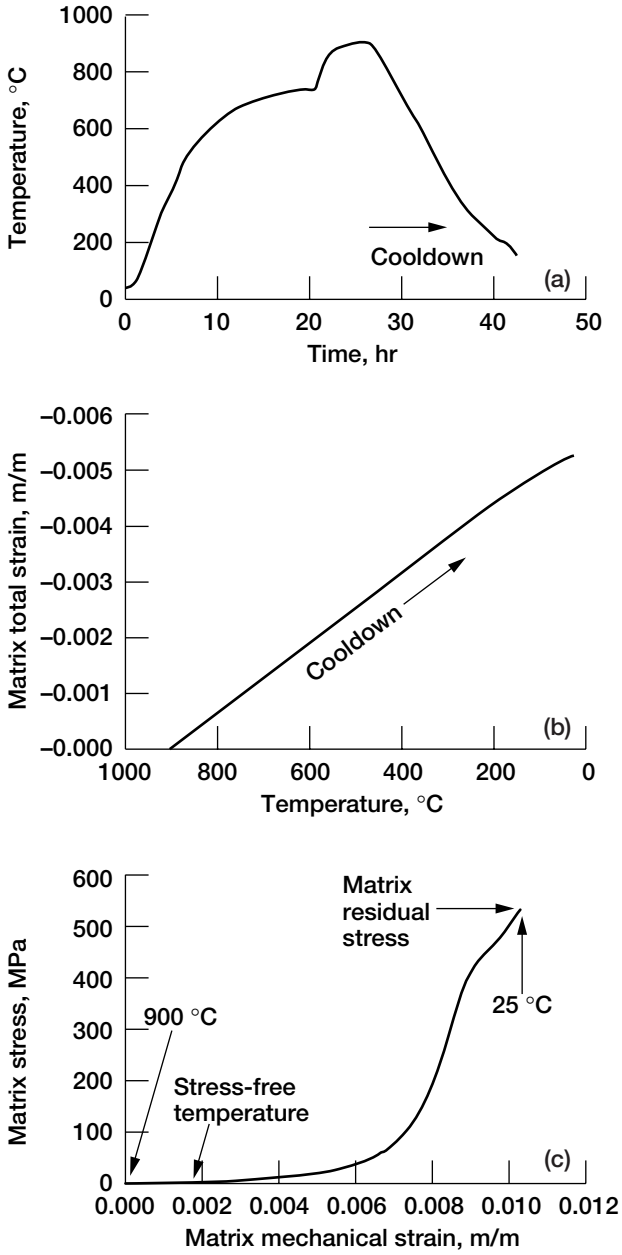

Thermomechanical test technique to simulate in situ metal matrix composite HIP cycle conditions on a standalone matrix. (a) Step 1—Measure composite cooldown strain. (b) Step 2—Enforce composite strain on matrix. (c) Step 3—Measure thermomechanical matrix response in terms of stress-free temperature; thermoelastic, thermoplastic, and thermoviscous behavior; and residual stress.

the measured macroscopic strain history is identical to that experienced by the individual constituents. With this information, the measured composite cooldown thermal strain response is "enforced" on the standalone matrix material during an identical cooldown cycle in a strain-controlled environment. This allows the thermomechanical matrix stress

response to be explicitly measured in real time without presupposing a given material behavior. From this technique, several critical measurements can be made, including (1) the time-dependent, stress-free temperature, (2) the degree of thermoelastic, thermoplastic, and thermoviscous behavior, (3) the real-time points within the HIP cycle where the respective behaviors occur, and (4) the residual stress locked into the matrix subsequent to the HIP cycle cooldown. Such results have been generated for several SiC-reinforced titanium matrix composites.

Glenn contact:
Michael G. Castelli, 216–433–8464,
Michael.G.Castelli@grc.nasa.gov

Deformation Behaviors of HIPped Foil Compared With Those of Sheet Titanium Alloys

Micromechanics-based modeling of composite material behaviors requires an accurate assessment of the constituent properties and behaviors. For the specific case of continuous-fiber-reinforced metal matrix composites (MMC's) manufactured from a foil/fiber/foil process, much emphasis has been placed on characterizing foil-based matrix materials that have been fabricated in the same way as the composite. Such materials are believed to yield mechanical properties and behaviors that are representative of the matrix constituent within the composite (in situ matrix). Therefore, these materials are desired for micromechanics modeling input. Unfortunately, such foils are extremely expensive to fabricate and procure because of the labor-intensive rolling process needed to produce them. As a potential solution to this problem that would maintain appropriately representative in situ properties, the matrix constituent could be characterized with sheet-based materials, which are considerably less expensive to manufacture than foils, are more readily procured, and result in fewer plies to obtain a desired panel thickness. The critical question is, however, does the consolidated sheet material exhibit the same properties and behaviors as do the consolidated foils? Researchers at NASA Lewis Research Center's Life Prediction Branch completed a detailed experimental investigation to answer this question for three titanium alloys commonly used in metal matrix composite form.

The experimental investigation compared the 427 °C (800 °F) mechanical properties and deformation behaviors of three HIPped (Hot Isostatic Pressed) foil and HIPped sheet titanium matrix materials commonly used in silicon-carbide-(SiC-) reinforced titanium composites. The alloys investigated were Ti-15V-3Cr-3Al-3Sn (Ti-15-3), Ti-15Mo-3Nb-3Al-0.2Si (Ti-21S), and Ti-6Al-4V (Ti-6-4). Elastic properties, creep deformation, and stress relaxation were examined along with the microstructural features before and after deformation. Differences in behavior were judged on the basis of statistical significance, where both a univariate analysis of variance (ANOVA) and a multivariate analysis of variance (MANOVA) were used and a two-parameter Norton-Bailey power law relationship was employed. In general, the HIPped foil and sheet were found to be significantly different in creep and stress relaxation at the 95-percent confidence level, with the only exceptions being Ti-15-3 in creep and Ti-21S in stress relaxation. Influencing this conclusion was the fact that the behaviors for any one alloy/product-form combination tended to be tightly grouped and exhibited relatively low sample-to-sample functional deviations. Of the three alloys, only the Ti-15-3 differed significantly within the microstructure in comparison to the foil and sheet forms.

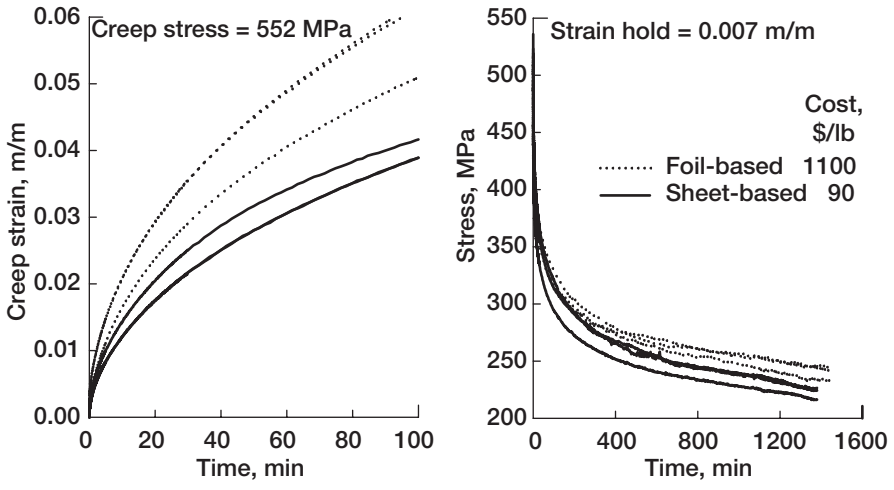

Creep and stress relaxation behavior of HIPped foil and sheet Ti-6-4 matrix at 427 °C (800 °F).

Furthermore, this was the only alloy to exhibit differences between the pre- and post-deformation states. This resulted from the metastable condition of the Ti-15-3 (even after a stabilization heat treatment). At 427 °C (800 °F), this alloy tends to experience a notable degree of deformation-assisted α-Ti precipitation within the β matrix. Although the strictly interpreted statistical analysis indicated that the foils and sheets exhibited significantly different behaviors, often a more practical engineering assessment and interpretation of the behaviors suggested that the sheet material could, in fact, be substituted for the foil, depending on the intended application of the data.

Glenn contacts:
Michael G. Castelli, 216–433–8464,
Michael.G.Castelli@grc.nasa.gov; and
Dr. Bradley A. Lerch, 216–433–5522,
Bradley.A.Lerch@grc.nasa.gov

Thermomechanical Fatigue Durability of T650–35/PMR–15 Sheet-Molding Compound Evaluated

High-performance polymer matrix composites (PMC's) continue to be the focus of a number of research efforts aimed at developing cost-effective, lightweight material alternatives for advanced aerospace and aeropropulsion applications. These materials not only offer significant advantages in specific stiffness and strength over their current metal counterparts, but they can be designed and manufactured to eliminate joints and fasteners by combining individual components into integral subassemblies, thus making them extremely attractive for commercial applications. With much emphasis on the low-cost manufacturing aspects of advanced composite structures, there is heightened interest in high performance sheet-molding compounds (SMC's). SMC's effectively reduce the costs associated with component production that uses prepregs, where variable costs are generally associated with labor, secondary processes, and scrap. With compression molding, SMC's can be fabricated into complex shapes facilitating the use of simple charge patterns, part consolidation, and molded-in inserts, which reduce labor, equipment, and operation costs for preparatory and secondary processes.

Researchers at the NASA Lewis Research Center, in cooperation with the Allison Advanced Development Company, completed an investigation examining the use of T650–35/PMR–15 SMC for a midstage inner-vane endwall application within a gas turbine engine compressor. This component resides in the engine flow path and is subjected not only to high airflow rates, but also to elevated temperatures and pressures. This application is unique in that it represents a very aggressive use of high-performance SMC's, raising obvious concerns related to durability and property retention in the presence of microstructural damage. Therefore, it was necessary to evaluate the fatigue behavior and damage tolerance of this material subjected to a representative thermomechanical fatigue (TMF) mission-cycle loading spectrum.

Damage progression was tracked through changes in the macroscopic deformation and elastic stiffness in the loading direction. Additional properties, such as the glass transition temperature and dynamic mechanical response also were examined. The fiber distribution orientation was characterized through a detailed quantitative image analysis, and material

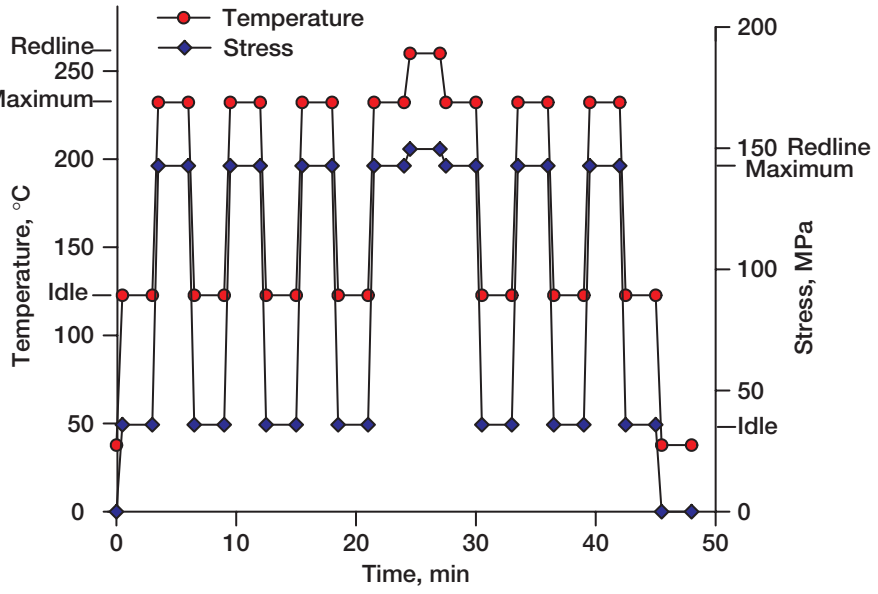

Thermomechanical fatigue mission cycle used for the T650–35/PMR–15 SMC inner-vane endwall application, showing idle, maximum, and redline (overload) conditions for temperature and stress.

durability and damage tolerance were quantified on the basis of residual static tensile properties after a prescribed number of TMF missions. Detailed microstructural examinations used optical and scanning electron microscopy to characterize the local damage.

Results indicate that the imposed TMF missions had only a modest effect on material durability as measured by the mechanical properties. Some microstructural damage was observed subsequent to 100 hours of TMF cycling. It consisted primarily of fiber debonding and transverse cracking local to predominantly transverse fiber bundles. No statistically significant degradation occurred in the residual tensile properties. Some of the more aggressive TMF scenarios examined, however, did promote notable creep damage and excessive strain accumulation that led to rupture. In some cases this creep behavior occurred at temperatures in excess of 150 °C below commonly cited values for the glass transition temperature. As a result, thermomechanical exploratory creep tests were conducted. These revealed that the SMC was subject to time-dependent deformation at stress/temperature thresholds of 150 MPa/230 °C and 170 MPa/180 °C.

Glenn contacts:
Michael G. Castelli, 216–433–8464,
Michael.G.Castelli@grc.nasa.gov; and
Dr. James K. Sutter, 216–433–3226,
James.K.Sutter@grc.nasa.gov

Test Standard Developed for Determining the Slow Crack Growth of Advanced Ceramics at Ambient Temperature

The service life of structural ceramic components is often limited by the process of slow crack growth. Therefore, it is important to develop an appropriate testing methodology for accurately determining the slow crack growth design parameters necessary for component life prediction. In addition, an appropriate test methodology can be used to determine the influences of component processing variables and composition on the slow crack growth and strength behavior of newly developed materials, thus allowing the component process to be tailored and optimized to specific needs.

At the NASA Lewis Research Center, work to develop a standard test method to determine the slow crack growth parameters of advanced ceramics was initiated by the authors in early 1994 in the C 28 (Advanced Ceramics) committee of the American Society for Testing and Materials (ASTM). After about 2 years of required balloting, the draft written by the authors was approved and established as a new ASTM test standard: ASTM C 1368–97, *Standard Test Method for Determination of Slow Crack Growth Parameters of Advanced Ceramics by Constant Stress-Rate Flexural Testing at Ambient Temperature*.

Briefly, the test method uses constant stress-rate testing to determine strengths as a function of stress rate at ambient temperature. Strengths are measured in a routine manner at four or more stress rates by applying constant displacement or loading rates. The slow crack growth parameters required for design are then estimated from a relationship between strength and stress rate. This new standard will be published in the Annual Book of ASTM Standards, Vol. 15.01, in 1998. Currently, a companion draft ASTM standard for determination of the slow crack growth parameters of advanced ceramics at elevated temperatures is being prepared by the authors and will be presented to the committee by the middle of 1998.

Consequently, Lewis will maintain an active leadership role in advanced ceramics standardization within ASTM. In addition, the authors have been and are involved with several international standardization organizations including the Versailles Project on Advanced Materials and Standards (VAMAS), the International Energy Agency (IEA), and the International Organization for Standardization (ISO). The associated standardization activities involve fracture toughness, strength, elastic modulus, and the machining of advanced ceramics.

Glenn contacts:
Dr. Sung R. Choi, 216–433–8366,
Sung.R.Choi@grc.nasa.gov, and
Jonathan A. Salem, 216–433–3313,
Jonathan.A.Salem@grc.nasa.gov

Accelerated Testing Methodology Developed for Determining the Slow Crack Growth of Advanced Ceramics

Constant stress-rate ("dynamic fatigue") testing has been used for several decades to characterize the slow crack growth behavior of glass and structural ceramics at both ambient and elevated temperatures. The advantage of such testing over other methods lies in its simplicity: strengths are measured in a routine manner at four or more stress rates by applying a constant displacement or loading rate. The slow crack growth parameters required for component design can be estimated from a relationship between strength and stress rate.

With the proper use of preloading in constant stress-rate testing, test time can be reduced appreciably. If a preload corresponding to 50 percent of the strength is applied to the specimen prior to testing, 50 percent of the test time can be saved as long as the applied preload does not change the strength. In fact, it has been a common, empirical practice in the strength testing of ceramics or optical fibers to apply some preloading (<40 percent). The purpose of this work at the NASA Lewis Research Center is to study the effect of preloading on measured strength in order to add a theoretical foundation to the empirical practice.

An analytical and numerical solution of strength as a function of preloading has been developed, as shown in the graphs. In this solution, $\bar{\sigma}_f$ is the normalized strength, in which the strength with preloading is normalized with respect to the strength with zero preloading; and α_p is the preloading fraction ($1 \le \alpha_p < 1$), where the preloading stress is normalized with respect to the strength with zero preloading. Finally, n is the slow crack growth parameter used in the expression of slow crack growth rate, $v = da/dt = A(K_I/K_{IC})^n$, where v, a, t, A, K_I, and K_{IC} are the crack velocity, crack size, time, slow crack growth parameter, stress intensity factor, and fracture toughness, respectively. The solution has been verified with experimental results obtained from constant stress-rate testing of glass and alumina at room temperature and of alumina, silicon nitride, and silicon carbide at elevated temperatures.

The most direct and powerful effect of preloading is the reduction of test time, which greatly affects test efficiency. For example, if it takes about 9 hr to perform constant stress-rate testing on one ceramic specimen and if a minimum of 20 specimens are required to obtain reliable statistical data, the total

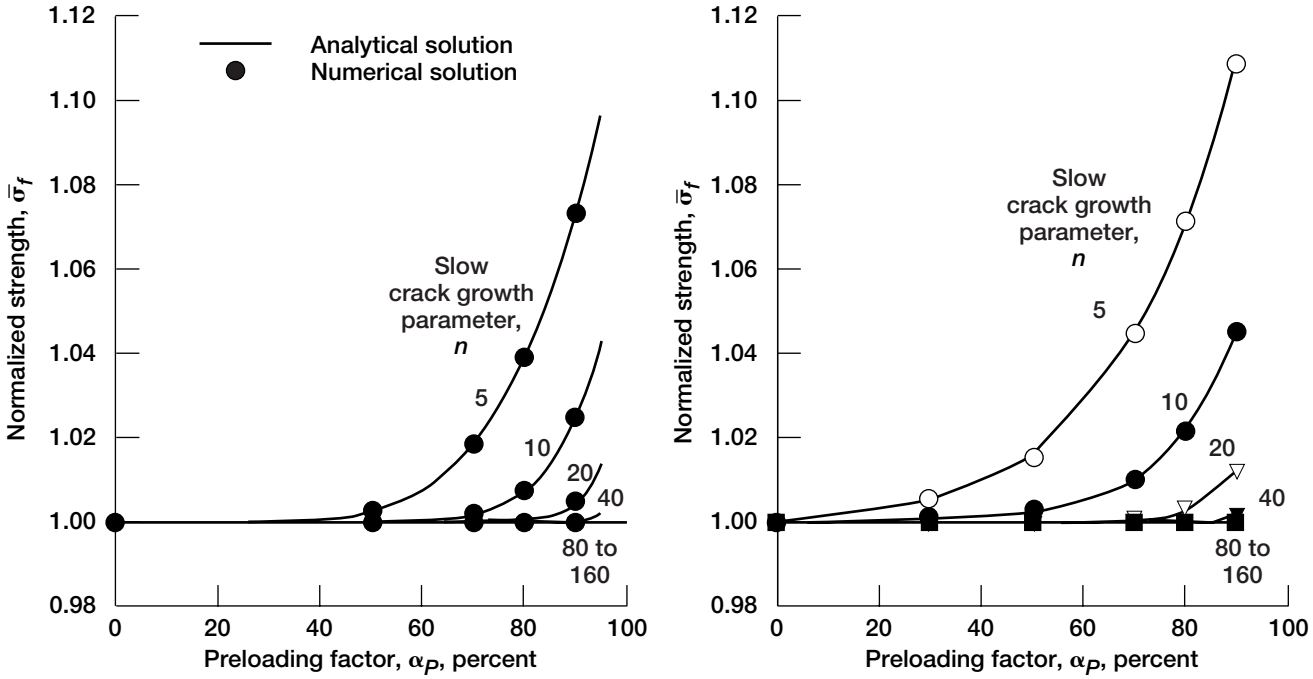

Normalized strength, $\bar{\sigma}_f$, as a function of preloading factor, α_p. Left: Natural flaw system. Right: Indentation-induced flaw system with residual stress field.

testing time at that stress-rate would be 180 hr. However, if a preloading of 80 percent was applied, the total testing time would be reduced to 36 hr, saving 80 percent of the total test time. For a preload of 70 percent, 70 percent of the time would be saved, and so on. The use of preloading has been adopted in a recently established American Society for Testing and Materials standard (C1368) on slow crack growth testing of advanced ceramics.

Glenn contacts:
Dr. Sung R. Choi, 216–433–8366,
Sung.R.Choi@grc.nasa.gov, and
Dr. John P. Gyekenyesi, 216–433–3210,
John.P.Gyekenyesi@grc.nasa.gov

"Ultra"-Fast Fracture Strength of Advanced Structural Ceramic Materials Studied at Elevated Temperatures

The accurate determination of inert strength is important in reliable life prediction of structural ceramic components. At ambient temperature, the inert strength of a brittle material is typically regarded as free of the effects of slow crack growth due to stress corrosion. Therefore, the inert strength can be determined either by eliminating active species, especially moisture, with an appropriate inert medium, or by using a very high test rate.

However, at elevated temperatures, the concept or definition of the inert strength of brittle ceramic materials is not clear, since temperature itself is a degrading environment, resulting in strength degradation through slow crack growth and/or creep. Since the mechanism to control strength is rate-dependent viscous flow, the only conceivable way to determine the inert strength at elevated temperatures is to utilize a very fast test rate that either minimizes the time for or eliminates slow crack growth. Few experimental studies have measured the elevated-temperature, inert (or "ultra"-fast fracture) strength of advanced ceramics. This is, in part, because conventional test frames are incapable of very high rate testing. In addition, data acquisition systems are inadequate, and there are safety concerns. Commonly, a maximum test rate of about 30 MPa/sec has been used to determine the elevated-temperature strength of ceramic materials. The strength that is determined at this test rate has been called the fast-fracture strength, implying that it is the maximum attainable, or ultimate, strength of the material at the temperature.

At the NASA Lewis Research Center, an experimental study was initiated to better understand the "ultra"-fast fracture strength behavior of advanced

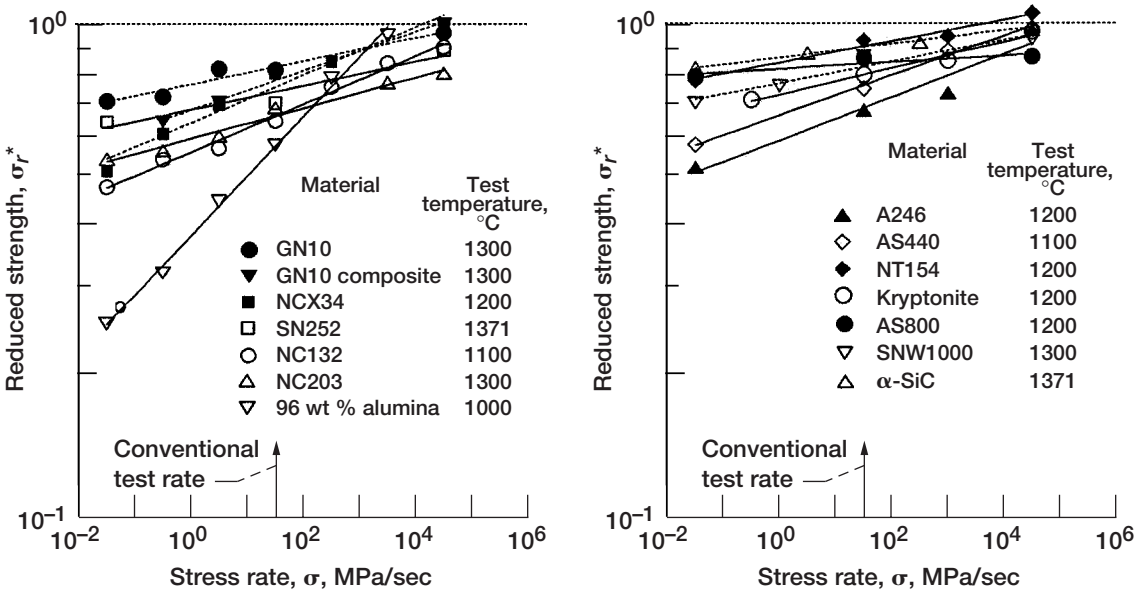

Summary of reduced strength as a function of stress rate for 14 advanced ceramics. Left: GN10, GN10 composite, NCX34, SN252 and NC132 silicon nitrides, NC203 silicon carbide, and 96 wt % alumina; Right: A2Y6, AS440, NT154, "Kryptonite" composite, AS800 and SNW1000 silicon nitrides, and α-silicon carbide.

ceramics at elevated temperatures. Fourteen advanced ceramics—one alumina, eleven silicon nitrides, and two silicon carbides—have been tested to date using constant stress-rate (dynamic fatigue) testing in flexure with a series of stress rates including the "ultra"-fast stress rate of 33 000 MPa/sec with digitally controlled test frames. The experimental results for these 14 advanced ceramics indicate that, notwithstanding possible changes in flaw populations as well as in flaw configurations because of elevated temperatures, the strength at 33 000 MPa/sec approached the room temperature strength or reached a higher value than that determined at the conventional test rate of 30 MPa/sec. The graphs summarize the test results for the 14 ceramics, where the reduced strength is an elevated-temperature strength normalized with respect to the corresponding room-temperature strength. On the basis of the experimental data, it can be stated that the elevated-temperature, inert strength of an advanced ceramic material can be defined as the strength where no slow crack growth takes place at the temperature. Specifically, the elevated-temperature inert strength is close to its room-temperature counterpart and can be obtained via a series of "ultra"-fast stress rates, including 33 000 MPa/sec in many cases. The strength determined at 33 000 MPa/sec must be used as an inert strength to determine the required life prediction parameters of the material.

Glenn contacts:
Dr. Sung R. Choi, 216–433–8366,
Sung.R.Choi@grc.nasa.gov; and
Dr. John P. Gyekenyesi, 216–433–3210,
John.P.Gyekenyesi@grc.nasa.gov

Test Standard Developed for Determining the Life Prediction Parameters of Advanced Structural Ceramics at Elevated Temperatures

The process of slow crack growth often limits the service life of structural ceramic components. Therefore, it is important to develop a test methodology for accurately determining the life prediction parameters required for component life prediction. In addition, this methodology should be useful in determining the influences of component processing variables and composition on the slow crack growth and strength behavior of newly developed or existing materials, thus allowing component processing to be tailored and optimized to specific needs.

In 1998, the authors initiated the development of a test method to determine the life prediction parameters of advanced structural ceramics at elevated temperatures. Performed at the NASA Glenn Research Center at Lewis Field, the work was done for the C28 Advanced Ceramics Committee of the American Society for Testing and Materials (ASTM). The draft standard written by the authors is going through the required balloting process. We expect it to be established in 2000 as a new ASTM test method, "Standard Test Method for Determining of Slow Crack Growth Parameters of Advanced Ceramics by Constant Stress-Rate Flexural Testing at Elevated Temperatures," and to be published in the year 2000 Annual Book of ASTM Standards, Vol. 15.01.

Briefly, the test method utilizes constant stress-rate testing to determine strengths as a function of the applied stress rate at elevated temperatures. The merit of this method lies in its simplicity: strengths are measured in a routine manner at four or more applied stress rates through the application of constant displacement or loading rates. The slow crack growth parameters necessary for life prediction are then determined from a simple relationship between the strength and the stress rate.

Glenn has maintained an active leadership role in the standardization of slow crack growth testing of advanced ceramics within ASTM. The authors also wrote a companion ambient-temperature standard, ASTM C 1368–97, "Standard Test Method for Determination of Slow Crack Growth Parameters of Advanced Ceramics at Ambient Temperature," which has been used by related industry, academia, and government agencies. In addition, Glenn has been actively involved with several international standardization organizations such as the Versailles Project on Advanced Materials and Standards (VAMAS) and the International Energy Agency. In 1988, for example, Glenn participated in a VAMAS round robin on fracture toughness of ceramics, using the Single-Edge-V-Notched Beam method.

Glenn contacts:
Dr. Sung R. Choi, 216–433–8366,
Sung.R.Choi@grc.nasa.gov; and
Dr. John P. Gyekenyesi, 216–433–3210,
John.P.Gyekenyesi@grc.nasa.gov

Nonlinearity and Strain-Rate Dependence in the Deformation Response of Polymer Matrix Composites Modeled

There has been no accurate procedure for modeling the high-speed impact of composite materials, but such an analytical capability will be required in designing reliable lightweight engine-containment systems. The majority of the models in use assume a linear elastic material response that does not vary with strain rate. However, for containment systems, polymer matrix composites incorporating ductile polymers are likely to be used. For such a material, the deformation response is likely to be nonlinear and to vary with strain rate. An analytical model has been developed at the NASA Glenn Research Center at Lewis Field that incorporates both of these features.

A set of constitutive equations that was originally developed to analyze the viscoplastic deformation of metals (Ramaswamy-Stouffer equations) was modified to simulate the nonlinear, rate-dependent deformation of polymers. Specifically, the effects of hydrostatic stresses on the inelastic response, which can be significant in polymers, were accounted for by a modification of the definition of the effective stress. The constitutive equations were then incorporated into a composite micromechanics model based on the mechanics of materials theory. This theory predicts the deformation response of a composite material from the properties and behavior of the individual constituents. In this manner, the nonlinear, rate-dependent deformation response of a polymer matrix composite can be predicted.

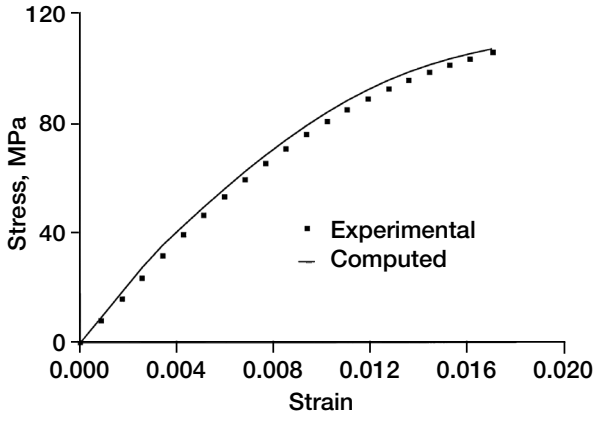

Model prediction for [45°] IM7/977–2 laminate compared with experimental results.

In the figure below, the tensile deformation response of a representative composite material that could be used in a fan-containment application is predicted. The predicted results compare favorably with experimentally obtained values. Currently, the deformation model is being implemented into a transient, dynamic finite element code. High-strain-rate data, which are required for the model, are also being obtained. The high-strain-rate data and the deformation model will be used to simulate ballistic impact tests that will be conducted in Glenn's Structures and Acoustics Division Ballistic Impact Facility.

Glenn contacts:
Dr. Robert K. Goldberg, 216–433–3330, Robert.K.Goldberg@grc.nasa.gov; and
Dr. J. Michael Pereira, 216–433–6738, J.M.Pereira@grc.nasa.gov

Constitutive Theory Developed for Monolithic Ceramic Materials

With the increasing use of advanced ceramic materials in high-temperature structural applications such as advanced heat engine components, the need arises to accurately predict thermomechanical behavior that is inherently time-dependent and that is hereditary in the sense that the current behavior depends not only on current conditions but also on the material's thermomechanical history. Most current analytical life prediction methods for both subcritical crack growth and creep models use elastic stress fields to predict the time-dependent reliability response of components subjected to elevated service temperatures. Inelastic response at high temperatures has been well documented in the materials science literature for these material systems, but this issue has been ignored by the engineering design community. From a design engineer's perspective, it is imperative to emphasize that accurate predictions of time-dependent reliability demand accurate stress field information.

Ceramic materials exhibit different time-dependent behavior in tension and compression. Thus, inelastic deformation models for ceramics must be

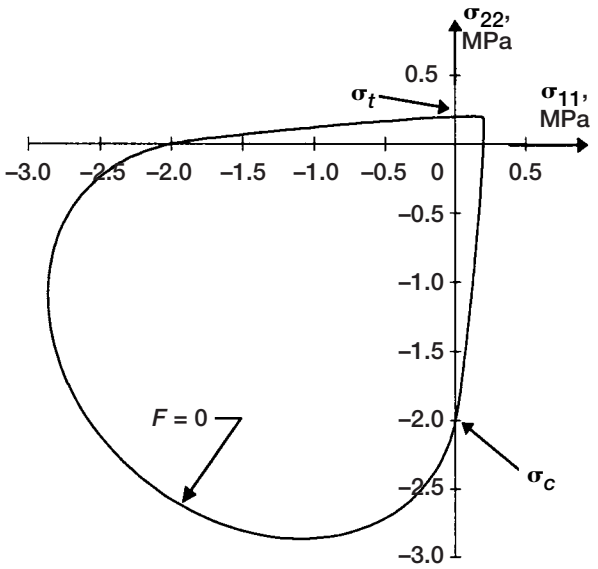

Threshold function projected onto the σ_{11}-σ_{22} stress plane.

constructed in a fashion that admits both sensitivity to hydrostatic stress and differing behavior in tension and compression. A number of constitutive theories for materials that exhibit sensitivity to the hydrostatic component of stress have been proposed that characterize deformation using time-independent classical plasticity as a foundation. However, none of these theories allow different behavior in tension and compression. In addition, these theories are somewhat lacking in that they are unable to capture the creep, relaxation, and rate-sensitive phenomena exhibited by ceramic materials at high temperatures.

The objective of this effort at the NASA Lewis Research Center has been to formulate a macroscopic continuum theory that captures these time-dependent phenomena. Specifically, the effort has focused on inelastic deformation behavior associated with these service conditions by developing a multiaxial viscoplastic constitutive model that accounts for time-dependent hereditary material deformation (such as creep and stress relaxation) in monolithic structural ceramics. Using continuum principles of engineering mechanics, we derived the complete viscoplastic theory from a scalar dissipative potential function. Constitutive equations for the flow law (strain rate) and evolutionary law were formulated on the basis of a threshold function, identified here as F (see the figure), that is sensitive to hydrostatic stress and allows different behavior in tension and compression. For illustration, a set of threshold flow stress values has been adopted that roughly corresponds to values anticipated for isotropic monolithic ceramics. Specifically, the compressive uniaxial threshold stress value σ_c is 2.00 MPa, and the tensile uniaxial threshold stress value σ_t is 0.20 MPa. Furthermore, inelastic deformation is treated as inherently time dependent. A rate of inelastic strain is associated with every state of stress. As a result, creep, stress relaxation, and rate sensitivity are phenomena resulting from applied boundary conditions and are not treated separately in an ad hoc fashion.

Complete details of the model and its attending geometrical implications have been developed, but a quantitative assessment has yet to be conducted since the material constants have not been suitably characterized for a specific material. Incorporating this model into a nonlinear finite element code would provide industry a means to numerically simulate the inherently time-dependent and hereditary phenomena exhibited by these materials in service. Utilization of this approach has the potential to improve the accuracy of life prediction results for structural ceramics in high-temperature power and propulsion applications.

Glenn contact:
Lesley A. Janosik, 216–433–5160,
Lesley.A.Janosik@grc.nasa.gov

Viscoplastic Constitutive Theory Demonstrated for Monolithic Ceramic Materials

Development of accurate three-dimensional (multiaxial) inelastic stress-strain models is critical in utilizing advanced ceramics for challenging 21st century high-temperature structural applications. The current state of the art uses elastic stress fields as a basis for both subcritical crack growth and creep life prediction efforts aimed at predicting the time-dependent reliability response of ceramic components subjected to elevated service temperatures. However, to successfully design components that will meet tomorrow's challenging requirements, design engineers must recognize that elastic predictions are inaccurate for these materials when subjected to high-temperature service conditions such as those encountered in advanced heat engine components. Analytical life prediction methodologies developed for advanced ceramics and

other brittle materials must employ accurate constitutive models that capture the inelastic response exhibited by these materials at elevated service temperatures.

A constitutive model recently developed at the NASA Lewis Research Center helps address this issue by accounting for the time-dependent (inelastic) material deformation phenomena (e.g., creep, rate sensitivity, and stress relaxation) exhibited by monolithic ceramics exposed to high-temperature service conditions. In addition, the proposed formulation is based on a threshold function that is sensitive to hydrostatic stress and allows different behavior in tension and compression, reflecting experimental observations obtained for these material systems.

The objective of this effort was to demonstrate the capabilities and inherent features of the mathematical formulation of the constitutive theory. In this regard, the viscoplastic constitutive equations formulated for the flow law (i.e., the strain rate) and the evolutionary law were incorporated into computer algorithms for predicting the multiaxial inelastic (creep) response of a given homogeneous state of stress. For the solution of a full multiaxial creep problem, 12 coupled differential equations had to be integrated. These represent the constitutive law: that is, six equations from the flow law (i.e., strain rate) and six from the evolutionary law.

Examples have been simulated numerically to illustrate the model's ability to qualitatively capture the time-dependent phenomena suggested here. For an imposed service (load) history, the computer algorithm can generate creep curves and viscoplastic flow surfaces that demonstrate its ability to capture the inelastic creep deformation response. No attempt was made to assess the accuracy of the model in comparison to the experiment. A quantitative assessment has been reserved for a later date—after the material constants have been suitably characterized for a specific ceramic material. Creep rupture is not considered in the model, although incorporating damage mechanics concepts into the present theory could yield a workable creep rupture model. This task also has been reserved for a future enhancement.

Glenn contact:
Lesley A. Janosik, 216–433–5160,
Lesley.A.Janosik@grc.nasa.gov

Noncontact Determination of Antisymmetric Plate Wave Velocity in Ceramic Matrix Composites

High-temperature materials are of increasing importance in the development of more efficient engines and components for the aeronautics industry. In particular, ceramic matrix composite (CMC) and metal matrix composite (MMC) structures are under active development for these applications.

The acousto-ultrasonic (AU) method has been shown to be useful for assessing mechanical properties in composite structures. In particular, plate wave analysis can characterize composites in terms of their stiffness moduli. It is desirable to monitor changes in mechanical properties that occur during thermomechanical testing and to monitor the health of components whose geometry or position make them hard to reach with conventional ultrasonic probes. In such applications, it would be useful to apply AU without coupling directly to the test surface.

For a number of years, lasers have been under investigation as remote ultrasonic input sources and ultrasound detectors. The use of an ultrasonic transducer coupled through an air gap has also been under study. So far at the NASA Lewis Research Center, we have been more successful in using lasers as ultrasonic sources than as output devices. On the other hand, we have been more successful in using an air-coupled piezoelectric transducer as an output device than as an input device. For this reason, we studied the laser in/air-coupled-transducer out combination—using a pulsed NdYAG laser as the ultrasonic source and an air-coupled-transducer as the detector.

The present work is focused on one of the AU parameters of interest, the ultrasonic velocity of the antisymmetric plate-wave mode. This easily identified antisymmetric pulse can be used to determine shear and flexure modulus. It was chosen for this initial work because the pulse arrival times are likely to be the most precise. The following schematic illustrates our experimental arrangement for using laser in/air-transducer out on SiC/SiC composite tensile specimens. The NdYAG pulse was directed downward by a 90° infrared prism to the top of the specimen, but at the edge of one end. An energy sensor measured a single pulse at 13 millijoules (mJ) before it passed through the

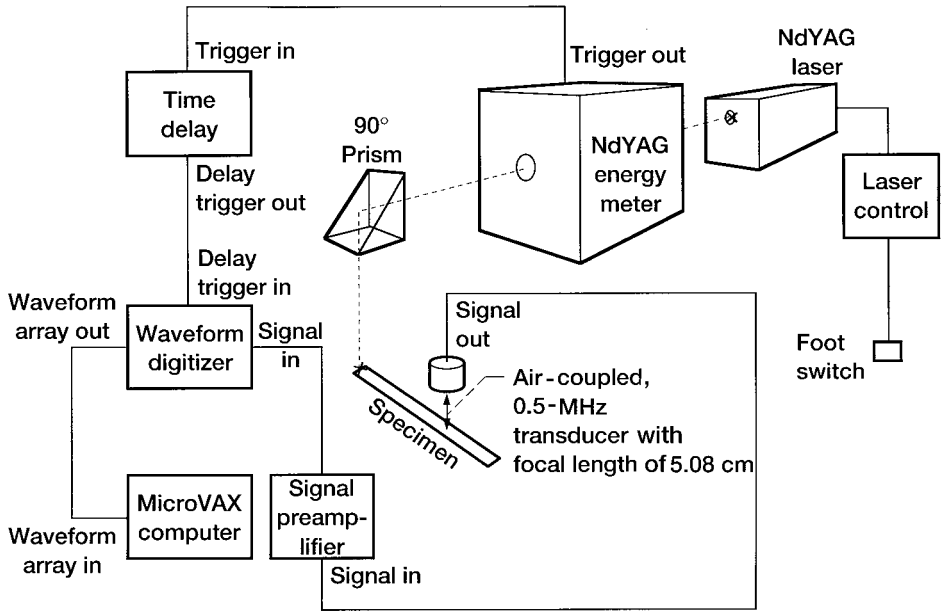

Experimental laser input/air-coupled-transducer output arrangement for collecting waveforms.

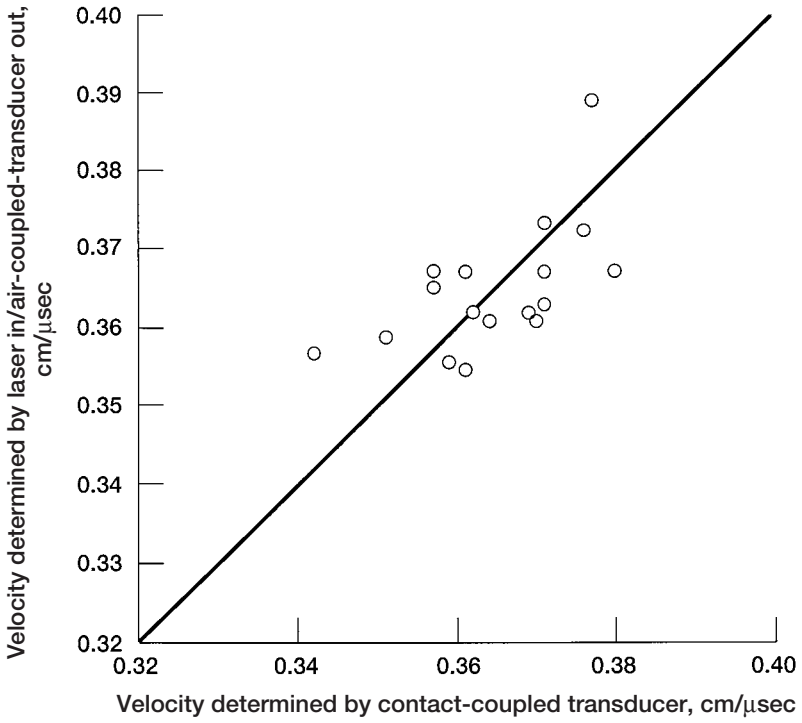

Plate-wave velocities from laser input/air-coupled-transducer output compared with those from contact-plate transducers.

prism, which attenuated 15 percent of its energy. It also provided an output trigger for the waveform time-delay synthesizer.

A broadband, air-coupled, piezoelectric transducer was centered nominally at 0.5 MHz and coupled to the air through a buffer that was shaped to focus the ultrasound 5.08 cm beyond its surface. We have shown that, for ceramic matrix composite specimens of the present geometry, this frequency range is very much dominated by the lowest antisymmetric plate mode.

Six specimens each of three layups, 0°/90°, ±45°, and $[0°/+45°/90°/-45°]_s$, of approximately 20-percent porous SiC/SiC were studied. For each layup, eight-ply panels were cut into 1.27- by 15.24-cm rectangular bars with thicknesses of 0.25 to 0.29 cm. Then, the bars, which had a 40-percent fiber fraction, were treated with a seal coating.

In the graph on the preceding page, the noncontact average plate-wave velocities are plotted against the contact average values. The standard deviation of the 18 sets of velocities was determined. For the noncontact data, the average was 2.8 percent, and for the contact data, it was 2.3 percent, indicating very similar reproducibility. Standard deviation bars are not plotted in the figure so that the correlation between the contact and noncontact velocity can be seen more readily. The laser in/air-coupled-transducer out system can provide data as accurate as that from contact-coupled transducers for determining the velocity associated with the lowest antisymmetric plate mode for SiC/SiC ceramic matrix composites.

Glenn contact:
Harold E. Kautz, 216–433–6015,
Harold.E.Kautz@grc.nasa.gov

Strain Measurement System Developed for Biaxially Loaded Cruciform Specimens

Components of mechanical equipment under load are routinely subjected to multiaxial states of stress at elevated temperatures. In addition, many construction materials exhibit anisotropic properties. For these conditions, in-plane biaxial testing of cruciform (cross-shaped) specimens is important for deriving mechanical properties used in design and life prediction.

Accurate strain measurement during biaxial testing is critical. It permits calculating specimen test area stresses under various loading conditions. Real-time measurement permits observation of deformation behavior under biaxial loading conditions. In addition, continuous electronic measurement is used in the closed-loop test control for strain-controlled experiments and in all test types for sensing test-termination strain limits.

A new extensometer system developed at the NASA Glenn Research Center at Lewis Field measures test area strains along two orthogonal axes in flat cruciform specimens. This system incorporates standard axial contact extensometers to provide a cost-effective high-precision instrument. The device was validated for use by extensive testing of a stainless steel specimen, with specimen temperatures ranging from room temperature to 1100 °F. In-plane loading conditions included several static biaxial load ratios, plus cyclic loadings of various waveform shapes, frequencies, magnitudes, and durations. The extensometer system measurements were compared with strain gauge data at room temperature and with calculated strain values for elevated-temperature measurements. All testing was performed in house in Glenn's Benchmark Test Facility in-plane biaxial load frame.

A summary of the verification testing results follows: (1) the new extensometer system was calibrated with a maximum error of 0.8 percent; (2) the room-temperature correlation with strain gauge data yielded an average variation of 58 microstrain; (3) operation under cyclic conditions resulted in tracking errors of less than 3 percent; (4) elevated-temperature results compared accurately with theoretical predictions; and (5) long-duration testing proved to be stable.

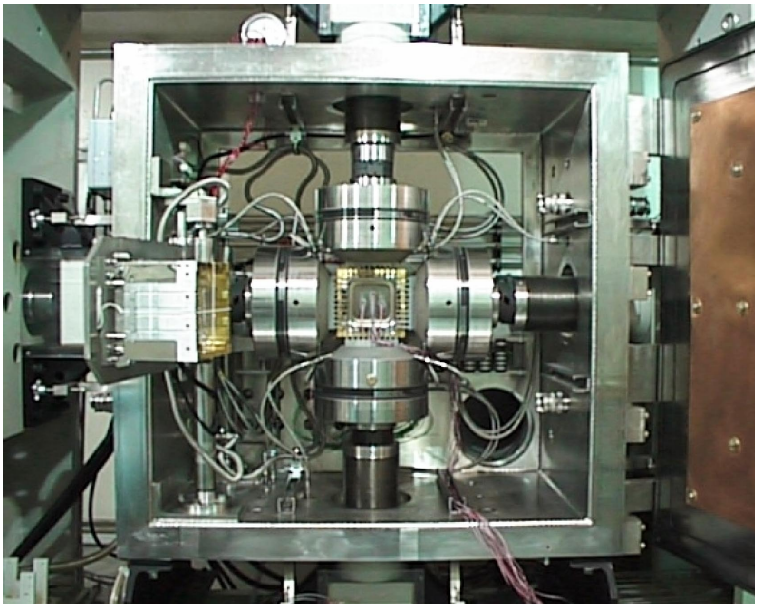

In-plane biaxial load frame with cruciform specimen.

This strain measurement system was developed to test advanced materials for the Advanced High Temperature Engine Materials Analysis Program (HITEMP) and the High-Speed Civil Transport propulsion system (HSR/EPM[2]). The candidate materials would be used in turbine engine components that are under highly multiaxial states of stress. Although monolithic, the mechanical properties of these cast materials exhibit directionality because of large grain sizes. The extensometer system could be used for the future testing of other high-temperature materials, including polymer and ceramic matrix composite materials.

Glenn contacts:
David L. Krause, 216–433–5465, David.L.Krause@grc.nasa.gov; and
Dr. Paul A. Bartolotta, 216–433–3338, Paul.A.Bartolotta@grc.nasa.gov

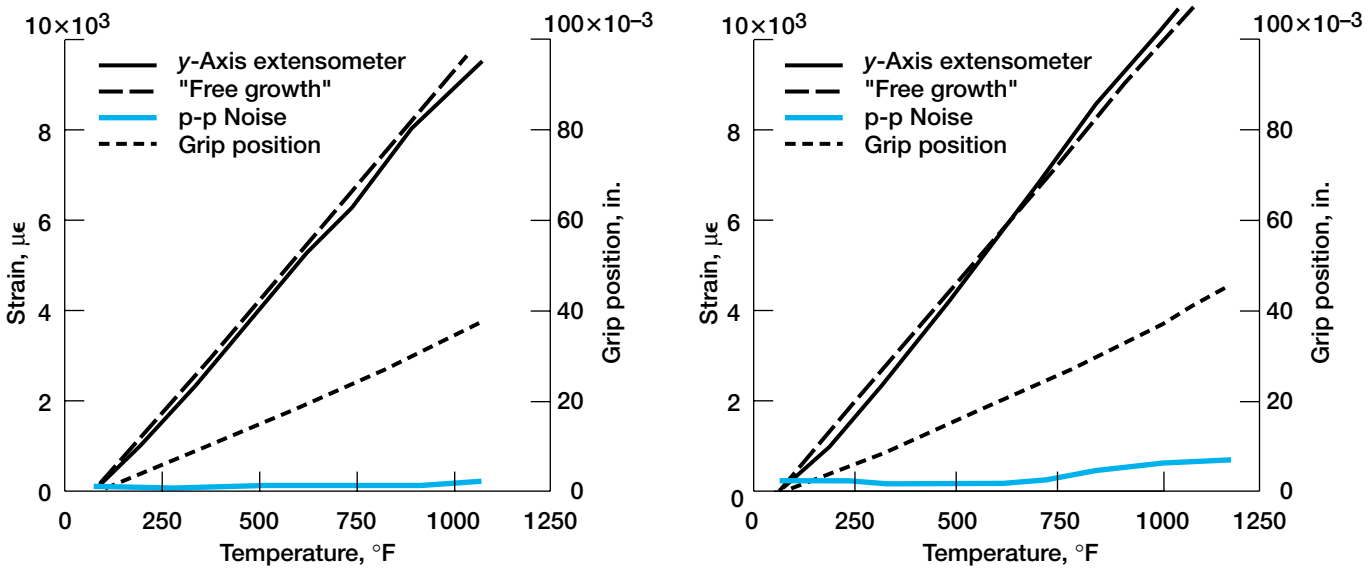

Extensometer operation for free thermal growth of AISI[1] Type 304 specimen. Left: x-direction. Right: y-direction.

[1]American Iron and Steel Institute (http://www.steel.org).
[2]http://www.grc.nasa.gov/WWW/HSR/HSR.html

Experimental Techniques Verified for Determining Yield and Flow Surfaces

Structural components in aircraft engines are subjected to multiaxial loads when in service. For such components, life prediction methodologies are dependent on the accuracy of the constitutive models that determine the elastic and inelastic portions of a loading cycle. A threshold surface (such as a yield surface) is customarily used to differentiate between reversible and irreversible flow. For elastoplastic materials, a yield surface can be used to delimit the elastic region in a given stress space. The concept of a yield surface is central to the mathematical formulation of a classical plasticity theory, but at elevated temperatures, material response can be highly time dependent. Thus, viscoplastic theories have been developed to account for this time dependency.

Since the key to many of these theories is experimental validation, the objective of this work (Lissenden et al., 1996 and 1997) at the NASA Lewis Research Center was to verify that current laboratory techniques and equipment are sufficient to determine flow surfaces at elevated temperatures. By probing many times in the axial-torsional stress space, we could define the yield and flow surfaces. A small offset definition of yield (10 με) was used to delineate the boundary between reversible and irreversible behavior so that the material state remained essentially unchanged and multiple probes could be done on the same specimen. The strain was measured with an off-the-shelf multiaxial extensometer that could measure the axial and torsional strains over a wide range of temperatures. The accuracy and resolution of this extensometer was verified by comparing its data with strain gauge data at room temperature. The extensometer was found to have sufficient resolution for these experiments. In addition, the amount of crosstalk (i.e., the accumulation of apparent strain in one direction when strain in the other direction is applied) was found to be negligible.

Tubular specimens were induction heated to determine the flow surfaces at elevated temperatures. The heating system induced a large amount of noise in the data. By reducing thermal fluctuations and using appropriate data averaging schemes, we could render the noise inconsequential. Thus, accurate and reproducible flow surfaces (see the figure) could be obtained.

With the experimental equipment verified, it is now possible to validate multiaxial, viscoplastic theories. Future work is planned to examine multiaxial effects in composites and superalloys commonly used in advanced aircraft engines.

Glenn contacts:
Dr. Brad A. Lerch, 216–433–5522, Bradley.A.Lerch@grc.nasa.gov, and
Dr. Rod Ellis, 216–433–3340, John.R.Ellis@grc.nasa.gov

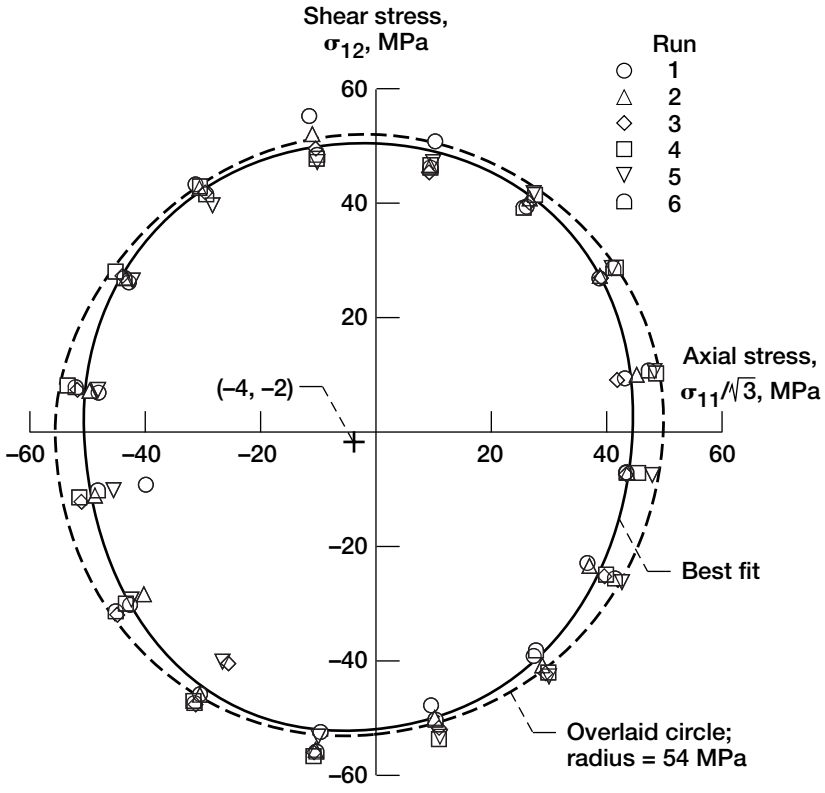

Flow surfaces for 316 stainless steel at 650 ° C.

Resistance of Titanium Aluminide to Domestic Object Damage Assessed

A team consisting of GE Aircraft Engines, Precision Cast Parts, Oremet, and Chromalloy were awarded a NASA-sponsored Aerospace Industry Technology Program (AITP) to develop a design and manufacturing capability that will lead to the engine test demonstration and eventual implementation of a γ-Ti-47Al-2Nb-2Cr (at. %) titanium aluminide (TiAl) low-pressure turbine blade into commercial service. One of the main technical risks of implementing TiAl low-pressure turbine blades is the poor impact resistance of TiAl in comparison to the currently used nickel-based superalloy. The impact resistance of TiAl is being investigated at the NASA Lewis Research Center as part of the Aerospace Industry Technology Program and the Advanced High Temperature Engine Materials Program (HITEMP).

The overall objective of this work is to determine the influence of impact damage on the high cycle fatigue life of TiAl-simulated low-pressure turbine blades. To this end, impact specimens were cast to size in a dogbone configuration and given a typical processing sequence followed by an exposure to 650 °C for 20 hours to simulate embrittlement at service conditions. Then, the specimens were impacted at 260 °C under a 69-MPa load. Steel projectiles with diameters 1.6 and 3.2 mm were used to impact the specimens at 90° to the leading edge. Two different impact energies (0.74 and 1.5 joules) were used to simulate fairly severe domestic object damage on a low-pressure turbine blade.

Fatigue tests were performed at 650 °C and at a frequency of 100 Hz. In addition, three different loading ratios, *R*, were used to assess the effect of mean stresses. As expected, the specimens impacted at the higher energy levels failed at lower fatigue stresses because of the larger "defect" associated with the impact. Both energy levels resulted in fatigue strengths that were significantly lower, yet predictable, than for the smooth bars (i.e., nonimpacted specimens). In addition, a Goodman mean stress approach could be used to accurately model the fatigue data for all impacted specimens.

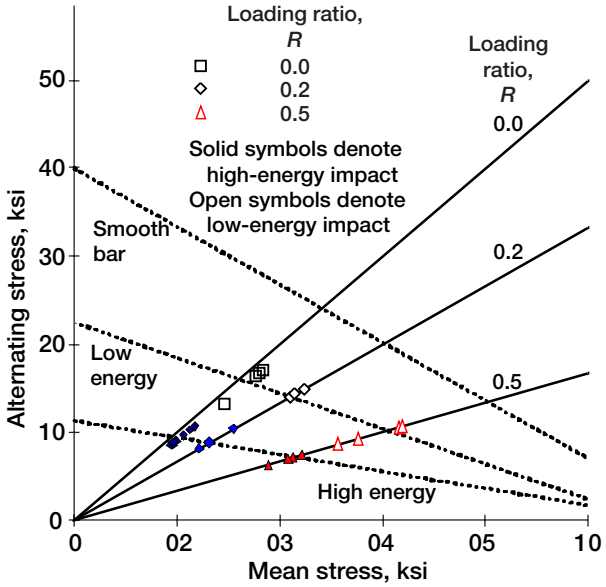

Goodman diagram for γ-TiAl specimens tested at 650 °C.

The industry-NASA team is using the results of this study to minimize the technical risks associated with impact issues. The actual damage tolerable for a low-pressure turbine blade application will be determined by a combination of fatigue testing and consideration of actual engine conditions. The current evaluations indicate that Ti-47Al-2Nb-2Cr possesses the level of damage tolerance required for implementation into service.

Glenn contact:
Dr. Bradley A. Lerch, 216–433–5522,
Bradley.A.Lerch@grc.nasa.gov

Multiaxial Experiments Conducted to Aid in the Development of Viscoplastic Models

Aeropropulsion components, such as disks, blades, and shafts, are commonly subjected to multiaxial stress states at elevated temperatures. Experimental results from loadings as complex as those experienced in service are needed to help guide the development of accurate viscoplastic, multiaxial deformation models that can be used to improve the design of these components. Typically, past studies investigated model materials, concentrating, for experimental simplicity, on room temperature. This study provides first-of-a-kind data by conducting axial-torsional tests at service-related temperatures on a popular aeropropulsion material, namely INCONEL 718 (IN–718, Inco Alloys International, Inc., Huntington, West Virginia). The data from this type of study can be used to develop the evolution equations necessary for this and similar engineering materials.

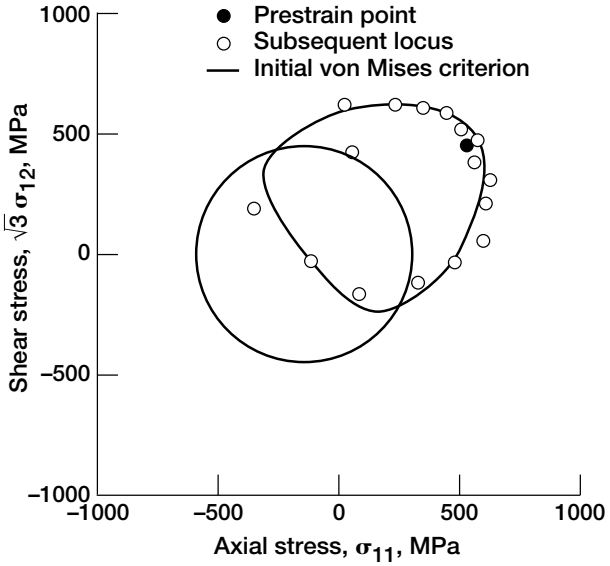

Yield locus subsequent to an axial-shear inelastic prestrain of 500-microstrain for IN–718 aged at 650 °C. Offset for individual probes, ε^{off}, 30 microstrain.

Yield loci were determined for aged IN–718 at 650 °C. This was done using experimental procedures developed over the past several years in a cooperative program between Penn State University and the NASA Lewis Research Center. This program represents an ongoing effort to develop test methods necessary for the validation of viscoplastic models. The von Mises (J_2) yield criterion was found to not fit the data well because of a strength differential in tension and compression. That is, the initial yield strength in compression was greater than it was in tension. The strength differential was present for the entire range of loading (up to at least strains of ±1 percent), but it decreased as plastic flow increased. In addition, the strength differential increased as the temperature increased in the range of 20 to 650 °C.

Yield surfaces also were obtained after preloading the material to various levels. After applying an axial-shear prestrain to an equivalent inelastic strain of 500 microstrain, the yield surface translated in the direction of the prestrain (see the figure). In addition, the yield surface elongated in the direction of prestraining and flattened on the back side. Thus, there is a component of distortional hardening that needs to be accounted for in the theoretical evolution equations.

We are presently developing techniques to transform the yield surface data to flow surfaces, which are similar to yield surfaces except that they are rate-dependent, and thus more meaningful for viscoplastic models. Since the von Mises yield criterion was inadequate for IN–718, experiments and associated modeling work are planned to determine the dependence of initial yielding on the stress invariants (I_1, J_2, and J_3) and to establish the importance of these invariants. In addition, we plan to examine load path dependence for the evolution of state and compare these results with predictions from viscoplastic models.

Glenn contact: Dr. Bradley A. Lerch, 216–433–5522, Bradley.A.Lerch@grc.nasa.gov

Damage Resistance of Titanium Aluminide Evaluated

As part of the aviation safety goal to reduce the aircraft accident rate, NASA has undertaken studies to develop durable engine component materials. One of these materials, γ-TiAl, has superior high-temperature material properties. Its low density provides improved specific strength and creep resistance in comparison to currently used titanium alloys. However, this intermetallic is inherently brittle, and long life durability is a potential problem. Of particular concern is the material's sensitivity to defects, which may form during the manufacturing process or in service. To determine the sensitivity of TiAl to defects, a team consisting of GE Aircraft Engines, Precision Cast Parts, and NASA was formed. The work at the NASA Glenn Research Center at Lewis Field has concentrated on the fatigue response to specimens containing defects.

The overall objective of this work is to determine the influence of defects on the high cycle fatigue life of TiAl-simulated low-pressure turbine blades. Two types of defects have been introduced into the specimens: cracking from impact damage and casting porosity. For both types of defects, the cast-to-size fatigue specimens were fatigue tested at 650 °C and 100 Hz until failure.

Impacting the specimens yielded two forms of cracks, dependent on the impact energy. At a high energy, hertzian cracks were dominant and often led to material being removed from the edge of the specimen. At lower impact energies, cracks formed on the backside of the specimen perpendicular to the specimen axis. Both types of cracks are described in Draper, Pereira, and Nathal (1997).

Additional specimens, which were originally rejected because of nondestructive evaluation (NDE) indications, were fatigue tested to study the degradation in fatigue life due to the presence of the casting defects. Before testing, these specimens were reexamined using microfocus x-ray and computed tomography (Lerch et al., 1999). Microfocus x-ray was successful in identifying 90 percent of the casting defects that caused failure and improved the detection capabilities over conventional radiography. Computed tomography, a time-consuming method, was only performed on two samples. This method gave cross-sectional information about the defects, which could be used to estimate the subsequent fatigue life.

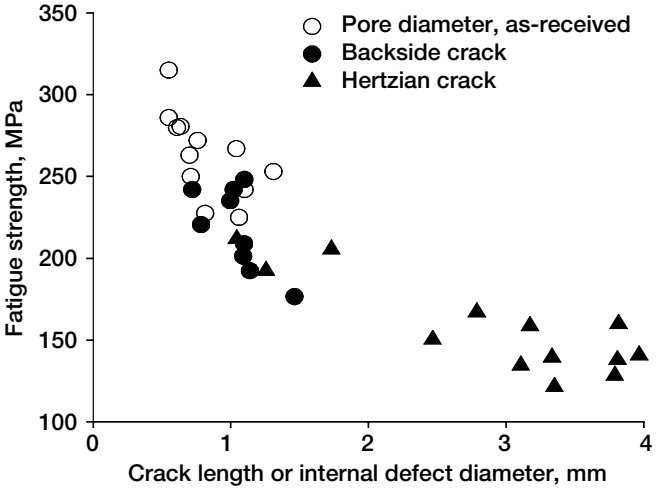

Decline in fatigue strength with increasing defect size.

Defect size played a large role in determining the critical fatigue loads. Increasing the defect size, regardless of whether the flaws resulted from casting porosity or from impact cracks, led to a decrease in the fatigue strength. Some of the severest impacts reduced the fatigue strength by almost a factor of three. The larger casting defects only reduced the fatigue strength by a maximum of 35 percent.

This information on the effects of defects in γ-TiAl will be used in several ways. First, it will help set accept-reject limits for castings at the foundry, and in some cases, depending on part cost and defect location, may indicate when casting repairs should be made. Second, it will help develop a damage-tolerant design and life-determination approach for γ, to make sure that γ-TiAl parts will have the necessary robustness to provide a long life in engine service. Third, it will help establish field inspection and repair limits for parts that develop damage in service.

Glenn contact:
Dr. Bradley A. Lerch, (216) 433–5522,
Bradley.A.Lerch@grc.nasa.gov

Multidisciplinary Probabilistic Heat Transfer/Structural Analysis Code Developed—NESTEM

High-Speed Civil Transport (HSCT) engine combustor liners are subjected to complex thermal environments and have to endure these for thousands of hours with assured reliability. In the past, several deterministic analyses have been performed, including detailed heat transfer analyses to obtain thermal profiles and deterministic stress analyses to identify critical locations of high stresses. Actual rig tests also have been performed for segments by simulating these loading situations as closely as possible. However, it is well known that many uncertainties exist in loading (primarily thermal loads due to heat transfer), boundary conditions (end fixity unknowns), and material properties (moduli, thermal-expansion coefficients, and conductivities). The present in-house effort at the NASA Lewis Research Center is directed toward accounting for these in a formal way to assess the performance of liner components under complex and uncertain loading conditions as well as subject to other geometry- and material-related uncertainties.

Under the sponsorship of the Enabling Propulsion Materials (EPM) project, Lewis' Structures and Acoustics Division recently developed a computational capability, NESTEM (see the figures), through a contract to Modern Technologies Corporation. NESTEM is a computer code that combines the heat transfer analysis capability of the EPM backbone computer code CSTEM (Coupled Structural, Thermal and Electro-Magnetic Tailoring) with Lewis' in-house probabilistic structural analysis code NESSUS (Numerical Evaluation of Stochastic Structures Under Stress). The code can now analyze and assess the complex combustor thermal environment with uncertainties, as well as its effects on the overall ceramic matrix composite (CMC) liner response. It enables us to formally assess the uncertainties in loads, material property variations, and geometric imperfections on the overall structural behavior (such as stability, frequencies, and stresses). Typical output of the code is

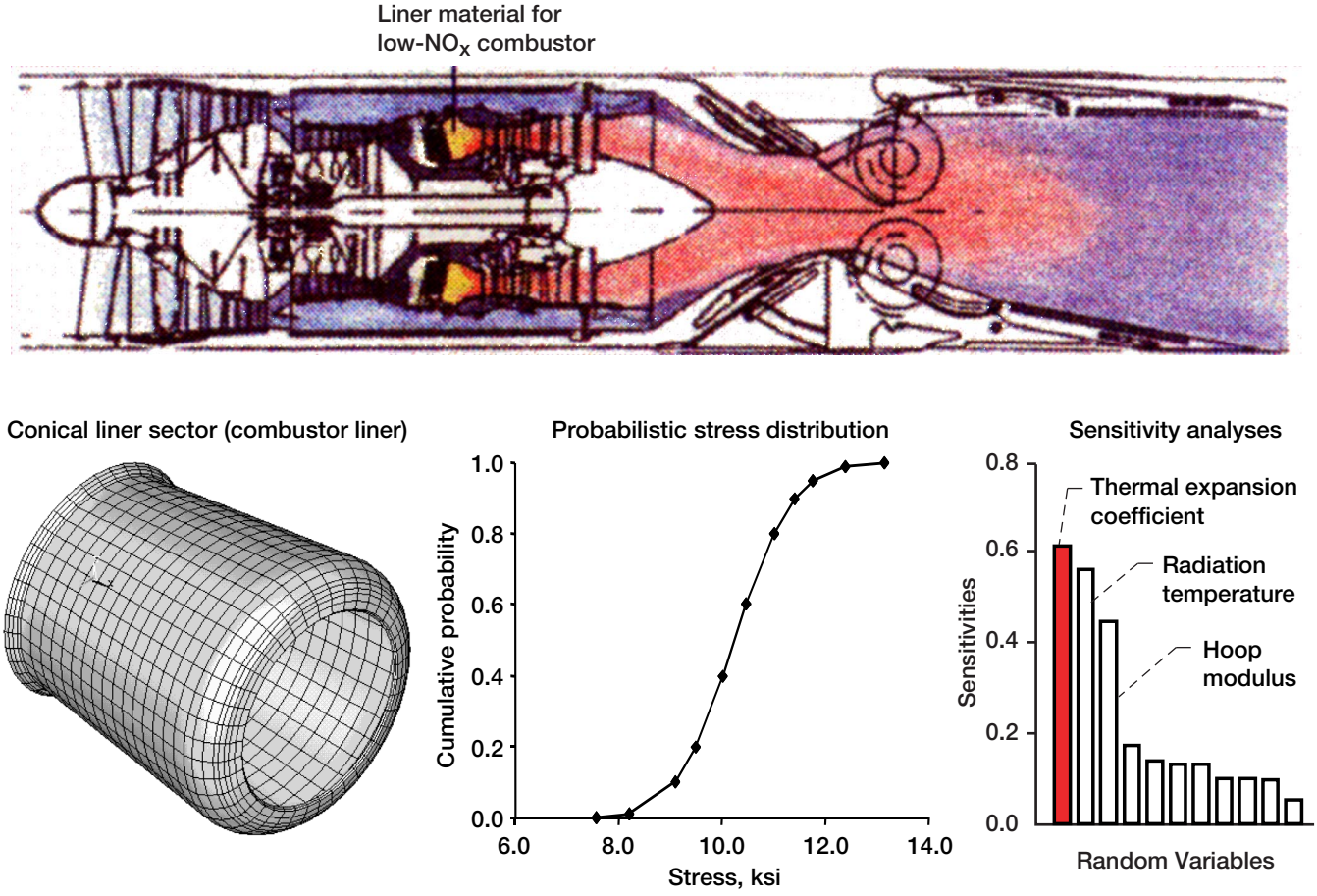

Sample output from NESTEM for a conical ceramic-matrix-composite liner segment.

probabilistic stress distributions at the hot spots, probabilistic frequencies, and buckling loads. This information allows designers to make more informed judgments regarding the preliminary design of the liner components without resorting to overly conservative deterministic approaches with ad hoc knockdown factors. The information also permits more accurate calculation of the reliability and life of such components. In addition, the code provides information on the sensitivities of the various uncertainties and ranks them in the order of importance as a byproduct. The accompanying figures show a sample output for a conical ceramic-matrix-composite liner segment.

NESTEM's features include

- Automatic geometry and finite element mesh generation
- Finite element property card generation for arbitrary composite layups
- Uncertainties in heat-transfer-related variables, combustor temperatures, geometry, material properties, and boundary conditions
- Heat transfer and structural analysis in the same run
- Cumulative distribution functions of response, including temperatures, stresses, natural frequencies, buckling loads, and displacements
- Sensitivities of variables with uncertainties at various probability levels

Glenn contacts:
Dr. Pappu L.N. Murthy, (216) 433–3332,
Pappu.L.Murthy@grc.nasa.gov; and
Dr. Shantaram S. Pai, (216) 433–3255,
Shantaram.S.Pai@grc.nasa.gov

Special recognition: Team Achievement Award

Design Tool Developed for Probabilistic Modeling of Ceramic Matrix Composite Strength

Ceramic matrix composites are being evaluated as candidate materials for many high-temperature applications such as engine combustor liners for the High-Speed Civil Transport (HSCT). They are required to have an assured life of several thousand hours. Estimating the reliability of these components is quite a complex process and requires knowledge of the uncertainties that occur at various scales. The properties of ceramic matrix composites (CMC) are known to display a considerable amount of scatter due to variations in fiber/matrix properties, interphase/coating properties, bonding, amount of matrix voids, and many geometry- and fabrication-related parameters such as ply thickness and ply orientations. The objective of this research effort is to account for these uncertainties in a formal way by probabilistically analyzing both the stiffness- and strength-related properties of CMC's. In current deterministic approaches, uncertainties are usually accounted for by safety

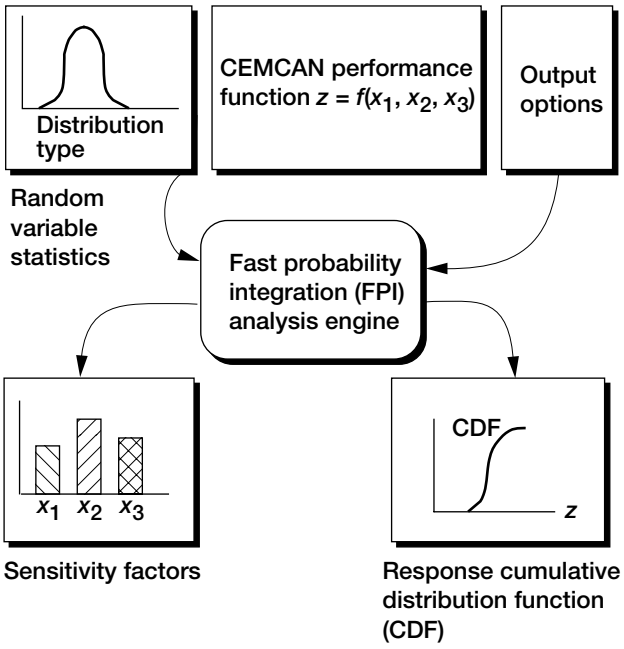

Fast probability integration input and output.

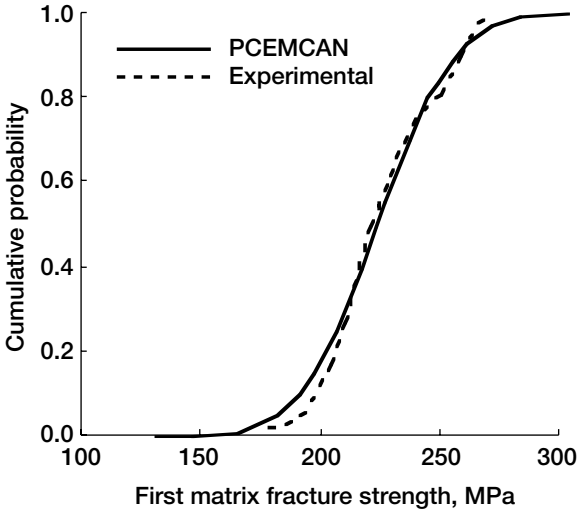

Comparison of the first matrix cracking strength cumulative-distribution-function simulation (PCEMCAN, Probabilistic Ceramic Matrix Composite Analyzer) with the experimental data for a $[0]_8$ SCS–6/RBSN composite laminate.

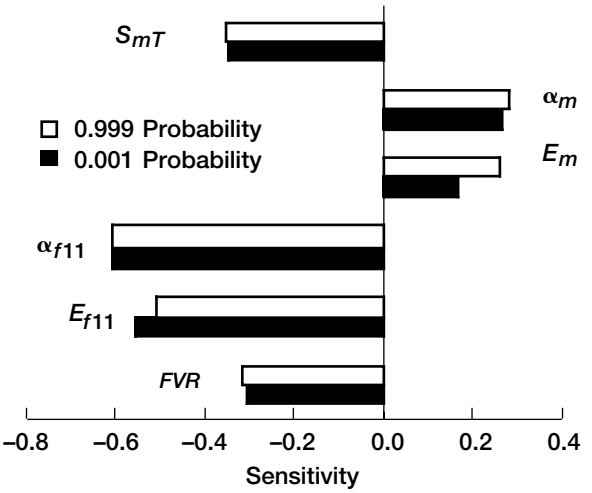

Sensitivity of the first matrix cracking strength to the primitive random variables of a $[0]_8$ SCS–6/RBSN composite laminate. Matrix tensile strength, S_{mT}; fiber coefficient of thermal expansion, α_{f11}; fiber longitudinal modulus, E_{f11}; fiber volume ratio, FVR.

factors. This approach often yields overly conservative designs, thereby reducing the potential of many advanced composite materials.

Work is underway at the NASA Lewis Research Center to incorporate the probabilistic distribution of material-behavior and fabrication-related parameters into the micromechanics and macromechanics of CMC's. The primary objective of this work was to develop an efficient computational design tool that could account for all the uncertainties in a more rigorous and formal manner, providing overall composite properties and their probabilistic distributions.

Therefore, we combined the CMC analysis embedded in the CEMCAN (Ceramic Matrix Composite Analyzer) computer code with the fast probability integration (FPI) techniques available in the NESSUS (Numerical Evaluation of Stochastic Structures Under Stress) code. CEMCAN provides functional relationships that tie the constituent properties and other geometry- and fabrication-related parameters to the overall composite properties. Fast probability integration is used to perform probabilistic analyses by utilizing the properties generated by CEMCAN. The results are cumulative distribution functions (CDF's) and probability density functions (PDF's) for the ply and laminate properties of the CMC. This technique is more efficient than a standard Monte-Carlo technique, where a large number of simulations are needed to generate a cumulative distribution function. The probabilistic sensitivities of the output variables with respect to inherent scatter in basic variables are obtained as a byproduct of the fast probability integration analyses. This provides very useful information to design and test engineers in evaluating the importance of variables that control the scatter in an overall property. The accompanying figures show sample results from the analyses.

Glenn contact:
Dr. Pappu L.N. Murthy, 216–433–3332,
Pappu.L.Murthy@grc.nasa.gov

University of Toledo contact:
Subodh K. Mital, 216–433–3261,
Subodh.K.Mital@grc.nasa.gov

CEMCAN Software Enhanced for Predicting the Properties of Woven Ceramic Matrix Composites

Major advancements are needed in current high-temperature materials to meet the requirements of future space and aeropropulsion structural components. Ceramic matrix composites (CMC's) are one class of materials that are being evaluated as candidate materials for many high-temperature applications. For example, combustor liners made of these materials can withstand very high temperatures. Furthermore, they can be operated uncooled, thereby improving engine performance

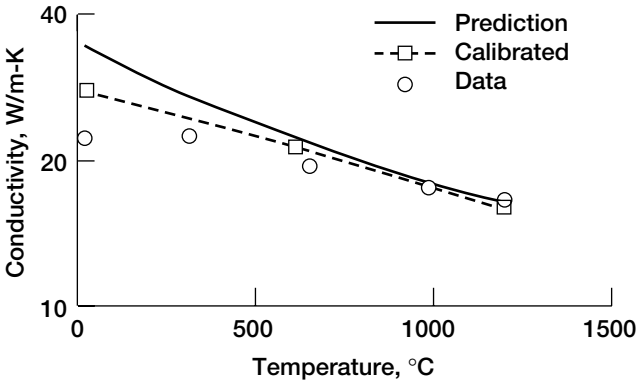

Through-the-thickness thermal conductivity. Constituents: F–34.[1]

[1]A set of constituents that leads to an overall fiber volume ratio of 34 vol % in the resulting composite.

as well as meeting or exceeding emission requirements. Past efforts to improve the performance of CMC's focused primarily on improving the properties of the fiber, interfacial coatings, and matrix constituents as individual phases. Design and analysis tools must take into consideration the complex geometries, microstructures, and fabrication processes involved in these composites and must allow the composite properties to be tailored for optimum performance. Major accomplishments during the past year include the development and inclusion of woven CMC micromechanics methodology into the CEMCAN (Ceramic Matrix Composites Analyzer) computer code.

Woven composite analysis, which is based on micromechanics techniques, is applicable to generalized two-dimensional woven architectures. The technique can account for the complex microstructure of these composites (i.e., the distribution and the volume fraction of the multiple constituent phases that these advanced composites are now employing). Such an analysis tool is useful for preliminary screening of new candidate materials and to help material developers perform tradeoff studies by evaluating different fiber architectures, constituents, and their volume fractions.

The code enables one to calibrate a consistent set of constituent properties as a function of temperature with the aid of experimentally measured data. Such properties, though hard to find, are quite useful in computational design and analysis. With the aid of this code, the properties of an advanced five-harness SiC/SiC composite were predicted as a function of temperature. However, we realized that there were still some issues regarding the constituent properties at high temperatures and the confidence that can be put in these properties. The composite property predictions were compared with measured data available from the High-Speed Research (HSR) program to create calibrated constituent properties as a function of temperature. This information is very useful for material developers and design engineers. Such analytical tools can be used to predict the complete set of material properties needed by design engineers, whereas only a handful of them can be measured experimentally. In the figure, the through-the-thickness thermal conductivity of an advanced SiC/SiC composite is shown as a function of temperature. The predictions are shown for the initially assumed constituent properties as well as for the calibrated set of constituent properties with the measured data.

Glenn contact:
Dr. Pappu L.N. Murthy, 216–433–3332,
Pappu.L.Murthy@grc.nasa.gov

University of Toledo contact:
Subodh K. Mital, 216–433–3261,
Subodh.K.Mital@grc.nasa.gov

GENOA–PFA: Progressive Fracture in Composites Simulated Computationally

GENOA–PFA is a commercial version of the Composite Durability Structural Analysis (CODSTRAN) computer program that simulates the progression of damage ultimately leading to fracture in polymer-matrix-composite (PMC) material structures under various loading and environmental conditions. GENOA–PFA offers several capabilities not available in other programs developed for this purpose, making it preferable for use in analyzing the durability and damage tolerance of complex PMC structures in which the fiber reinforcements occur in two- and three-dimensional weaves and braids.

GENOA–PFA implements a progressive-fracture methodology based on the idea that a structure fails when flaws that may initially be small (even microscopic) grow and/or coalesce to a critical dimension where the structure no longer has an adequate safety margin to avoid catastrophic global fracture. Damage is considered to progress through five stages: (1) initiation, (2) growth, (3) accumulation (coalescence of propagating flaws), (4) stable propagation (up to the critical dimension), and (5) unstable or very rapid propagation (beyond the critical dimension) to catastrophic failure. The computational simulation of progressive failure involves formal procedures for identifying the five different stages of damage and for relating the amount of damage at each stage to the overall behavior of the deteriorating structure.

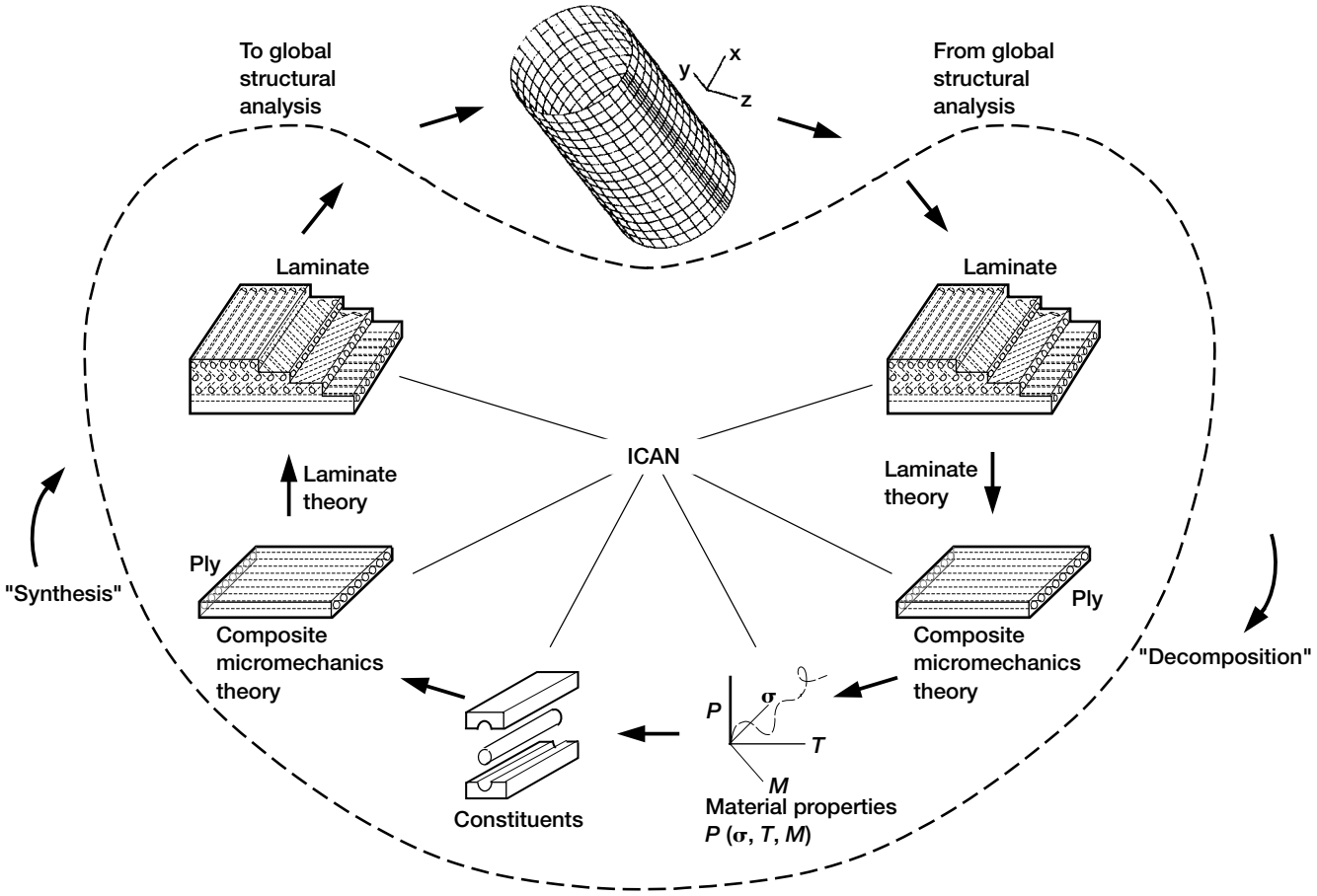

Simulation of composite damage and fracture propagation via CODSTRAN (where M is moisture; P, property; T, temperature; and σ, stress).

In GENOA–PFA, mathematical modeling of the composite physical behavior involves an integration of simulations at multiple, hierarchical scales ranging from the macroscopic (lamina, laminate, and structure) to the microscopic (fiber, matrix, and fiber/matrix interface), as shown in the figure. The code includes algorithms to simulate the progression of damage from various source defects, including (1) through-the-thickness cracks and (2) voids with edge, pocket, internal, or mixed-mode delaminations.

Some of the salient features of the GENOA–PFA software follow:

(1) Inclusion of the material's nonlinearities through periodic updates of the stiffness and inclusion of geometric nonlinearities through Lagrangian updating

(2) Simulation of the initiation and growth of cracks and of the ultimate failure of the composite under static, cyclic, creep, and impact loads

(3) Identification of the fractional contributions of various possible composite failure modes involved in critical damage events, and determination of the sensitivities of failure modes to such design parameters as fiber volume fractions, ply thicknesses, fiber orientations, and adhesive bond thicknesses

Glenn contacts:
Dr. Pappu L.N. Murthy, 216–433–3332,
Pappu.L.Murthy@grc.nasa.gov; and
Dr. Christos C. Chamis, 216–433–3252,
Christos.C.Chamis@grc.nasa.gov

Special recognition: 1999 Software of the Year Award

CARES/*Life* Ceramics Durability Evaluation Software Used for Mars Microprobe Aeroshell

The CARES/*Life* computer program, which was developed at the NASA Lewis Research Center, predicts the probability of a monolithic ceramic component's failure as a function of time in service. The program has many features and options for materials evaluation and component design. It couples commercial finite element programs—which resolve a component's temperature and stress distribution—to reliability evaluation and fracture mechanics routines for modeling strength-limiting defects. These routines are based on calculations of the probabilistic nature of the brittle material's strength. The capability, flexibility, and uniqueness of CARES/*Life* has attracted many users representing a broad range of interests and has resulted in numerous awards for technological achievements and technology transfer.

One noteworthy highlight was the use of CARES/*Life* to assess the survivability of the Mars Microprobe Aeroshell from launch-induced stresses. When the two Mars Microprobes piggyback aboard the Mars Surveyor '98 Lander (scheduled for launch in January 1999), they will be encased in basketball-sized, protective aeroshells made of silicon carbide. These aeroshells will free fall through the Martian atmosphere and crash into the polar surface. Shattering upon impact, the shells will release a miniature science probe designed to determine the presence of water ice. Although the shells are designed to shatter on Mars, they must, nonetheless, survive the high stresses associated with the launch. Analysis with CARES/*Life* indicated a high likelihood that the shells will remain intact after launch.

A key to maintaining interest in CARES/*Life* has been to actively maintain and promote the program as well as to enhance the program's ease of use. Toward this end, ANSCARES 2.0 was created. This computer program couples CARES/*Life* to the ANSYS finite element analysis program. Most noteworthy is that ANSCARES 2.0 contains an automatic surface recognition feature that frees CARES/*Life* users from manually modeling component surfaces. The majority of CARES/*Life* customers are also ANSYS users, so upgrading the links between the two codes was an imperative goal.

For more information, visit NASA Lewis' Life Prediction Branch:
http://www.grc.nasa.gov/WWW/LifePred
Or go directly to CARES:
http://www.grc.nasa.gov/WWW/LifePred/BrittleStructures/CARES/

Glenn contacts:
Noel N. Nemeth, 216–433–3215, Noel.N.Nemeth@grc.nasa.gov;
Lynn M. Powers, 216–433–8374, Lynn.M.Powers@grc.nasa.gov; and
Lesley A. Janosik, 216–433–5160, Lesley.A.Janosik@grc.nasa.gov

Special recognition: American Ceramic Society's 1997 Corporate Technical Achievement Award was given jointly to NASA Lewis and Philips Display Components Company for the development and commercialization of new design, durable, lightweight, and environmentally friendly television picture tubes.

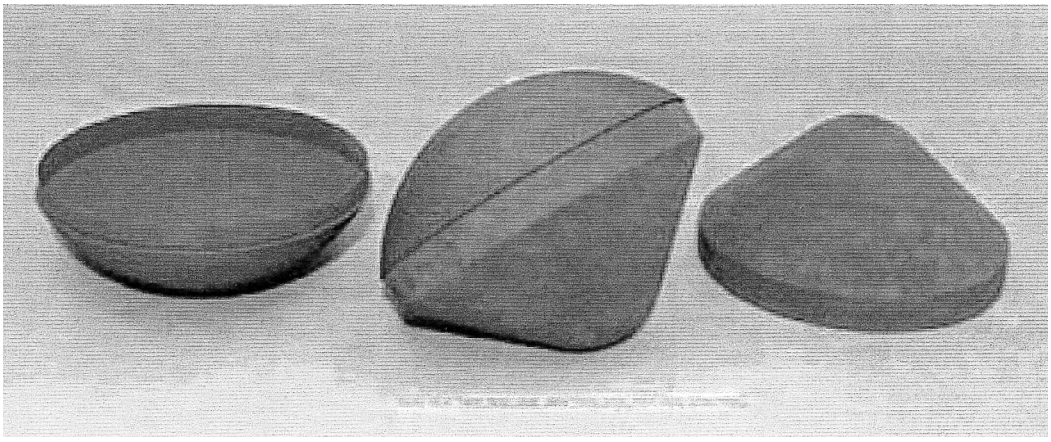

Mars Microprobe Aeroshell made of heat-resistant silicon carbide material. (Copyright Jet Propulsion Laboratory; used with permission.)

CARES/*Life* Ceramics Durability Evaluation Software Enhanced for Cyclic Fatigue

The CARES/*Life* computer program predicts the probability of a monolithic ceramic component's failure as a function of time in service. The program has many features and options for materials evaluation and component design. It couples commercial finite element programs—which resolve a component's temperature and stress distribution—to reliability evaluation and fracture mechanics routines for modeling strength-limiting defects. The capability, flexibility, and uniqueness of CARES/*Life* have attracted many users representing a broad range of interests and has resulted in numerous awards for technological achievements and technology transfer.

Recent work with CARES/*Life* was directed at enhancing the program's capabilities with regards to cyclic fatigue. Only in the last few years have ceramics been recognized to be susceptible to enhanced degradation from cyclic loading. To account for cyclic loads, researchers at the NASA Lewis Research Center developed a crack growth model that combines the Power Law (time-dependent) and the Walker Law (cycle-dependent) crack growth models. This combined model has the characteristics of Power Law behavior (decreased damage) at high *R* ratios (minimum load/maximum load) and of Walker law behavior (increased damage) at low *R* ratios. In addition, a parameter estimation methodology for constant-amplitude, steady-state cyclic fatigue experiments was developed using nonlinear least squares and a modified Levenberg-Marquardt algorithm. This methodology is used to give best estimates of parameter values from cyclic fatigue specimen rupture data (usually tensile or flexure bar specimens) for a relatively small number of specimens. Methodology to account for runout data (unfailed specimens over the duration of the experiment) was also included.

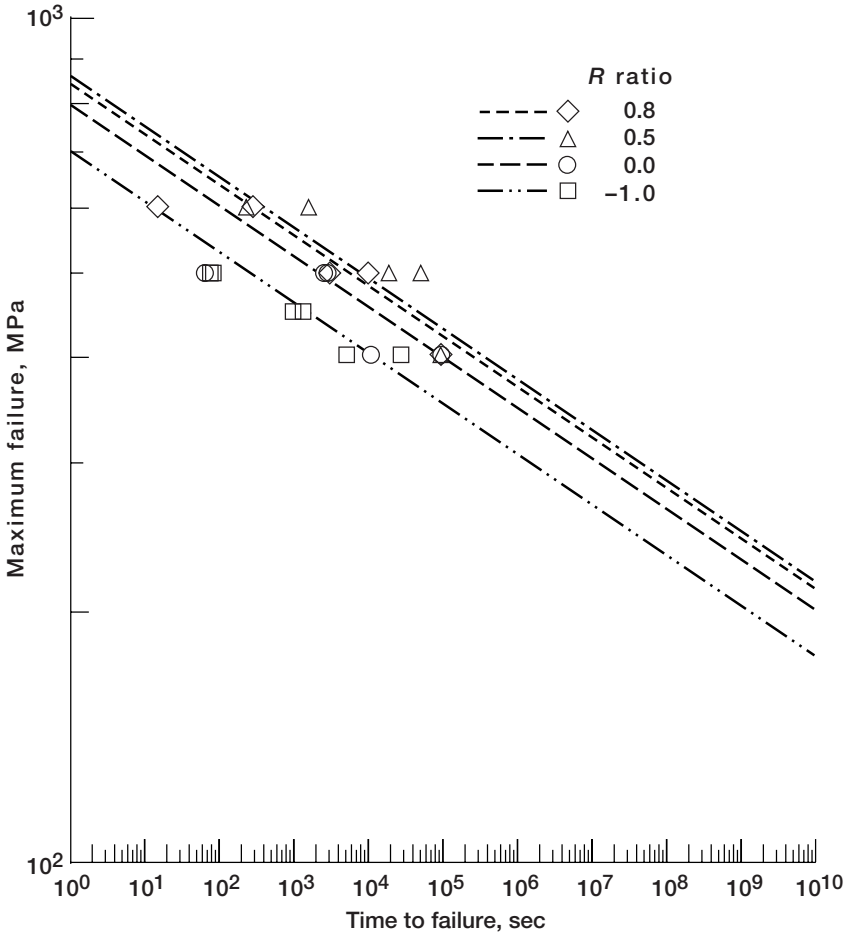

Median regression lines for partially stabilized zirconia tensile specimens with various R-ratios (combined law model).

The graph shows an example of this regression technique for tensile specimen data for partially stabilized zirconia. Data for various *R* ratios and their corresponding median regression lines are shown for the combined fatigue law model. Note that at lower *R* ratios (0 and –1) the combined law predicted increased material strength degradation, whereas at higher *R* ratios (0.5 and 0.8) this trend was reversed.

Find out more on the World Wide Web: http://www.grc.nasa.gov/WWW/LPB/cares/life/software.html

Glenn contacts:
Noel N. Nemeth, 216–433–3215, Noel.N.Nemeth@grc.nasa.gov;
Lynn M. Powers, 216–433–8374, Lynn.M.Powers@grc.nasa.gov; and
Lesley A. Janosik, 216–433–5160, Lesley.A.Janosik@grc.nasa.gov

Special recognition:
Numerous awards including 1998 EDI (Enterprise Development Inc.) Innovation Award given to Lewis for the development of CARES

Continuum Damage Mechanics Used to Predict the Creep Life of Monolithic Ceramics

Significant improvements in propulsion and power generation for the next century will require revolutionary advances in high-temperature materials and structural design. Advanced ceramics are candidate materials for these elevated temperature applications. High-temperature and long-duration applications of monolithic ceramics can place their failure mode in the creep rupture regime.

An analytical methodology in the form of the integrated design program—Ceramics Analysis and Reliability Evaluation of Structures/*Creep* (CARES/*Creep*) has been developed by the NASA Lewis Research Center to predict the life of ceramic structural components subjected to creep rupture conditions. This program utilizes commercially available finite element packages and takes into account the transient state of stress and creep strain distributions (stress relaxation as well as the asymmetric response to tension and compression). The creep life of a component is discretized into short time steps, during which the stress distribution is assumed constant. Then, the damage is calculated for each time step on the basis of a modified Monkman-Grant (MMG) creep rupture criterion. The cumulative damage is subsequently calculated as time elapses in a manner similar to Miner's rule for cyclic fatigue loading. Failure is assumed to occur when the normalized cumulative damage at any point in the component reaches unity. The corresponding time is the creep rupture life for that component.

To account for the deteriorating state of the material due to creep damage (cavitation) as time elapses as well as the effects of tertiary creep, we implemented a creep life prediction methodology based on a modified form of the Kachanov-Rabotnov Continuum Damage Mechanics (CDM) theory. In this theory, the uniaxial creep rate is described in terms of stress, temperature, time, and the current state of material damage. This scalar damage state parameter is basically an abstract measure of the current state of creep in the material. The damage rate is assumed to vary with stress, temperature, time, and the current state of damage itself. Multiaxial creep and creep rupture formulations of the CDM approach have been characterized.

The CARES/*Creep* code predicts the deterministic life of a ceramic component. Future work involves the role of probabilistic models in this design process. The complete package will predict the life of monolithic ceramic components, using simple, uniaxial creep laws to account for multiaxial creep loading. The combination of the CARES/*Creep* and CARES/*Life* codes gives design engineers the tools necessary to predict component life for the two dominant delayed failure mechanisms—creep and slow crack growth.

More information is available on the World Wide Web:
http://www.grc.nasa.gov/WWW/LifePred/BrittleStructures/CARES/creep/

Glenn contacts:
Lynn M. Powers, 216–433–8374, Lynn.M.Powers@grc.nasa.gov, and
Lesley A. Janosik, 216–433–5160, Lesley.A.Janosik@grc.nasa.gov

Single-Transducer, Ultrasonic Imaging Method for High-Temperature Structural Materials Eliminates the Effect of Thickness Variation in the Image

NASA Lewis Research Center's Life Prediction Branch, in partnership with Sonix, Inc., and Cleveland State University, recently advanced the development of, refined, and commercialized an advanced nondestructive evaluation (NDE) inspection method entitled the *Single Transducer Thickness-Independent Ultrasonic Imaging Method* (Roth, 1996 and 1997; and Roth et al., 1996a and 1996b). Selected by *R&D Magazine* as one of the 100 most technologically significant new products of 1996, the method uses a single transducer to eliminate the superimposing effects of thickness variation in the ultrasonic images of materials. As a result, any variation seen in the image is due solely to microstructural variation. This nondestructive method precisely and accurately characterizes material gradients (pore fraction, density, or chemical) that affect the uniformity of a material's physical performance (mechanical, thermal, or electrical). Advantages of the method over conventional ultrasonic imaging include (1) elimination of machining costs (for precision thickness control) during the quality control stages

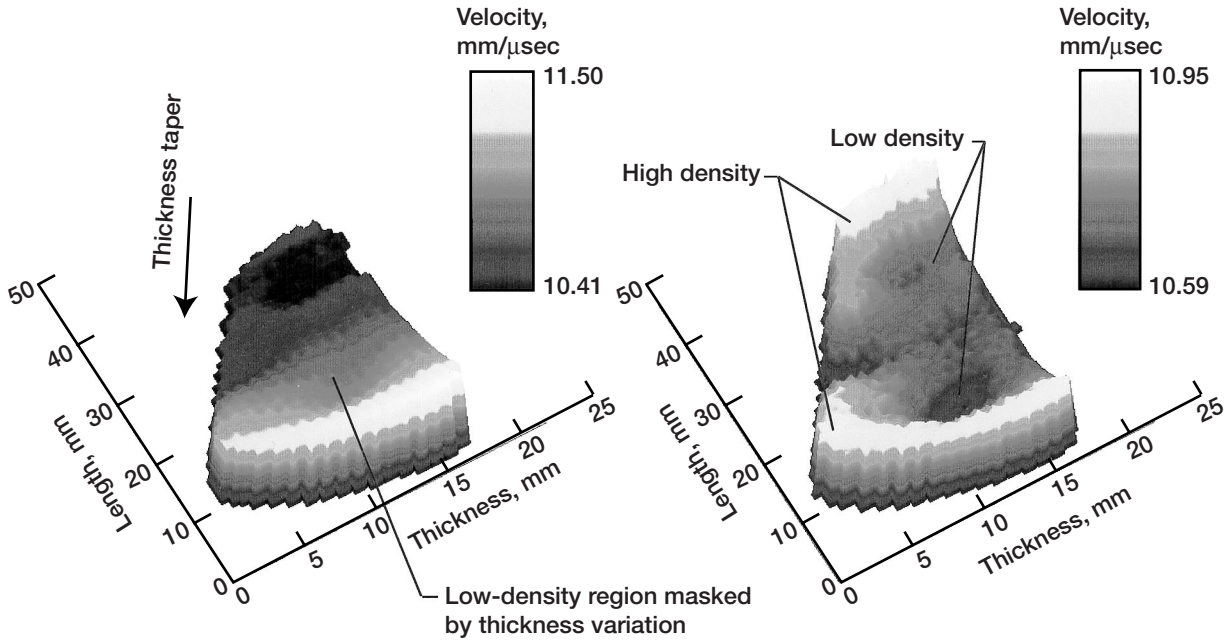

Conventional ultrasonic imaging versus thickness-independent ultrasonic imaging for silicon nitride monolithic ceramic with pore fraction variations and 10-percent thickness variation. Left: Conventional ultrasonic image. Thickness effect not eliminated; defects not revealed. Right: New thickness-independent ultrasonic imaging. Thickness eliminated; defects revealed. Images are shown in color in the online version of this article (http://www.grc.nasa.gov/WWW/RT1997/5000/5920roth.htm).

of material processing and development and (2) elimination of labor costs and subjectivity involved in further image processing and image interpretation.

At NASA Lewis, the method has been used primarily for accurate inspections of high-temperature structural materials including monolithic ceramics, metal matrix composites, and polymer matrix composites. Data were published this year for platelike samples, and current research is focusing on applying the method to tubular components.

The initial publicity regarding the development of the method generated 150 requests for further information from a wide variety of institutions and individuals including the Federal Bureau of Investigation (FBI), Lockheed Martin Corporation, Rockwell International, Hewlett Packard Company, and Procter & Gamble Company. In addition, NASA has been solicited by the 3M Company and Allison Abrasives to use this method to inspect composite materials that are manufactured by these companies.

Glenn contact:
Dr. Don J. Roth, 216–433–6017, Don.J.Roth@grc.nasa.gov

Special recognition: 1996 R&D 100 Award

Novel Method Used to Inspect Curved and Tubular Structural Materials

At the NASA Lewis Research Center, a technique for the ultrasonic characterization of plates has been extended to tubes and to curved structures in general. In this technique, one performs measurements that yield a thickness-independent value of the local through-the-thickness speed of sound in a specimen. From such measurements at numerous locations across the specimen, one can construct a map of velocity as a function of location. The gradients of velocity indicated by such a map indicate local through-the-thickness-averaged microstructural parameters that affect the speed of sound. Such parameters include the pore volume fraction, mass density, fiber volume fraction (in the case of a composite material), and chemical composition. Apparatus was designed to apply the technique to tubular and other curved specimens.

The specimen was mounted on a horizontal turntable in a water tank, with its axis vertical and coincident with the turntable axis. A machined metal reflector plate narrow enough to fit within the inner diameter of the specimen was suspended vertically from above and positioned inside the specimen about 1 cm from the inner tube wall.

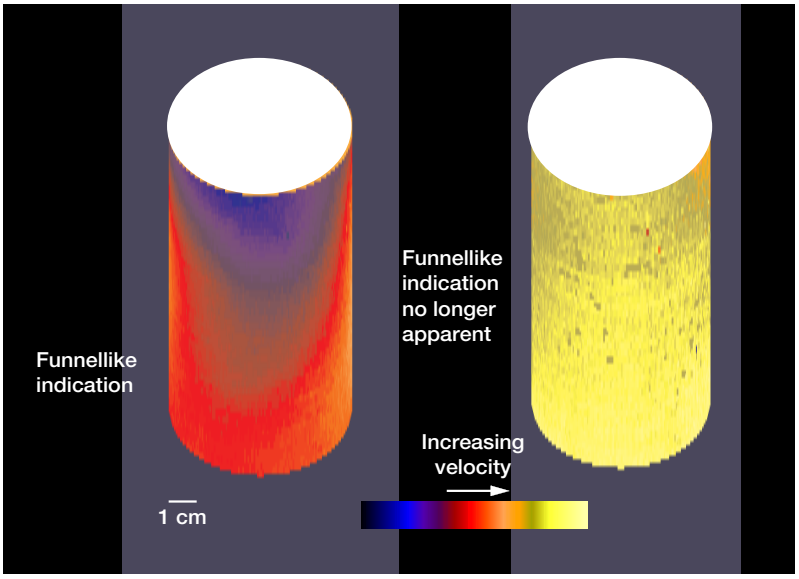

Apparent and thickness-independent velocity images of silicon nitride tube as decaled onto tubular models. Baseline orientation. Left: Apparent velocity image. Right: Thickness-independent velocity image.

A horizontally oriented ultrasonic transducer was positioned outside the specimen, facing the reflector plate. Then, pulse/echo measurements were taken in basically the same manner as for the plate specimens. The transducer was translated vertically to obtain measurements at various axial positions (e.g., increments of 1 mm), and the turntable was rotated to obtain measurements at various azimuthal positions (e.g., increments of 1°).

The technique has been demonstrated in experiments on tubular specimens of mullite (silica/alumina), a polymer-matrix composite, a composite of SiC fibers in an SiC matrix, and a high-temperature structural grade of silicon nitride. Although the turntable, specimen, reflector plate, and transducer should be aligned as nearly perfectly as possible and the specimen should approximate a perfect round tube, it was observed that, in general, some misalignment and out of roundness can be tolerated. This is an advantage over peak-amplitude-based ultrasonic techniques in which measurements are altered drastically by refractive effects associated with out of roundness. The present technique made it possible to eliminate most of the effects of variations in tube-wall thicknesses upon velocity maps (through-the-thickness velocities as functions of axial and azimuthal positions). However, edge effects associated with discontinuous changes in thickness were not eliminated completely. In the case of the silicon nitride tube, differences between velocities at different locations were found to be correlated with differences between densities and pore volume fractions revealed by x-radiography and destructive metallographic analysis at those locations. The illustration shows the apparent (without thickness variation subtracted) and thickness-independent velocity images of the silicon nitride tube as decaled onto tubular models.

For more information about this research, visit us on the World Wide Web:
http://www.grc.nasa.gov/WWW/LPB/tiui/

Glenn contact:
Dr. Don J. Roth, 216–433–6017, Don.J.Roth@grc.nasa.gov

Special recognition: Part of the effort that received an R&D100 Award and the Federal Laboratory Consortium Excellence in Technology Transfer Award; to be featured on the cover of the International Journal of Materials Evaluation in 1998

New Technology—Large-Area Three-Dimensional Surface Profiling Using Only Focused Air-Coupled Ultrasound—Given 1999 R&D 100 Award

Surface topography, which significantly affects the performance of many industrial components, is normally measured with diamond-tip profilometry over small areas or with optical scattering methods over larger areas. To develop air-coupled surface profilometry, the NASA Glenn Research Center at Lewis Field initiated a Space Act Agreement with Sonix, Inc., through two Glenn programs, the Advanced High Temperature Engine Materials Program (HITEMP) and COMMTECH. The work resulted in quantitative surface topography profiles obtained using only high-frequency, focused ultrasonic pulses in air. The method is nondestructive, noninvasive, and noncontact, and it does not require light-reflective surfaces. Air surface profiling may be desirable when diamond-tip or laser-based methods are impractical, such as over large areas, when a significant depth range is required, or for curved surfaces. When the configuration is optimized, the method is reasonably rapid and all the quantitative analysis facilities are online, including two- and three-dimensional visualization, extreme value filtering (for faulty data), and leveling.

The method is simple and reproducible because it relies mainly on the knowledge of and the constancy of the velocity of sound through air. When the air transducer is scanned across the surface, it sends pulses to the sample surface, where they are reflected back along the same path as the incident wave. (We recommend an air transducer with a ~1-MHz nominal center frequency to generate the air pulses.) Time-of-flight images of the sample surface are acquired and converted to depth and surface profile images using the simple relation $d = V(t/2)$, where d is the distance, t is the time of flight, and V is the velocity of sound in air.

The system can resolve surface depression variations as small as 25 µm with 400-µm lateral resolution, is useable over a 1.4-mm vertical depth range, and can profile large areas limited only by the scan limits of the particular ultrasonic system. (The best-case depth resolution is 0.25-µm, which may be achievable with improved isolation from air currents and vibrations—both external vibrations and those due to motor or bridge assembly movement.) Results are shown for several proof-of-concept samples: plastic samples burned in microgravity on the STS–54 space shuttle mission and a partially coated, cylindrical ceramic composite sample. When compared with diamond-tip profiles and measurements from micrometers, the topographical representations for all the samples are impressive. Funding for this work came from the NASA HITEMP and COMMTECH programs and from Sonix, Inc.

Find out more about this research on the World Wide Web:
http://www.grc.nasa.gov/WWW/LPB/research/nde/rnd100.html

Glenn contact:
Dr. Don J. Roth, 216–433–6017, Don.J.Roth@grc.nasa.gov

Special recognition: 1999 R&D 100 Award

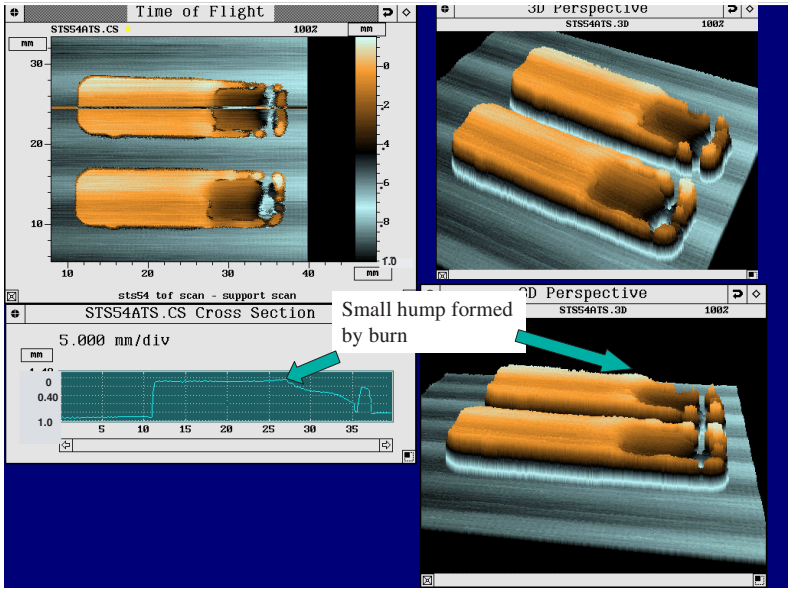

Air surface profiles for Burned Space Experiment samples. Left: Two-dimensional view and line profile across one scan line of top sample. Right: Three-dimensional views.

Composite Nozzle/Thrust Chambers Analyzed for Low-Cost Boosters

The Low Cost Booster Technology Program is an initiative to minimize the cost of future liquid engines by using advanced materials and innovative designs, and by reducing engine complexity. NASA Marshall Space Flight Center's 60K FASTRAC Engine is one example where these design philosophies have been put into practice. This engine burns a liquid kerosene/oxygen mixture. It uses a one-piece, polymer composite thrust chamber/nozzle that is constructed of a tape-wrapped silica phenolic liner, a metallic injector interface ring, and a filament-wound epoxy overwrap (figure on the left). This integral chamber/nozzle design minimizes engine operations costs because it simplifies engine refurbishment procedures.

A cooperative effort between NASA Lewis Research Center's Structures Division and Marshall is underway to perform a finite element analysis of the FASTRAC chamber/nozzle under all the loading and environmental conditions that it will experience during its lifetime. The chamber/nozzle is a complex composite structure. Of its three different materials, the two composite components have distinctly different fiber architectures and, consequently, require separate material model descriptions. Since the liner is tape wrapped, it is orthotropic in the nozzle global coordinates; and since the overwrap is filament wound, it is treated as a monoclinic material. Furthermore, the wind angle on the overwrap (figure on the right) varies continuously along the length of the chamber/nozzle. The angle is very shallow in the throat region and becomes steep toward the ends.

During early fabrication attempts, cracking of the liner posed a significant problem. The cracking was the result of residual stresses that developed during processing because of the large differences between the thermal expansion coefficients of the silica phenolic and the epoxy overwrap. The final figure (facing page) shows the tangential thermal expansion coefficient as a function of the axial position for both the liner and the overwrap. Although the liner tangential thermal expansion coefficient is constant with position, the overwrap thermal coefficient varies considerably along the length because of the varying wind angle.

A finite element analysis of the chamber/nozzle was performed under processing conditions. The results were instrumental in resolving the residual-stress cracking problem and helped to establish a representative analog using straight cylinders. The analyses verified that cylindrical analogs will duplicate the highest stress states in the nozzle, which occur at the nozzle throat. Furthermore, they helped to identify large discrepancies between the material strengths measured using the traditional dogbone configuration and the strengths measured in a cylindrical configuration.

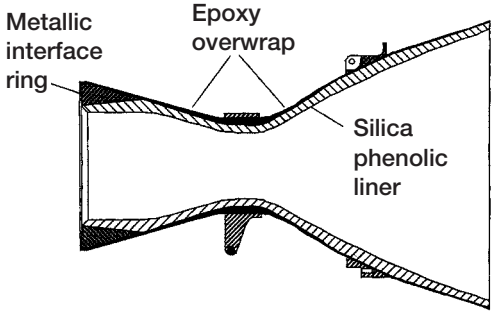

Thrust chamber/nozzle of 60K FASTRAC Engine.

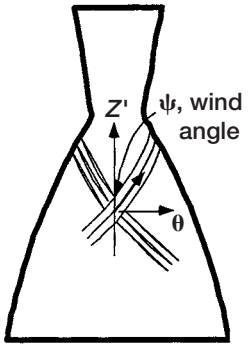

Thrust chamber/nozzle showing filament wind angles.

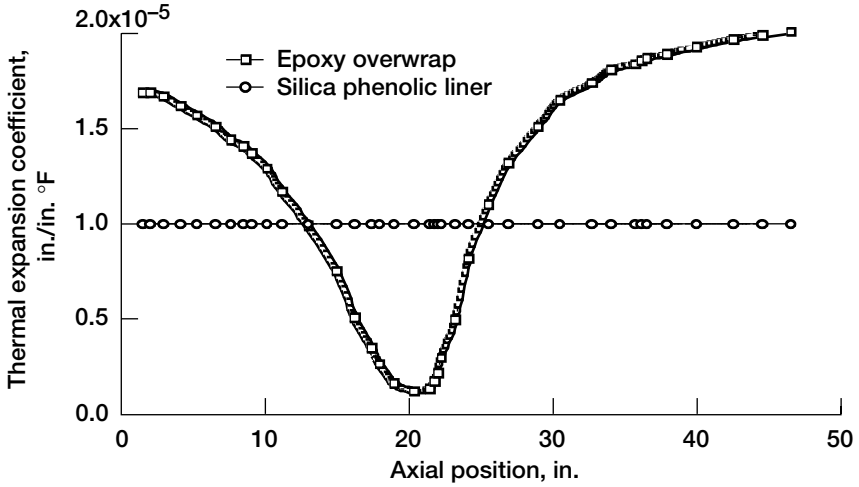

Tangential thermal expansion coefficient versus axial position.

Future analyses of the chamber/nozzle are planned to determine the residual stress levels for a variety of possible material systems, nozzle designs, and fiber architectures. The objective is to choose the optimal material system to minimize residual stresses. Furthermore, we plan to perform finite element analyses for all the loading and temperature conditions that the chamber/nozzle will experience during 60K FASTRAC Engine operation.

Glenn contact:
Roy M. Sullivan, 216–433–3249,
Roy.M.Sullivan@grc.nasa.gov

Structural Mechanics and Dynamics

Flutter Version of Propulsion Aeroelasticity Code Completed

NASA's Advanced Subsonic Technology (AST) Program seeks to develop new technologies to increase the fuel efficiency of commercial aircraft engines, improve the safety of engine operation, and reduce emissions and engine noise. For new designs of ducted fans, compressors, and turbines to achieve these goals, a basic aeroelastic requirement is that there should be no flutter or high resonant blade stresses in the operating regime. For verifying the aeroelastic soundness of the design, an accurate prediction/analysis code is required. Such a three-dimensional viscous propulsion aeroelastic code, named TURBO–AE, is being developed at the NASA Lewis Research Center. The development and verification of the flutter version of the TURBO–AE code (version 4) has been completed. Validation of the code is partially complete.

The TURBO–AE aeroelastic code is based on a three-dimensional unsteady aerodynamic Euler/Navier-Stokes turbomachinery code TURBO, developed previously under a grant from Lewis. This code can model viscous flow effects, which play an important role in certain aeroelastic problems such as flutter with flow separation, flutter at high loading conditions near the stall line (stall flutter), and flutter in the presence of shock and boundary-layer interaction. In the TURBO–AE code, the structural dynamics representation of the blade is based on a normal mode representation. Any finite-element analysis code can be used to calculate in-vacuum vibration modes and the associated natural frequency. As an alternative, experimental measurements of these vibration characteristics can be used.

A work-per-cycle approach is used to determine aeroelastic stability (flutter). With this approach, the motion of the blade is prescribed to be a harmonic vibration in a specified in-vacuum normal mode. The work done by aerodynamic forces on the vibrating blade during a cycle of vibration is calculated. If this work is positive, the blade is dynamically unstable, because it will extract energy from the flow, leading to an increase in the amplitude of the blade's oscillation.

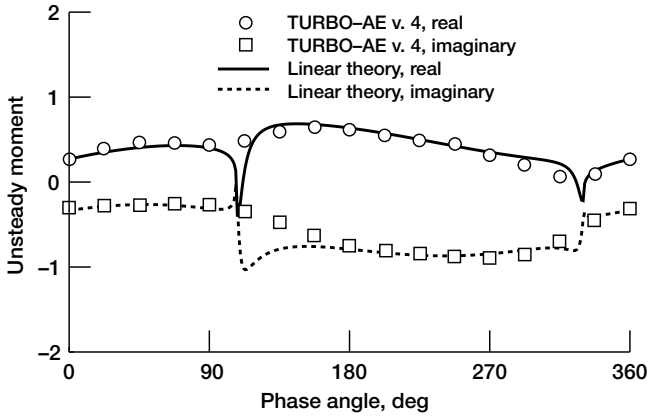

Unsteady moment for the torsional blade vibrations of a helical fan.

As part of the verification of the TURBO–AE code, calculations were performed for a helical fan test configuration. This configuration was used to compare the code to two-dimensional linear potential (classical linear/flat plate) theory. Results from the midspan of the blade undergoing torsional vibrations were compared with linear theory results for the pitching motion of a flat plate cascade. Excellent agreement was observed for this test case, providing a fundamental verification of the TURBO–AE code.

TURBO–AE code will provide a useful aeroelastic prediction/analysis capability for engine manufacturers. It will reduce design cycle times by allowing new blade designs to be verified for aeroelastic soundness before blades are built and tested. Using this prediction capability, it will be possible to build thinner, lighter, and faster rotating blades without encountering aeroelastic problems like stall flutter and high-cycle fatigue due to forced vibrations.

Glenn contacts:
Milind A. Bakhle, 216–433–6037, Milind.A.Bakhle@grc.nasa.gov;
Rakesh Srivastava, 216–433–6045, Rakesh.Srivastava@grc.nasa.gov; and
George L. Stefko, 216–433–3920, George.L.Stefko@grc.nasa.gov

Propulsion Aeroelastic Analysis Developed for Flutter and Forced Response

The NASA Glenn Research Center at Lewis Field develops new technologies to increase the fuel efficiency of aircraft engines, improve the safety of engine operation, reduce emissions, and reduce engine noise. With the development of new designs for fans, compressors, and turbines to achieve these goals, the basic aeroelastic requirements are that there should be no flutter (self-excited vibrations) or high resonant blade stresses (due to forced response) in the operating regime. Therefore, an accurate prediction and analysis capability is required to verify the aeroelastic soundness of the designs. Such a three-dimensional viscous propulsion aeroelastic analysis capability has been developed at Glenn with support from the Advanced Subsonic Technology (AST) program.

This newly developed aeroelastic analysis capability is based on TURBO, a three-dimensional unsteady aerodynamic Reynolds-averaged Navier-Stokes turbomachinery code developed previously under a grant from Glenn. TURBO can model the viscous flow effects that play an important role in certain aeroelastic problems—such as flutter with flow separation, flutter at high loading conditions near the stall line (stall flutter), flutter in the presence of shock and boundary-layer interaction, and forced response due to wakes and shock impingement. In aeroelastic analysis, the structural dynamics representation of the blades is based on normal modes. A finite-element analysis code is used to calculate these in-vacuum vibration modes and the associated natural frequencies.

In an aeroelastic analysis using the TURBO code, flutter and forced response are modeled as being uncoupled. To calculate if a blade row will flutter, one prescribes the motion of the blade to be a harmonic vibration in a specified in-vacuum normal mode. An aeroelastic analysis preprocessor is used to generate the displacement field required for the analysis. The work done by aerodynamic forces on the vibrating blade during a cycle of vibration is calculated. If this work is positive, the blade is dynamically unstable, since it will extract energy from the flow, leading to an increase in the blade's oscillation amplitude. The forced-response excitations on a blade row are calculated by modeling the flow through two adjacent blade rows using the TURBO code. The blades are assumed to be rigid. As an option, a single blade row can be modeled with the upstream blade row influence represented by a time-varying disturbance (gust) at the inlet boundary. The unsteady forces on a blade row from such analyses are used in a structural analysis along with the blade structural dynamics characteristics and aerodynamic damping associated with blade vibration to calculate the resulting dynamic stresses on the blade.

As part of the verification and validation of the aeroelastic analysis capability in TURBO, flutter and forced-response calculations were performed in collaboration with engine companies for various standard configurations and industry configurations. The aeroelastic analysis capability in the TURBO code will allow engine manufacturers to reduce design cycle times by allowing new blade designs to be verified for aeroelastic soundness before they are built and tested. With this prediction capability, it will be possible to build thinner, lighter, and faster rotating blades without encountering aeroelastic problems like stall flutter and high-cycle fatigue due to forced vibrations.

Glenn contacts:
Milind A. Bakhle, 216–433–6037,
Milind.A.Bakhle@grc.nasa.gov;
Rakesh Srivastava, 216–433–6045,
Rakesh.Srivastava@grc.nasa.gov; and
George L. Stefko, 216–433–3920,
George.L.Stefko@grc.nasa.gov

Stability of the Tilt Modes of an Actively Controlled Flywheel Analyzed

Applications of strongly gyroscopic rotors are becoming important, including flywheels for terrestrial and space energy storage and various attitude control devices for spacecraft. Some of these applications, especially the higher speed ones for energy storage, will have actively controlled magnetic bearings. These bearings will be required where speeds are too high for conventional bearings, where adequate lubrication is undesirable or impossible, or where bearing losses must be minimized for efficient energy storage.

Flywheel rotors are highly gyroscopic, and above some speed that depends on the bandwidth of the feedback system, they always become unstable in an actively controlled magnetic bearing system.

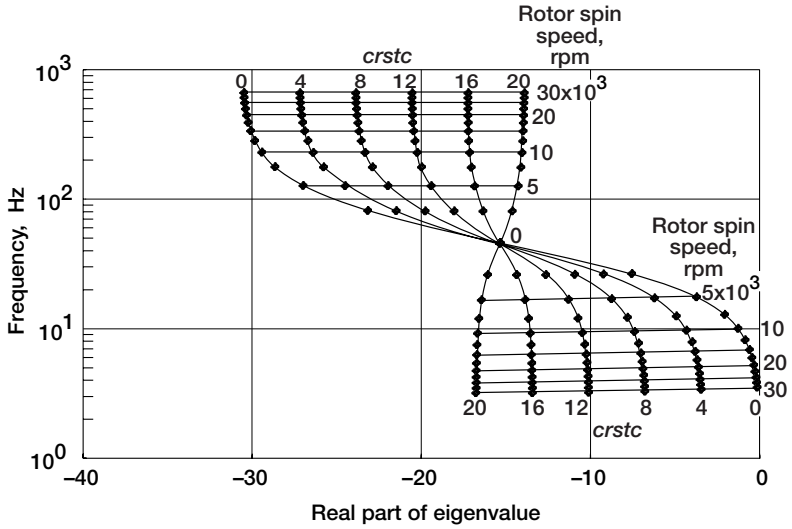

Effect of position cross coupling with Ω factor; five corners at 50 kHz.

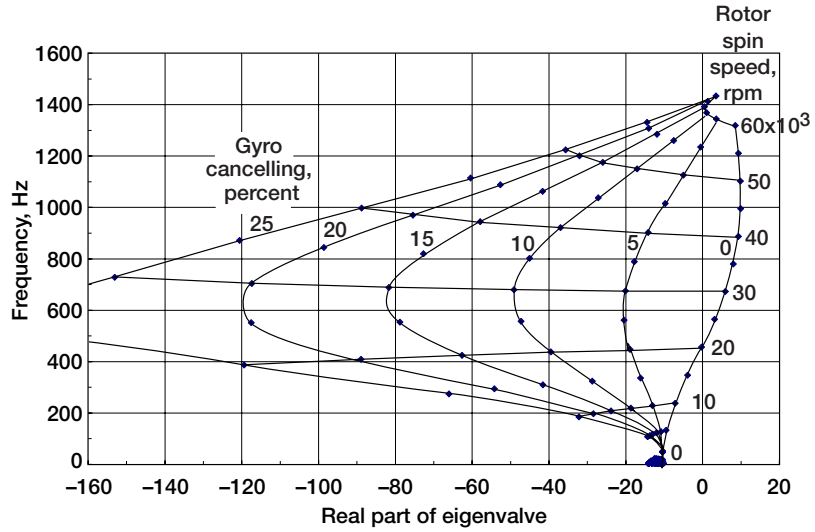

Effect of small-percent gyro canceling with position cross coupling; five corners at 2 kHz; crstc, 12.

To assess ways to prevent instability until speeds well above the desired operating range, researchers at the NASA Lewis Research Center used a commercial controls code to calculate the eigenvalues of the tilt modes of a rigid gyroscopic rotor supported by active magnetic bearings. The real part of the eigenvalue is the negative of the damping of the mode, and the imaginary part is approximately equal to the mode's frequency.

A modal controller was presumed in which the pure translation and pure tilt modes were separated. We addressed only the tilt modes. The controller included simple proportional-derivative (PD) gains for each tilt angle and proportional and derivative cross-coupling gains. Bandwidths were imposed in the control loop to represent the various phase lags of a magnetic bearing system. The effects of bandwidths, cross-axis proportional gain, and cross-axis derivative gain (gyroscopic canceling) were considered individually and in combination to show the qualitative and quantitative effects of each. Both cross-axis gains were "scheduled" by being multiplied by the rotor spin speed Ω since they were needed only to counteract the effects of gyroscopic torques.

The tilt mode of a nonspinning rotor becomes two modes under rotation: one mode (called the forward whirl mode) goes up in frequency with the rotor speed; the other (called the backward whirl mode) goes down. We found that cross-axis proportional gain, *crstc*, increases the damping of the backward whirl mode, which is otherwise a poorly damped, low-frequency mode at high rotor spin speed (see the top figure, which was calculated with high bandwidth). The point common to all curves is for zero rpm. Damping increases toward the left. This gain (*crstc*) decreases the damping of the forward whirl mode, which is otherwise better damped, but which could be subject to strong forcing by rotor unbalance as rotor speed increases (top figure). Cross-axis derivative gain (also called gyroscopic cancelling) can improve the forward whirl mode damping but has little effect on the backward whirl mode. An appropriate combination of these cross-axis gains can result in a closed-loop system that is stable over a wide speed range without additional gain scheduling, as shown in the bottom figure, which was calculated with more realistic bandwidths. Again, the point common to all curves is for zero rpm. Modes to the right of the vertical axis are unstable; modes to the left are progressively more stable as damping increases. Note that with 10-percent gyroscopic canceling, for example, the flywheel would be stable to nearly 60 000 rpm.

Glenn contacts: Dr. Gerald V. Brown, 216–433–6047, Gerald.V.Brown@grc.nasa.gov; and Albert F. Kascak, 216–433–6024, Albert.F.Kascak@grc.nasa.gov

Neural Network Control of a Magnetically Suspended Rotor System

Magnetic bearings offer significant advantages because they do not come into contact with other parts during operation, which can reduce maintenance. Higher speeds, no friction, no lubrication, weight reduction, precise position control, and active damping make them far superior to conventional contact bearings. However, there are technical barriers that limit the application of this technology in industry. One of them is the need for a nonlinear controller that can overcome the system nonlinearity and uncertainty inherent in magnetic bearings. At the NASA Lewis Research Center, a neural network was selected as a nonlinear controller because it generates a neural model without any detailed information regarding the internal working of the magnetic bearing system. It can be used even for systems that are too complex for an accurate system model to be derived. A feed-forward architecture with a back-propagation learning algorithm was selected because of its proven performance, accuracy, and relatively easy implementation.

The neural net plant emulator was first trained to emulate a theoretical model of the nonlinear plant. A discrete theoretical model of the plant dynamics in state-space notation was used to choose the present states of the plant (rotor displacement and velocity) and the plant input (control current) as the input to the emulator. The next states, the rotor displacement and velocity after one sample time, were chosen as the output. During the learning procedure, we minimized the errors between the actual network output and the desired values by upgrading the weights. After training, the neural emulator perfectly predicted the next states (delayed by one sample time) of the magnetic bearing system for the current states and control force, which were not in the training sample data.

Our second step was to use the trained neural emulator to train a neural net controller to make the whole system meet conventional performance specifications on such parameters as the bandwidth, settling time, and overshoot. We wanted the controller to take the current magnetic bearing states $\vec{x}(t)$ and the demand r as input parameters, and to output a control force $u(t)$ to the magnetic bearing system. These current state values should make the magnetic bearing's next state vector $\vec{x}(t+1)$ be identical to that defined by the desired linear reference system, satisfying performance specifications in either the frequency or time domain.

The left side of the following figure is the Bode plot of a simple second-order linear reference model derived from frequency domain specifications; the right side shows the closed-loop magnetic bearing system after training. They are almost identical even after 200 training epochs. Another neural controller based on time domain specifications was trained and tested by simulating its response for the initial

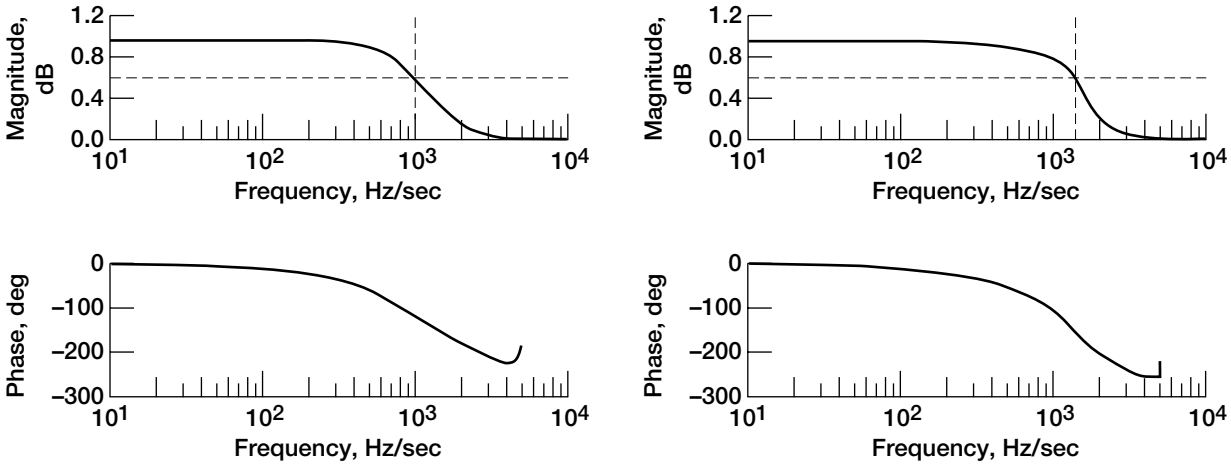

Bode plots of desired and neural network models in frequency domain, showing averaged transfer function. Left: Simple second-order linear reference model for a frequency domain of peak magnitude, m_p, 1.1, and cutoff frequency, w_c, 1000 Hz. Right: Trained closed-loop system.

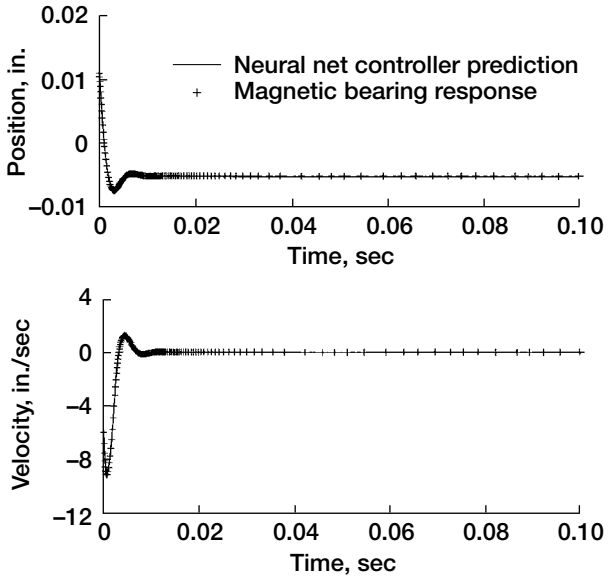

Desired and actual response in time domain. Top: Simple second-order linear reference model response for percent of overshoot, P_0, 4.3 percent, and settling time, T_s, 0.0001 sec. Bottom: Trained closed-loop system response for initial position, x_0, 0.0011 in.; initial velocity, x_0, –6 in./sec; and reference position, r_f, –0.005 in.

condition and comparing the results to the actual magnetic bearing response (see the figure above). The neural net controller was so accurate that it perfectly overlapped the magnetic bearing response (+ markers).

In summary, a neural network controller that circumvents the magnetic bearing's nonlinearity was developed and successfully demonstrated on a small Bentley-Nevada magnetic bearing rig. The neural plant emulator and neural controller were so accurate that the neural network controller did a near perfect job of making the nonlinear magnetic bearing system act like the linear reference model. This novel approach demonstrated the feasibility of using it for advanced turbomachinery systems with large-scaled magnetic bearings with unknown dynamics.

Glenn contacts:
Dr. Benjamin B. Choi, 216–433–6040, Benjamin.B.Choi@grc.nasa.gov;
Dr. Gerald V. Brown, 216–433–6047, Gerald.V.Brown@grc.nasa.gov; and
Dr. Dexter Johnson, 216–433–6046, Dexter.Johnson@grc.nasa.gov

Neural Network Control of Dynamic Spin Rig

In 1997, researchers at the NASA Glenn Research Center developed a neural network controller that circumvents a magnetic bearing's nonlinearity and they successfully demonstrated it on a Bentley-Nevada rig—a small-scaled magnetically suspended rotor system. In 2000, they extended a neural network approach to control the Dynamic Spin Rig that is a full-scale magnetic bearing suspension system at Glenn.

Magnetic bearings have significant advantages over conventional contact bearings: such as a no-oil system, higher speeds, no friction, weight reduction, precise position control, and active damping. However, there are technical barriers that limit the application of this technology in industry. One of them is the need for a nonlinear controller that can overcome the system nonlinearity and uncertainty inherent in magnetic bearings.

A neural network was selected for a nonlinear controller because it generates a neural model without any detailed information regarding the internal working of the magnetic bearing system, even though it might be too complex or impossible to derive an accurate system model. A feed-forward architecture with a back-propagation learning algorithm was selected because of its proven performance, accuracy, and relatively easy implementation.

The neural network plant emulator is first trained to emulate a theoretical model of the nonlinear plant. A discrete theoretical mode of the plant dynamics in state-space notation is utilized to choose the present states of the plant (rotor displacement and velocity) and the plant input (control current) as the input to the emulator. The next states, the rotor displacement and velocity after one sample time, are chosen as the output of the plant emulator. During the learning procedure, the weights are upgraded to minimize the errors between the actual network output and the desired values. After training, the neural emulator perfectly predicts the next states (delayed by one sample time) of the magnetic bearing system for the current states and control force, which are not in the training sample data.

The second step is to use the trained neural emulator to train a neural network controller that

makes the whole system meet conventional performance specifications such as bandwidth, settling time, and overshoot. We want the controller to take the current magnetic bearing states $\vec{x}(t)$ and demand r as input parameters, and to output a control force $u(t)$ to the magnetic bearing system. These current state values should make the magnetic bearing's next state vector $\vec{x}(t+1)$ be identical to that defined by the desired linear reference system, which satisfies performance specifications in either the frequency or the time domain.

A Bode plot of a simple second-order linear reference model was derived from frequency domain specifications and then compared with the closed-loop magnetic bearing system after training. They were almost identical even after 320 training epochs. Another neural controller based on time domain specifications was trained and tested by simulating its response for the initial condition and comparing the results with the actual magnetic bearing response. The neural network controller was so accurate that it perfectly overlapped the magnetic bearing response.

In summary, a neural network controller that circumvents the magnetic bearing's nonlinearity was developed and successfully demonstrated on a full-scaled magnetic bearing system. The neural plant emulator and neural controller were so accurate that the neural network controller did a near perfect job of making the nonlinear magnetic bearing system act like the linear reference model. The results demonstrate the feasibility of using this novel approach for advance turbomachinery systems with large-scaled magnetic bearings with unknown dynamics.

Glenn contacts:
Dr. Benjamin B. Choi, 216–433–6040, Benjamin.B.Choi@grc.nasa.gov; and
Dr. Gerald V. Brown, 216–433-6047, Gerald.V.Brown@grc.nasa.gov

Feasibility of Using Neural Network Models to Accelerate the Testing of Mechanical Systems

Verification testing is an important aspect of the design process for mechanical mechanisms, and full-scale, full-length life testing is typically used to qualify any new component for use in space. However, as the required life specification is increased, full-length life tests become more costly and lengthen the development time. In addition, this type of testing becomes prohibitive as the mission life exceeds 5 years, primarily because of the high cost and the slow turnaround time for new technology. As a result, accelerated testing techniques are needed to reduce the time required for testing mechanical components.

Current accelerated testing methods typically consist of increasing speeds, loads, or temperatures to simulate a high cycle life in a short period of time. However, two significant drawbacks exist with this technique. The first is that it is often not clear what the accelerated factor is when the operating conditions are modified. Second, if the conditions are changed by a large degree (an order of

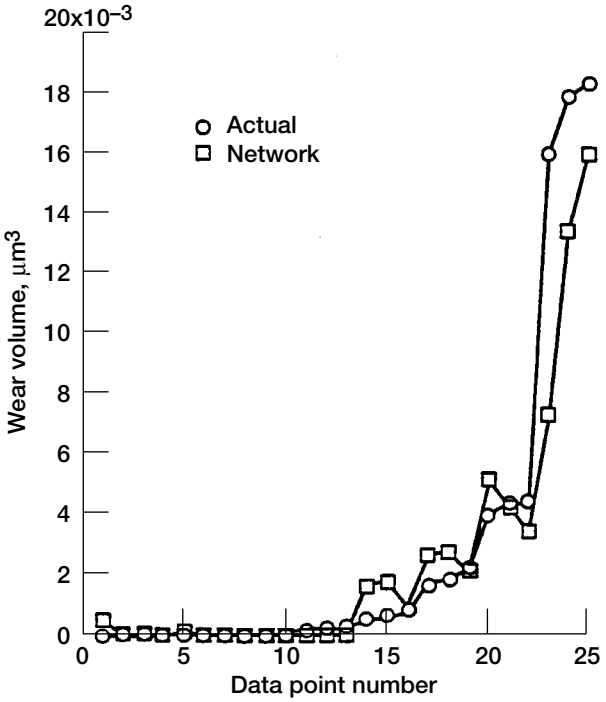

Comparison of previously unknown rub-shoe wear volumes (actual data) to those of a neural network model approximation.

magnitude or more), the mechanism is forced to operate out of its design regime. Operation in this condition often exceeds material and mechanical system parameters and renders the test meaningless.

At the NASA Lewis Research Center, we theorized that neural network systems may be able to model the operation of a mechanical device. If so, the resulting neural network models could simulate long-term mechanical testing with data from a short-term test. This combination of computer modeling and short-term mechanical testing could then be used to verify the reliability of mechanical systems, thereby eliminating the costs associated with long-term testing. Neural network models could also enable designers to predict the performance of mechanisms at the conceptual design stage by entering the critical parameters as input and running the model to predict performance.

The purpose of this study was to assess the potential of using neural networks to predict the performance and life of mechanical systems. To do this, we generated a neural network system to model wear obtained from three accelerated testing devices: (1) a pin-on-disk tribometer, (2) a line-contact rub-shoe tribometer, and (3) a four-ball tribometer. Critical parameters such as load, speed, oil viscosity, temperature, sliding distance, friction coefficient, wear, and material properties were used to produce models for each tribometer.

The study showed that neural networks were able to model these simple tribological systems, illustrating the feasibility of using neural networks to perform accelerated life testing on more complicated mechanical systems (e.g., bearings). The graph to the left compares actual wear data generated on a rub-shoe tribometer with data that were generated from a neural network. As the graph on the preceding page illustrates, the correlation is very good.

Neural networks can also be used to predict input variables for conditions that have not been run experimentally. The following plot is a neural-network-generated, three-dimensional plot of wear rate (for the pin-on-disk tribometer) as a function of sliding distance and sliding speed. This figure depicts wear rate values that would be obtained for different distances and speeds.

Glenn contact: Robert L. Fusaro, 216–433–6080, Robert.L.Fusaro@grc.nasa.gov

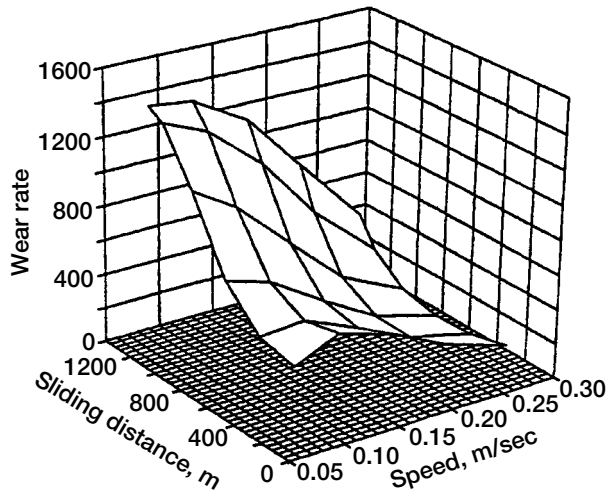

Three-dimensional plots generated from a neural network model illustrating the relationship between speed, load, and pin-on-disk wear rate.

Magnetic Suspension for Dynamic Spin Rig

NASA Lewis Research Center's Dynamic Spin Rig, located in Building 5, Test Cell CW–18 (see the top photo), is used to test turbomachinery blades and components by rotating them in a vacuum chamber. A team from Lewis' Machine Dynamics Branch successfully integrated a magnetic bearing and control system into the Dynamic Spin Rig (see the bottom photo). The magnetic bearing worked very well both to support and shake the shaft. It was demonstrated that the magnetic bearing can transmit more vibrational energy into the shaft and excite some blade modes to larger amplitudes than the existing electromagnetic shakers can.

Experiments were successfully conducted with the University of California, San Diego, on the damping of composite plates. These experiments demonstrated the system's robustness for long-term testing. Also, our team discovered that the bearing can use feedback from the blade's strain gauges to provide blade damping. This is an additional benefit since insufficient blade damping is a critical problem in advanced turbomachinery blades.

The success of the initial work led to the development and design of a full magnetic suspension system (using three magnetic bearings) for the Dynamic Spin Rig. The upgraded facility provides either a mechanical or magnetic support system for rotors. The magnetic support will enable longer run times for rotating blades at higher speeds and larger vibration amplitudes.

Glenn contacts:
Dr. Dexter Johnson, 216–433–6046,
Dexter.Johnson@grc.nasa.gov;
Oral Mehmed, 216–433–6036,
Oral.Mehmed@grc.nasa.gov; and
Dr. Gerald V. Brown, 216–433–6047,
Gerald.V.Brown@grc.nasa.gov

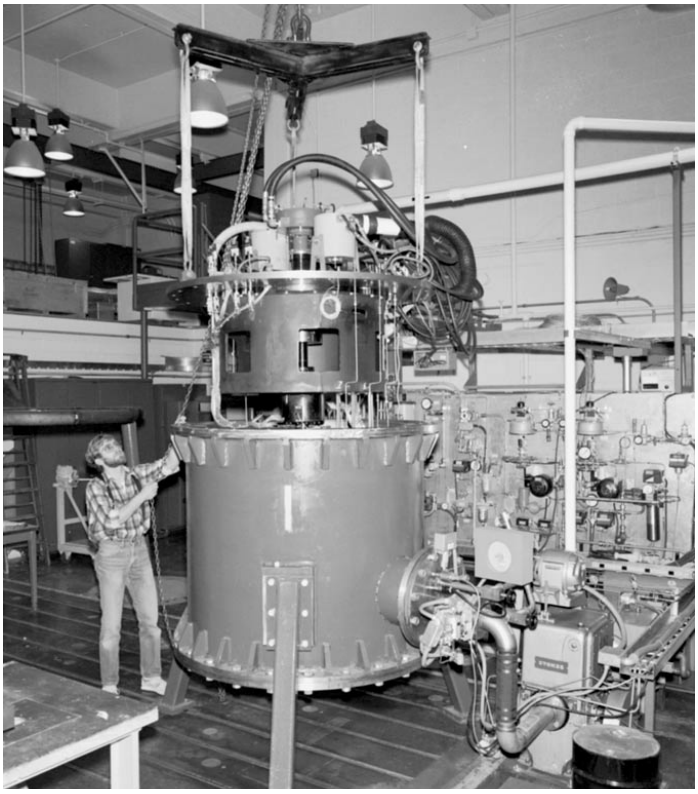

NASA Lewis' Dynamic Spin Rig.

Radial magnetic bearing in NASA Lewis' Dynamic Spin Rig showing viscoelastic damped composite plates attached to the rotor.

High-Temperature Magnetic Bearings Being Developed for Gas Turbine Engines

Magnetic bearings are the subject of a new NASA Lewis Research Center and U.S. Army thrust with significant industry participation, and cooperation with other Government agencies. The NASA/Army emphasis is on high-temperature applications for future gas turbine engines. Magnetic bearings could increase the reliability and reduce the weight of these engines by eliminating the lubrication system. They could also increase the DN (diameter of bearing times the rpm) limit on engine speed and allow active vibration cancellation systems to be used, resulting in a more efficient, "more electric" engine. Finally, the Integrated High Performance Turbine Engine Technology (IHPTET) program, a joint Department of Defense/industry program, identified a need for a high-temperature (1200 °F) magnetic bearing that could be demonstrated in their Phase III engine.

This magnetic bearing is similar to an electric motor. It has a laminated rotor and stator made of cobalt steel. Wound around the stator's circumference are a series of electrical wire coils which form a series of electric magnets that exert a force on the rotor. A probe senses the position of the rotor, and a feedback controller keeps it centered in the cavity. The engine rotor, bearings, and casing form a flexible structure with many modes. The bearing feedback controller, which could cause some of these modes to become unstable, could be adapted to varying flight conditions to minimize seal clearances and monitor the health of the system.

Cobalt steel has a curie point greater than 1700 °F, and copper wire has a melting point beyond that. However, practical limitations associated with the maximum magnetic field strength in the cobalt steel and the stress in the rotating components limit the temperature of the magnetic bearing to about 1200 °F. The objective of this effort is to determine the temperature and speed limits of a magnetic bearing operating in an engine. Our approach was to use Lewis' in-house experience in magnets, mechanical components, high-temperature materials, and surface lubrication to build and test a magnetic bearing in both a rig and an engine. Testing was to be done at Lewis or through cooperative programs in industrial facilities.

During the last year, we made significant progress. We have a cooperative program with Allison Engine Company to work on a high-temperature magnetic thrust bearing. During this program, we uncovered a problem with the conventional design of the magnetic thrust bearing. Because the thrust bearing is not laminated, it causes eddy currents that severely reduce the bandwidth. Also, we worked at Allison to bring their high-temperature magnetic bearing rig to full speed. We predicted both in-house and Allison magnetic bearing stability limits, and we tested a high-temperature displacement probe. Our flexible casing rig is being converted to a high-temperature magnetic bearing rig (see the illustration). Testing should start in the third quarter of 1997.

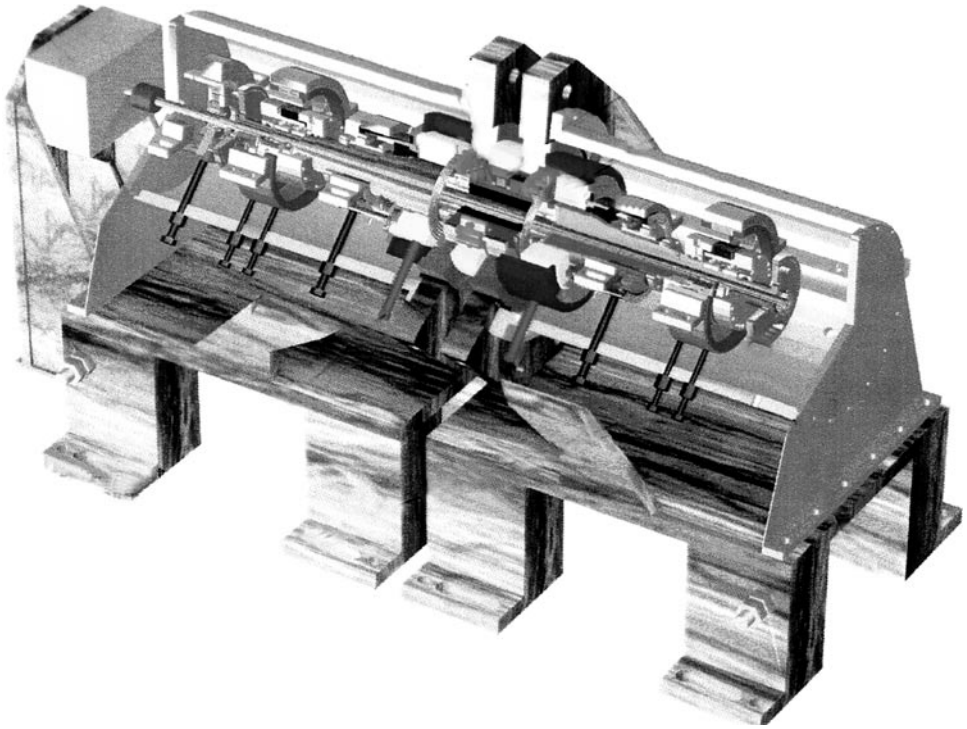

NASA Lewis' 1000 °F Magnetic Bearing Test Rig.

Our plan is to develop a high-temperature compact wire insulation, and to fiber

reinforce the core lamination to operate at higher temperature and DN values. We also plan to modify our stability analysis and controller theory by including a nonlinear magnetic bearing model. We are developing an expert system that adapts to changing flight conditions and that diagnoses the health of the system. Then, we will demonstrate the bearing on our rotor dynamics rig and, finally, in a engine.

Glenn contacts:
Albert F. Kascak, 216–433–6024,
Albert.F.Kascak@grc.nasa.gov, and
Dr. Gerald V. Brown, 216–433–6047,
Gerald.V.Brown@grc.nasa.gov

Integrated Fiber-Optic Light Probe: Measurement of Static Deflections in Rotating Turbomachinery

At the NASA Lewis Research Center, in cooperation with Integrated Fiber Optic Systems, Inc., an integrated fiber-optic light probe system was designed, fabricated, and tested for monitoring blade tip deflections, vibrations, and to some extent, changes in the blade tip clearances of a turbomachinery fan or a compressor rotor. The system comprises a set of integrated fiber-optic light probes that are positioned to detect the passing blade tip at the leading and trailing edges. In this configuration, measurements of both nonsynchronous blade vibrations and steady-state blade deflections can be made from the timing information provided by each light probe—consisting of an integrated fiber-optic transmitting channel and numerical aperture receiving fibers, all mounted in the same cylindrical housing. With integrated fiber-optic technology, a spatial resolution of 50 μm is possible while the outer diameter is kept below 2.5 mm. To evaluate these probes, we took measurements in a single-stage compressor facility and an advanced fan rig in Lewis' 9- by 15-Foot Low-Speed Wind Tunnel.

Glenn contact:
Dr. Anatole P. Kurkov, 216–433–5695,
Anatole.P.Kurkov@grc.nasa.gov

Dual-Laser Probe for Measuring Blade-Tip Clearance Tested

A dual-probe, integrated fiber-optic laser system for measuring blade tip clearance in rotating turbomachinery was developed cooperatively with Integrated Fiber Optic Systems, Inc., and tested at the NASA Lewis Research Center. Because the probes are nearly flush with the casing inner lining, there is minimal flow disturbance. The two probes are closely spaced in a circumferential plane and are slanted at an angle relative to each other so that the time it takes the blade tip to traverse the space between the two beams varies with the tip radius, making it possible to determine the tip clearance at rotor operating conditions. The tip clearance can be obtained for all the blades in a rotor with a single system, provided there are no synchronous vibrations present at a particular operating condition.

The two probes for the laser system were installed in two holders. For one, the included angle between the probes was 20°, and for the other, it was 40°. The two configurations were calibrated in a vacuum spin-rig facility that can reproduce realistic blade-tip speeds. A specially designed, nondeflecting rotor was used to calibrate the probes. This rotor consisted of a tapered titanium bar with three teeth on each end, the thickness of which was representative of a typical blade-tip thickness. The bar and measuring teeth were in a horizontal plane in the spin rig, and the axis of rotation was vertical. To set the clearances, we used a remotely controlled optical stage that could be traversed vertically.

The 40° probe system also was used to measure the tip clearance during an engine fan prototype test in a wind tunnel. Using the spin-rig calibrations, we estimated the accuracy of the tip-clearance measurement in the test to be 0.005 in. This program is ongoing.

Glenn contact:
Dr. Anatole P. Kurkov, 216–433–5695,
Anatole.P.Kurkov@grc.nasa.gov

Optical Measurements of Axial and Tangential Steady-State Blade Deflections Obtained Simultaneously

Case-mounted fiber-optic sensors have been used by aircraft engine manufacturers mainly to monitor blade vibration in fans and compressors. The simplest probe arrangement is a spot probe where, typically, a center fiber transmits laser light, and the outer fibers collect the reflected light from the blade tips and transmit it to a photodetector. Because the spot of incident light is fixed in space, whereas the blade deflects dynamically, the reflected light will originate from slightly different portions of the blade tip under different operating conditions. Unless corrections are developed to compensate for this effect, some error in vibratory tangential amplitude will occur. For monitoring vibrations, this error is usually not critical.

However, when steady-state blade deflections are being measured, it is very important to fix the spot on the blade tip at a particular location because the operating speed blade deflections are evaluated against a low-speed reference run. The change in speed usually implies a significant change in the blade orientation and possibly its shape brought about by the aerodynamic and centrifugal loading.

It is most convenient to select the blade's leading and trailing edges as the fixed points for which deflections will be evaluated. To capture the blade edges at various speeds, the light probe must be movable. This was achieved by mounting the probe in an eccentric hole in a bushing that fit the fan case in the region that overlapped the path of the blade edge. The probe was actuated to search for a blade edge while all the blades were viewed on an oscilloscope. The blade edge was considered to be captured when a pulse associated with a particular blade was significantly reduced in magnitude but was clearly distinguishable from the background noise level. By tracing the axial position of either blade edge, one could extend the deflection measurement to two dimensions: axial and tangential. These blade deflection measurements were obtained during a wind tunnel test of a fan prototype.

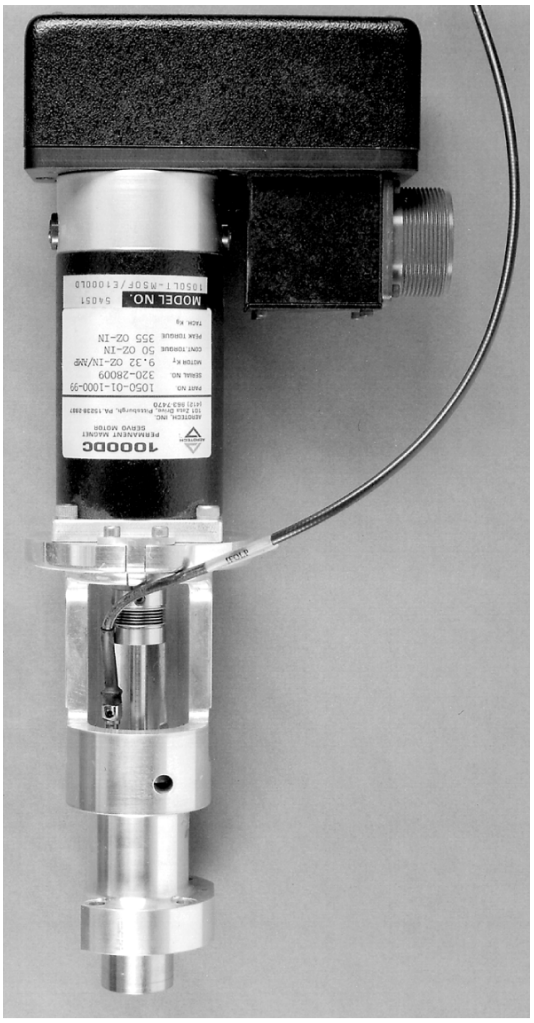

Probe-actuator/motor assembly.

As shown in this photograph of the servomotor-actuator assembly, the cylindrical enclosure that accommodates the eccentrically positioned optical probe was open on one side to provide an exit path for the fiber-optic cable. The 180° opening in the housing was oriented such that its base (along the diameter) was parallel to the fan rotor axis. Thus, when the motor was actuated, the probe moved over a semicircular path, maximizing the extent of the motion in the axial direction. The two noncontacting limit switches (not shown in the photograph) restricted the extent of rotation to 180°. The servomotor had a resolution of 4000 counts per revolution and was controlled remotely by a computer.

Glenn contact:
Dr. Anatole P. Kurkov, 216–433–5695,
Anatole.P.Kurkov@grc.nasa.gov

Structural Simulations of Engine-Airframe Systems Being Improved

The current environment for designing engine and engine-airframe structural systems requires extensive efforts to prepare and integrate models, generate analysis results, and postprocess data. Despite these efforts, the accuracy of the simulations is inadequate, leading to less than optimal designs, costly testing and redesigns, and most important, significant uncertainties in safety factors. The goal of this project is to develop improved tools for structural simulations of engine-airframe systems. To develop these new tools, the NASA Glenn Research Center at Lewis Field has teamed with GE Aircraft Engines, Pratt & Whitney, and Boeing Commercial Aircraft. Boeing brings a wealth of large-scale, complex, structural systems analysis experiences and capabilities to the team, while GE and Pratt & Whitney bring aircraft-engine-specific structural expertise.

The tools that the team is creating are being used to assess a multitude of structurally related problems. The primary problem being addressed is the accurate simulation of a blade-out event and the subsequent windmilling of the engine. Reliable simulations of the loss of a blade are required to ensure structural integrity during flight as well as to guarantee successful blade-out certification testing. Simulation of the windmilling that occurs after blade-out is critical to avoiding excessive vibration levels, which may damage the aircraft and endanger passengers. In addition to blade-out and windmilling, the structural simulation tools are being used to determine structural response during regular aircraft operations and under loadings resulting from flight maneuvers. The loads generated by these analyses are critical for the teams designing several airplane components, including the engine, nacelle, strut, and wing.

The approach being used for the system simulation is to first develop a detailed high-fidelity simulation

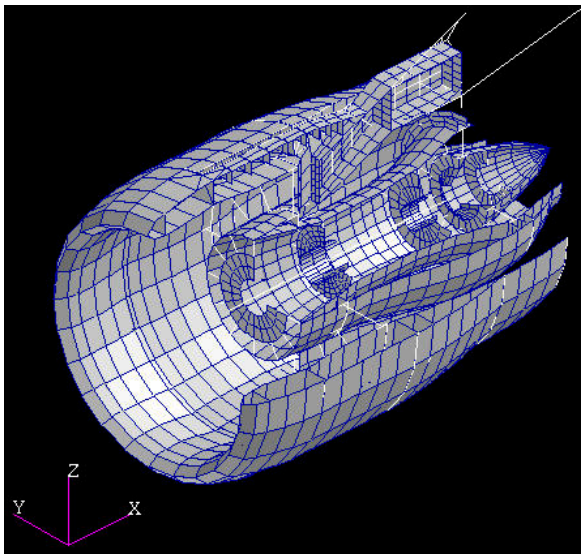

Engine-wing structural system model.

to capture the structural loads resulting from blade loss, and then use these loads in an overall system model that includes complete structural models of both the engines and airframe. The detailed simulation includes the time-dependent trajectory of the lost blade and its interactions with the containment structure, whereas the system simulation includes the lost blade loadings and the interactions between the rotating turbomachinery and the remainder of the aircraft's structural components. General-purpose finite-element structural analysis codes are being used to accomplish this task, and provisions are being added to include transient effects from the blade loss and rotational effects resulting from the engine's turbomachinery. The figure depicts the generic structural model that was constructed to demonstrate and validate the tools that are being developed under this project.

Glenn contacts:
Dr. Charles Lawrence, 216–433–6048,
Charles.Lawrence@grc.nasa.gov; and
Dr. Kelly S. Carney, 216–433–2386,
Kelly.S.Carney@grc.nasa.gov

Curved Thermopiezoelectric Shell Structures Modeled by Finite Element Analysis

"Smart" structures composed of piezoelectric materials may significantly improve the performance of aeropropulsion systems through a variety of vibration, noise, and shape-control applications. The development of analytical models for piezoelectric smart structures is an ongoing, in-house activity at the NASA Glenn Research Center at Lewis Field focused toward the experimental characterization of these materials.

Research efforts have been directed toward developing analytical models that account for the coupled mechanical, electrical, and thermal response of piezoelectric composite materials. Current work revolves around implementing thermal effects into a curvilinear-shell finite element code. This enhances capabilities to analyze curved structures and to account for coupling effects arising from thermal effects and the curved geometry.

The current analytical model implements a unique mixed multifield laminate theory to improve computational efficiency without sacrificing accuracy. The mechanics can model both the sensory and active behavior of piezoelectric composite shell structures. Finite element equations are being implemented for an eight-node curvilinear shell element, and numerical studies are being conducted to demonstrate capabilities to model the response of curved piezoelectric composite structures (see the figure).

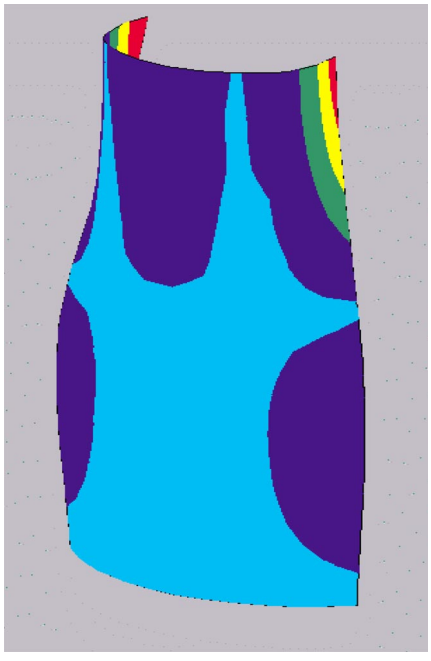

Response of a curved piezoelectric composite shell under thermal loading.

Glenn contact: Ho-Jun Lee, 216–433–3316, Ho-Jun.Lee@grc.nasa.gov

Damping Experiment of Spinning Composite Plates With Embedded Viscoelastic Material

One way to increase gas turbine engine blade reliability and durability is to reduce blade vibration. It is well known that vibration can be reduced by adding damping to metal and composite blade-disk systems. As part of a joint research effort of the NASA Lewis Research Center and the University of California, San Diego, the use of integral viscoelastic damping treatment to reduce the vibration of rotating composite fan blades was investigated. The objectives of this experiment were to verify the structural integrity of composite plates with viscoelastic material patches embedded between composite layers while under large steady forces from spinning, and to measure the damping and natural frequency variation with rotational speed.

Data were obtained from in-vacuum vibration spin experiments of flat and twisted graphite composite plates damped with 3M ISD 113 viscoelastic material patches embedded between composite layers. The photograph on the following page shows the rotor installation in the spin rig. The rotor has a tip diameter of 792 mm, and the plates have an aspect ratio of 3 and a chord of 76 mm.

Damping was calculated from measured transfer functions of blade base acceleration to blade strain. Damping was repeatable, and there were no failures or delaminations of the plates. This is significant since 3M ISD 113 has a low creep modulus at room temperature, and the plates had a centrifugal load of up to 28,000 g at the tip. Centrifugal stiffening

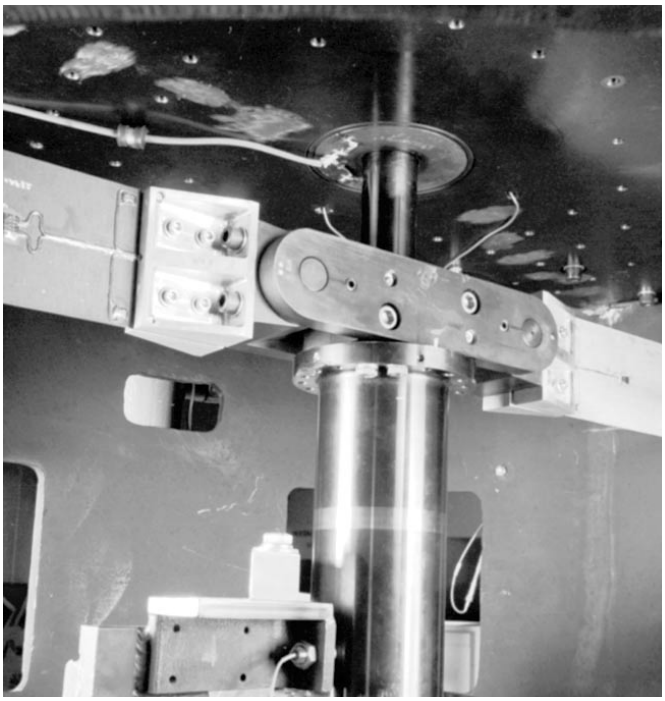

Viscoelastic damped composite plates in NASA Lewis' Dynamic Spin Rig.

was large for the plates and caused a significant drop in the damping ratios, but the viscoelastic material damping remained about constant. Even though the damping ratios decreased, they were always greater than 2 times the damping ratios of undamped control plates. Real fan blades have smaller increases in natural frequencies with rotational speed, and therefore, the decrease in fan blade damping ratio should be smaller than measured in this experiment.

From the results, we concluded that the presence of centrifugal forces, which are well-known to increase blade bending stiffness and corresponding natural frequencies, decreased damping ratios. This phenomenon occurred because as the blade stiffened the percent of modal strain energy in the damping material decreased, thus decreasing the modal damping ratios. To further improve damping, designers will need to consider how to increase the strain energy level in the viscoelastic material, such as using a stiffer viscoelastic damping material than used here. This study reveals not only the potential of integral viscoelastic material damping in composite fan blades, but also illustrates that there are technical challenges that still must be overcome before it can be effectively used as a design option.

Glenn contact: Oral Mehmed, 216–433–6036, Oral.Mehmed@grc.nasa.gov

Novel Vibration Damping of Ceramic Matrix Composite Turbine Blades Developed for RLV Applications

The Reusable Launch Vehicle (RLV) represents the next generation of space transportation for the U.S. space program. The goal for this vehicle is to lower launch costs by an order of magnitude from $10,000/lb to $1,000/lb. Such a large cost reduction will require a highly efficient operation, which naturally will require highly efficient engines. The RS–2200 Linear Aerospike Engine is being considered as the main powerplant for the RLV. Strong, lightweight, temperature-resistant ceramic matrix composite (CMC) materials such as C/SiC are critical to the development of the RS–2200. Preliminary engine designs subject turbopump components to extremely high frequency dynamic excitation, and ceramic matrix composite materials are typically lightly damped, making them vulnerable to high-cycle fatigue. The combination of low damping and high-frequency excitation creates the need for enhanced damping. Thus, the goal of this project has been to develop well-damped C/SiC turbine components for use in the RLV.

Foster-Miller and Boeing Rocketdyne have been using an innovative, low-cost process to develop light, strong, highly damped turbopump components for the RS–2200 under NASA's Small Business Innovation Research (SBIR) program. The NASA Glenn Research Center at Lewis Field is managing this work. The process combines three-dimensionally braided fiber reinforcement with a preceramic polymer. The three-dimensional reinforcement significantly improves the structure over conventional two-dimensional laminates, including high through-the-thickness strength and stiffness.

Phase I of the project successfully applied the Foster-Miller preceramic polymer infiltration and pyrolysis (PIP) process to the manufacture of dynamic specimens representative of engine components. An important aspect of the program has been the development of the manufacturing process. Results show that the three-dimensionally braided carbon-fiber reinforcement provides good processability and good mechanical stiffness and strength in comparison to materials produced with competing processes as shown in the graphs.

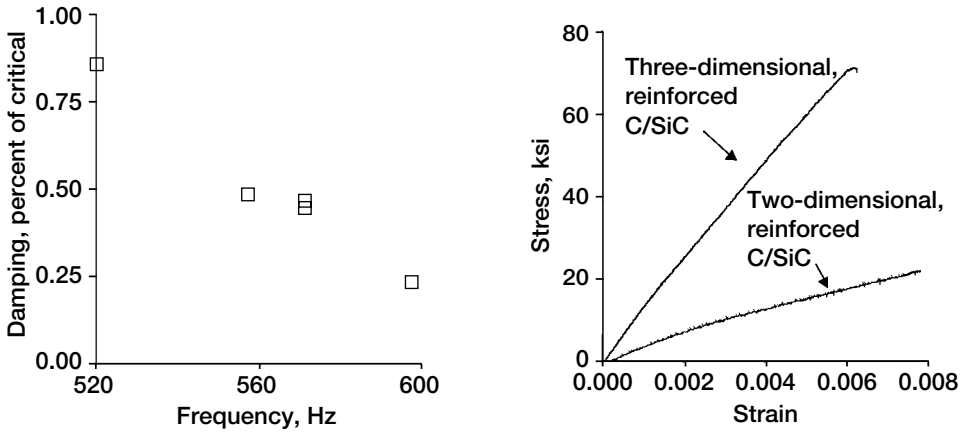

Left: Dynamic characterization. Right: Static characterization.

The RS–2200 turbopump turbine blades are susceptible to high-frequency vibration with motion dominated by leading- and trailing-edge motion. The most effective approach to controlling these vibrations is by increasing internal damping. Baseline C/SiC damping appears to decrease as a function of frequency and is too small, less than 0.2 percent for the turbine applications. Phase I results show that fiber architecture has little effect on damping. Previous research indicates that incorporating highly damped materials in the form of particulate fillers and coatings increases damping substantially. Several materials were identified that could be added to the base material to enhance damping, in particular, compounds containing boron. BN has a critical damping value as high as 2 percent.

The next step of this work will include end-to-end component development, encompassing process development and refinement, structural design, and structural dynamic testing. Damping materials will be incorporated into the material in the form of coatings and particulates, and the polymer infiltration and pyrolysis manufacturing will be modified to optimize mechanical behavior. The physical and mechanical properties of these materials will be completely characterized as a function of temperature and of microcracking caused by sustained centrifugal loads.

Foster-Miller and Boeing Rocketdyne will use these properties to design and manufacture insertable blades for the RS–2200 turbopump. The blades will be dynamically tested under simulated environmental and operational engine conditions.

Glenn contact: Dr. James B. Min, 216–433–2587, James.B.Min@grc.nasa.gov

Cascade Optimization Strategy With Neural Network and Regression Approximations Demonstrated on a Preliminary Aircraft Engine Design

A preliminary aircraft engine design methodology is being developed that utilizes a cascade optimization strategy together with neural network and regression approximation methods. The cascade strategy employs different optimization algorithms in a specified sequence. The neural network and regression methods are used to approximate solutions obtained from the NASA Engine Performance Program (NEPP), which implements engine thermodynamic cycle and performance analysis models. The new methodology is proving to be more robust and computationally efficient than the conventional optimization approach of using a single optimization algorithm with direct reanalysis. The methodology has been demonstrated on a preliminary design problem for a novel subsonic turbofan engine concept that incorporates a wave rotor as a cycle-topping device. Computations of maximum thrust were obtained for a specific design point in the engine mission profile. The results (depicted in the figure) show a significant improvement in the maximum thrust obtained using the new methodology in comparison to benchmark solutions obtained using NEPP in a manual design mode.

Glenn contact:
Dale A. Hopkins, 216–433–3260,
Dale.A.Hopkins@grc.nasa.gov

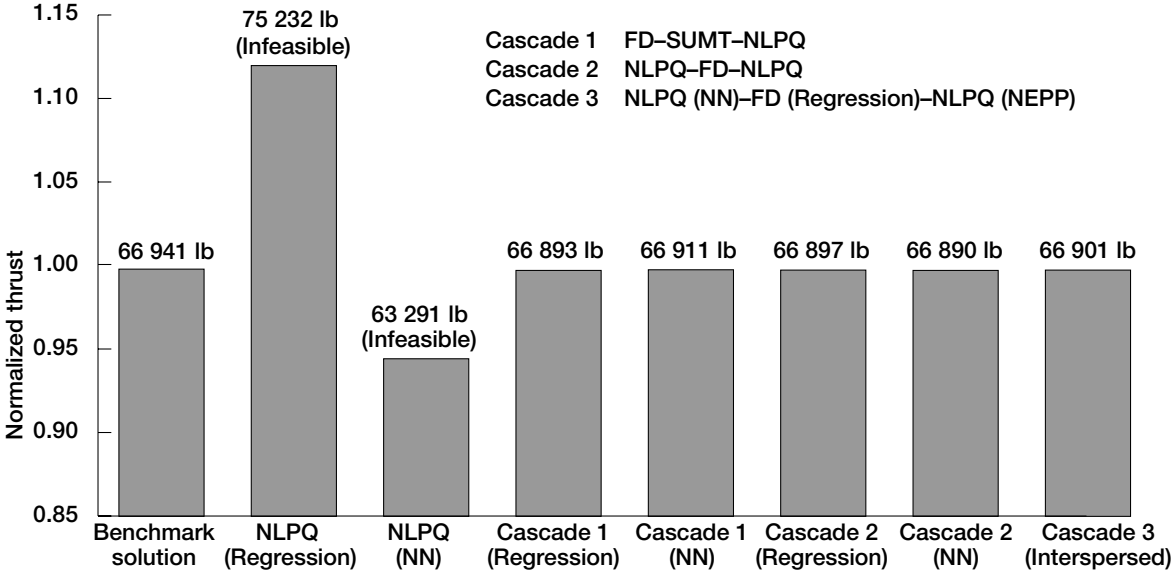

Optimum thrust for a subsonic wave-rotor-topped engine for the sixth operating point.

Optimization method	Description
Benchmark solution	Average thrust obtained using 10 different initial designs.
NLPQ (Regression)	Thrust obtained using NLPQ and regression approximation.
NLPQ (NN)	Thrust obtained using the quadratic programming algorithm (NLPQ) and the neural network (NN) approximation.
Cascade 1[a] (Regression)	Thrust obtained using the Cascade 1 strategy and the regression approximation.
Cascade 1[a] (NN)	Thrust obtained using the Cascade 1 strategy and the neural network approximation.
Cascade 2 (Regression)	Thrust obtained using the Cascade 2 strategy and the regression approximation.
Cascade 2 (NN)	Thrust obtained using the Cascade 2 strategy (NLPQ-FD-NLPQ) and the neural network approximation.
Cascade 3 (Interspersed)	Thrust obtained using the interspersed cascade strategy (NLPQ with NN, FD with regression, and NLPQ with the NASA Engine Performance Program (NEPP) reanalysis).

[a]The Cascade 1 strategy uses three algorithms: the Method of Feasible Directions (FD) followed by the Sequential Unconstrained Minimization Technique (SUMT) and the quadratic programming algorithm (NLPQ).

Effects of Various Heat Treatments on the Ballistic Impact Properties of Inconel 718 Investigated

Uncontained failures of aircraft engine fan blades are serious events that can cause equipment damage and loss of life. Federal Aviation Administration (FAA) certification requires that all engines demonstrate the ability to contain a released fan blade with the engine running at full power. However, increased protection generally comes at the expense of weight. Proper choice of materials is therefore imperative to an optimized design. The process of choosing a good casing material is done primarily through trial and error. This costly procedure could be minimized if there was a better understanding of the relationships among static material properties, impact properties, and failure mechanisms. This work is part of a program being conducted at the NASA Glenn Research Center at Lewis Field to study these relationships. Ballistic impact tests were conducted on flat, square sheets of Inconel 718 that had been subjected to different heat treatments. Two heat treatments and the as-received condition were studied. In addition, results were compared with those from an earlier study involving a fourth heat treatment. The heat treatments were selected on the basis of their effects on the static tensile properties of the material.

The impact specimens used in this study were 17.8-cm square panels that were centered and clamped over a 15.2-cm square hole in a 1.27-cm-thick steel plate. Three nominal plate thickness dimensions were studied, 1.0, 1.8, and 2.0 mm. For each thickness, all the specimens were taken from the same sheet of material. The projectile was a Ti-6Al-4V cylinder with a length of 25.4 mm, a diameter of 12.7 mm, and a mass ranging from 14.05 to 14.20 g. The projectiles were accelerated toward the specimens at normal incidence using a gas gun with a 2-m-long, 12.7-mm inner-diameter barrel. The ballistic limit for each heat treatment condition and thickness was determined by conducting a number of impact tests that bracketed as closely as possible the velocity required to penetrate the specimen.

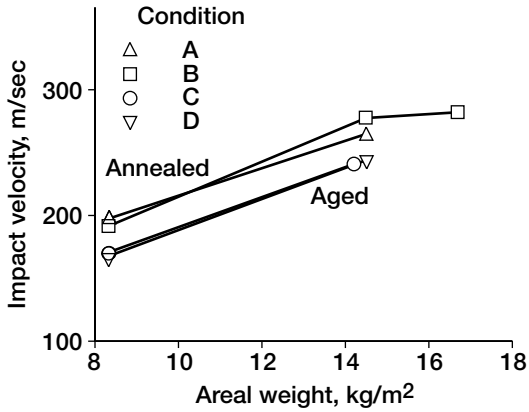

Ballistic limit of Inconel 718 as a function of areal weight and heat treatment.

We found that both the static and impact properties as well as the failure mechanisms of Inconel 718 can be changed significantly by varying the heat treatment. Under the conditions used in this study, softer annealed material performed dramatically better in ballistic impact tests than harder annealed and aged material (see the figure). Micrographs indicated highly localized areas of large shear deformation in impacted aged specimens. In the annealed material, the deformation was not as localized. Future studies will attempt to determine what specific material properties have the greatest influence on impact properties.

Glenn contacts:
Dr. J. Michael Pereira, 216–433–6738, J.M.Pereira@grc.nasa.gov; and
Dr. Bradley A. Lerch, 216–433–5522, Bradley.A.Lerch@grc.nasa.gov

Failure Accommodation Tested in Magnetic Suspension Systems for Rotating Machinery

The NASA Glenn Research Center at Lewis Field and Texas A&M University are developing techniques for accommodating certain types of failures in magnetic suspension systems used in rotating machinery. In recent years, magnetic bearings have become a viable alternative to rolling element bearings for many applications. For example, industrial machinery such as machine tool spindles and turbomolecular pumps can today be bought off the shelf with magnetically supported rotating components. Nova Gas Transmission Ltd. has large gas compressors in Canada that have been running flawlessly for years on magnetic bearings.

To help mature this technology and quiet concerns over the reliability of magnetic bearings, NASA researchers have been investigating ways of making the bearing system tolerant to faults. Since the potential benefits from an oil-free, actively controlled bearing system are so attractive, research that is focused on assuring system reliability and safety is justifiable. With support from the Fast Quiet Engine program, Glenn's Structural Mechanics and Dynamics Branch is working to demonstrate fault-tolerant magnetic suspension systems targeted for aerospace engine applications. The Flywheel Energy Storage Program is also helping to fund this research.

The fault-tolerant magnetic suspension facility in Glenn's Engine Research Building, test cell SW18, was completed in fiscal year 1999. The test rig has two eight-pole heteropolar magnetic bearings that suspend the rotor radially. Each pole is individually controlled with its own pulse-width-modulated amplifier. Opening the circuit between the pulse-width-modulated amplifier and the coil simulates coil failures. Turning off the amplifier supply power simulates amplifier failures. All possible combinations of failures can be realized by flipping switches on the facility control panel.

In fiscal year 1999, Glenn researchers tested unique solutions to 22 different combinations of single and multiple coil failures on a single bearing at zero speed. In all cases, levitation of the rotor was achievable. In addition, levitation with only three of the eight coils operational was demonstrated. A test case where every other coil in the outboard bearing was unpowered behaved satisfactorily to 3000 rpm. In fiscal year 2000, we plan to develop a controller that can detect any combination of failures and accommodate it without loss of levitation.

Glenn contact:
Andy J. Provenza, 216–433–6025,
Andrew.J.Provenza@grc.nasa.gov

Ohio Aerospace Institute contact:
Ralph H. Jansen, 216–433–6038,
Ralph.H.Jansen@grc.nasa.gov

Texas A&M University contact:
Dr. Alan Palazzolo, 409–845–5280,
abp8849@acs.tamu.edu

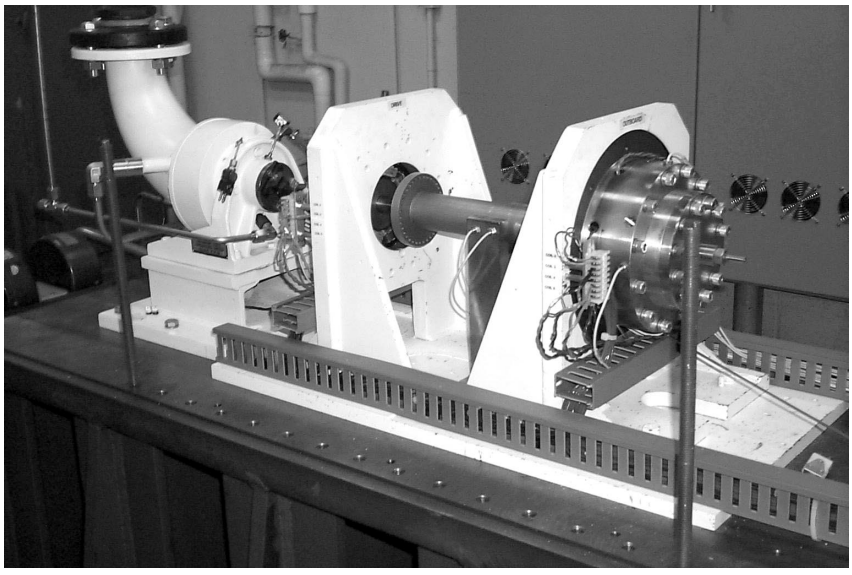

Fault-tolerant magnetic bearing rig.

Time-Shifted Boundary Conditions Used for Navier-Stokes Aeroelastic Solver

Under the Advanced Subsonic Technology (AST) Program, an aeroelastic analysis code (TURBO–AE) based on Navier-Stokes equations is currently under development at NASA Lewis Research Center's Machine Dynamics Branch. For a blade row, aeroelastic instability can occur in any of the possible interblade phase angles (IBPA's). Analyzing small IBPA's is very computationally expensive because a large number of blade passages must be simulated. To reduce the computational cost of these analyses, we used time-shifted, or phase-lagged, boundary conditions in the TURBO–AE code. These conditions can be used to reduce the computational domain to a single blade passage by requiring the boundary conditions across the passage to be lagged depending on the IBPA being analyzed. The time-shifted boundary conditions currently implemented are based on the direct-store method. This method requires large amounts of data to be stored over a period of the oscillation cycle. On CRAY computers this is not a major problem because solid-state devices can be used for fast input and output to read and write the data onto a disk instead of storing it in core memory.

In aeroelastic analyses using TURBO–AE, the unsteady aerodynamic loads are obtained by solving the Reynolds-averaged Navier-Stokes equations. The aerodynamic equations are solved via a finite volume scheme. Flux vector splitting is used to evaluate the flux Jacobians on the left side, and a higher order Total Variation Diminishing (TVD) scheme based on Roe's flux vector splitting is used to discretize the fluxes on the right side. Newton subiterations are used at each time step to maintain higher accuracy. Then, symmetric Gauss-Sidel iterations are applied to the discretized equations, and a dynamic grid deformation technique is used to simulate the blade motions. TURBO–AE updates the grid at each time step by recalculating it using linear interpolation and by assuming the far field to be fixed. It determines the aeroelastic characteristics of the blade row by calculating the energy exchange between the vibrating blade and its surrounding fluid for all possible frequencies and IBPA's of interest. Positive work on the blade indicates instability.

To verify and validate the time-shifted analysis, we used a flat-plate, helical-fan geometry. The helical fan consisted of 24 flat-plate blades with zero thickness. The inflow conditions and stagger angle were set to induce an inflow with a relative Mach number of 0.7 at an incidence of zero at the midspan. The results were obtained for several IBPA's and compared with those of the analysis using multiple blade passages. Only a few typical results are shown here; for more detail please refer to the reference. The graphs show the unsteady pressure difference for the 180° IBPA pitching and plunging cases. The time-shifted results were compared with results from a two-passage analysis. A very good comparison was obtained in both cases, indicating that the time-shifted boundary condition was properly implemented and reproduced the results of the multiple-passage analysis.

In the graph on the left (following page), the rate of convergence for the time-shifted analysis for –90° IBPA pitching is compared with that of the multiple-passage analysis. From this figure, it can be seen that the work-per-cycle for the four-passage

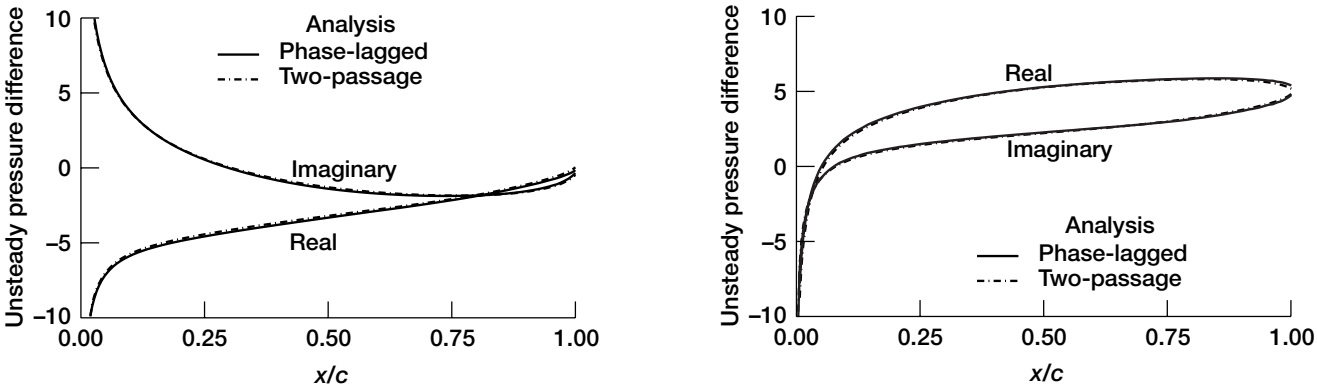

Comparison of the unsteady pressure difference variation at midspan for 180° IBPA oscillations; distance along chord from leading edge, x; chord, c. Left: Pitching. Right: Plunging.

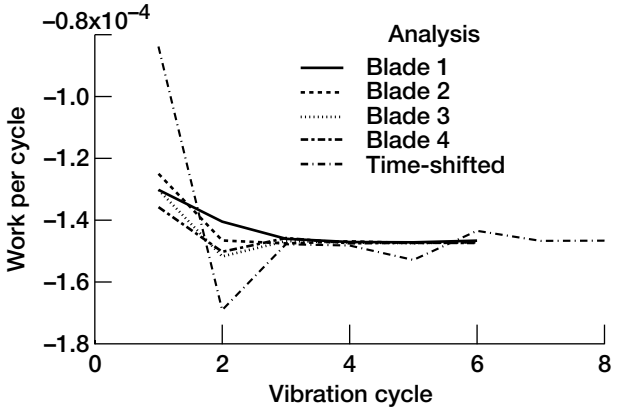

Comparison of the work-per-cycle convergence for a time-shifted analysis with multiple passages.

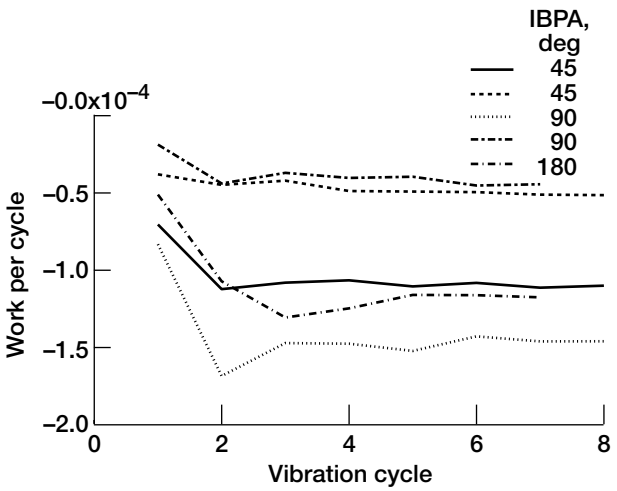

Comparison of the work-per-cycle convergence history for various interblade-phase-angle pitching oscillations.

analysis converged within four to five oscillation cycles, whereas roughly seven to eight cycles were required for the time-shifted analysis. Even though approximately 40-percent more cycles were required for convergence, the computational time was reduced by almost 60 percent. This is because only one blade passage was needed in the time-shifted analysis. We also found that the convergence rate for the time-shifted analysis was independent of the IBPA analyzed (see the graph on the right).

Glenn contacts:
Rakesh Srivastava, 216–433–6045, Rakesh.Srivastava@grc.nasa.gov;
Milind A. Bakhle, 216–433–6037, Milind.A.Bakhle@grc.nasa.gov; and
George L. Stefko, 216–433–3920, George.L.Stefko@grc.nasa.gov

Design Process for High Speed Civil Transport Aircraft Improved by Neural Network and Regression Methods

A key challenge in designing the new High Speed Civil Transport (HSCT) aircraft is determining a good match between the airframe and engine. Multidisciplinary design optimization can be used to solve the problem by adjusting parameters of both the engine and the airframe. Earlier (Patniak, et al., 1997), an example problem was presented of an HSCT aircraft with four mixed-flow turbofan engines and a baseline mission to carry 305 passengers 5000 nautical miles at a cruise speed of Mach 2.4. The problem was solved by coupling NASA Lewis Research Center's design optimization testbed (COMETBOARDS) with NASA Langley Research Center's Flight Optimization System (FLOPS). The computing time expended in solving the problem was substantial, and the instability of the FLOPS analyzer at certain design points caused difficulties.

In an attempt to alleviate both of these limitations, we explored the use of two approximation concepts in the design optimization process. The two concepts, which are based on neural network and linear regression approximation (Patnaik et al., 1998), provide the reanalysis capability and design sensitivity analysis information required for the optimization process. The HSCT aircraft optimization problem was solved by using three alternate approaches; that is, the original FLOPS analyzer and two approximate (derived) analyzers. The approximate analyzers were calibrated and used in three different ranges of the design variables; narrow (interpolated), standard, and wide (extrapolated).

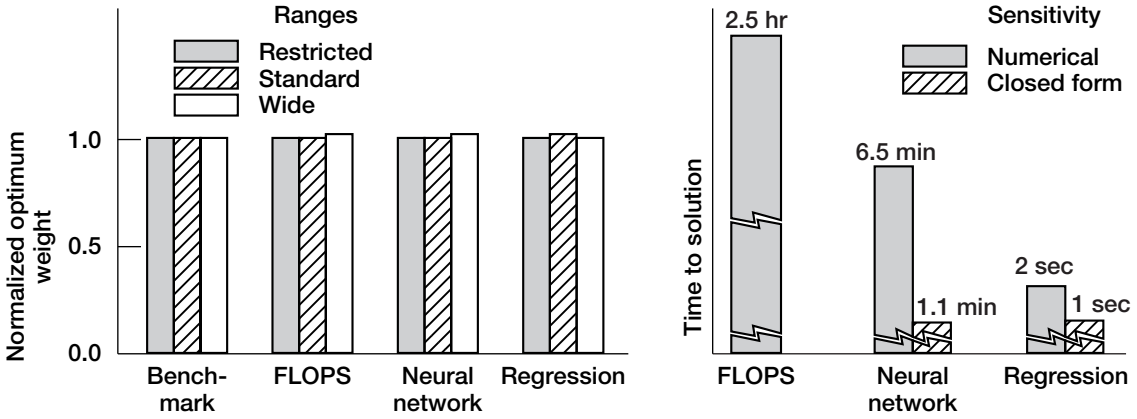

Optimum solutions for HSCT aircraft. Left: Normalized optimum weight of aircraft. Right: Central processing unit (CPU) time to solution.

Performance of the regression and neural network approximation methods for both the analysis and design of the HSCT aircraft could be considered satisfactory. For example, in the restricted range, 1-percent deviation was observed in the optimum gross takeoff weight of the aircraft. In the standard and wide ranges, the deviation increased to 2 percent. The approximation concepts significantly reduced the computing time expended during the optimization process. For the FLOPS-based optimization process, computing time was measured in hours, whereas for both approximation-based optimization processes, it was measured in minutes. Furthermore, difficulties associated with the instability of the FLOPS analyzer were eliminated with the approximation methods. However, calibrating the approximate (derived) analyzers required substantial computational time for both neural network and regression methods. For the HSCT aircraft problem, it was preferable to calibrate the approximate analyzers over a wider (standard) range and then use them to optimize over a narrower (restricted) range. Overall, neural network and regression approximation concepts were found to be satisfactory for the analysis and design optimization of the HSCT aircraft problem.

Glenn contact: Dale A. Hopkins, 216–433–3260, Dale.A.Hopkins@grc.nasa.gov

Ohio Aerospace Institute contact: Dr. Surya N. Patnaik, 216–433–5916, Surya.N.Patnaik@grc.nasa.gov

Thermal Effects Modeling Developed for Smart Structures

Applying smart materials in aeropropulsion systems may improve the performance of aircraft engines through a variety of vibration, noise, and shape-control applications. To facilitate the experimental characterization of these smart structures, researchers have been focusing on developing analytical models to account for the coupled mechanical, electrical, and thermal response of these materials.

One focus of current research efforts has been directed toward incorporating a comprehensive thermal analysis modeling capability. Typically, temperature affects the behavior of smart materials by three distinct mechanisms: (1) induction of thermal strains because of coefficient of thermal expansion mismatch, (2) pyroelectric effects on the piezoelectric elements, and (3) temperature-

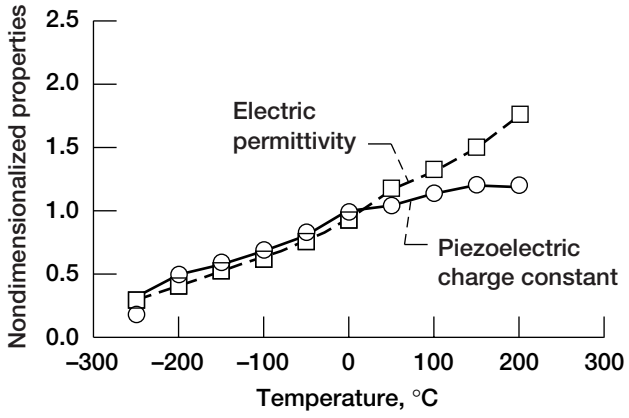

Temperature dependence of piezoelectric material properties.

dependent changes in material properties. Previous analytical models only investigated the first two thermal effects mechanisms. However, since the material properties of piezoelectric materials generally vary greatly with temperature (see the graph), incorporating temperature-dependent material properties will significantly affect the structural deflections, sensory voltages, and stresses.

Thus, the current analytical model captures thermal effects arising from all three mechanisms through thermopiezoelectric constitutive equations. These constitutive equations were incorporated into a layerwise laminate theory with the inherent capability to model both the active and sensory response of smart structures in thermal environments. Corresponding finite element equations were formulated and implemented for both the beam and plate elements to provide a comprehensive thermal effects modeling capability.

Glenn contacts: Ho-Jun Lee, 216–433–3316, Ho-Jun.Lee@grc.nasa.gov, and Dale A. Hopkins, 216–433–3260, Dale.A.Hopkins@grc.nasa.gov

Procedure Developed for Ballistic Impact Testing of Composite Fan Containment Concepts

The fan-containment system in a jet engine is designed to prevent a fan blade from penetrating the engine case in the event that the blade or a portion of the blade separates from the rotor during operation. Usually, these systems consist of a thick metal case that is strong enough to survive such an impact. Other systems consist of a dry aramid fabric wrapped around a relatively thin metal case. In large turbofan engines, metal-containment systems can weigh well over 300 kg, and there is a strong impetus to reduce their weight. As a result, the NASA Lewis Research Center is involved in an effort to develop polymer matrix composite (PMC) fan-containment systems to reduce the weight and cost while maintaining the high levels of safety associated with current systems. Under a Space Act Agreement with AlliedSignal Aircraft Engines, a new ballistic impact test procedure has been developed to quantitatively evaluate the performance of polymer matrix composite systems.

The test procedure uses a curved (half-ring) specimen with an inside diameter of 38 cm (15 in.) and a width of 20.3 cm (8 in.). A metal specimen with this geometry is shown in the photo; however, typical polymer matrix composite test specimens are considerably thicker. During testing, the specimen is supported along both ends and on one edge.

The projectile used in this test is designed to simulate the most important features of a full-scale fan blade at a low cost (see the figure on the next page). It features a relatively thick shank section to simulate the blade attachment region, and the stiffness induced by the geometry of a twisted fan blade is approximated by tapering the thickness of the projectile from tip to shank. The projectile material has a mass of 330 g, and the projectile material is Ti-6Al-4V. In the test, the projectile is accelerated toward the specimen by NASA Lewis' 20.3-cm-diameter gas gun, which can achieve speeds of over 350 m/sec.

Transient finite element analyses showed that the blade simulating projectile performs in a manner similar to that of a scaled fan blade. In a typical test, the projectile was oriented at a 45° angle from the vertical, so that the tip of the projectile would impact the specimen first. The blade then began to

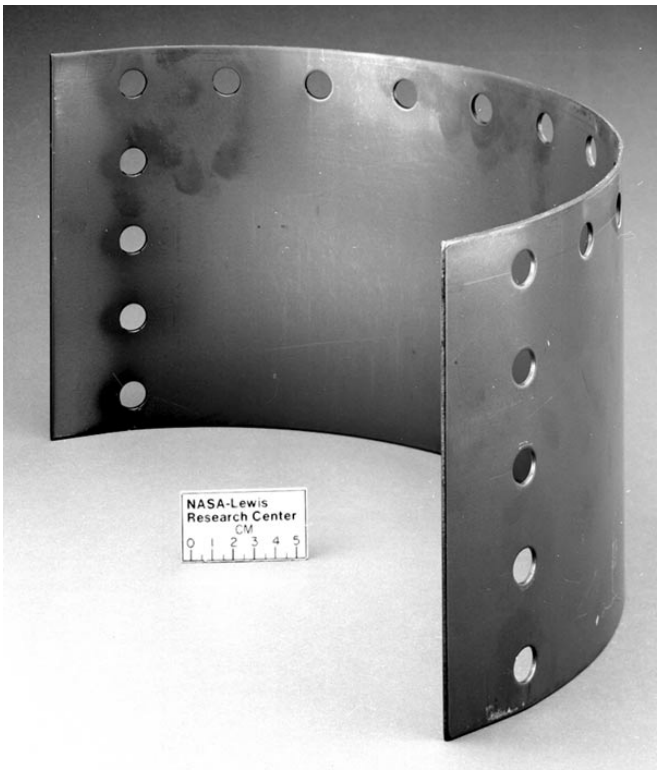

Metal test specimen.

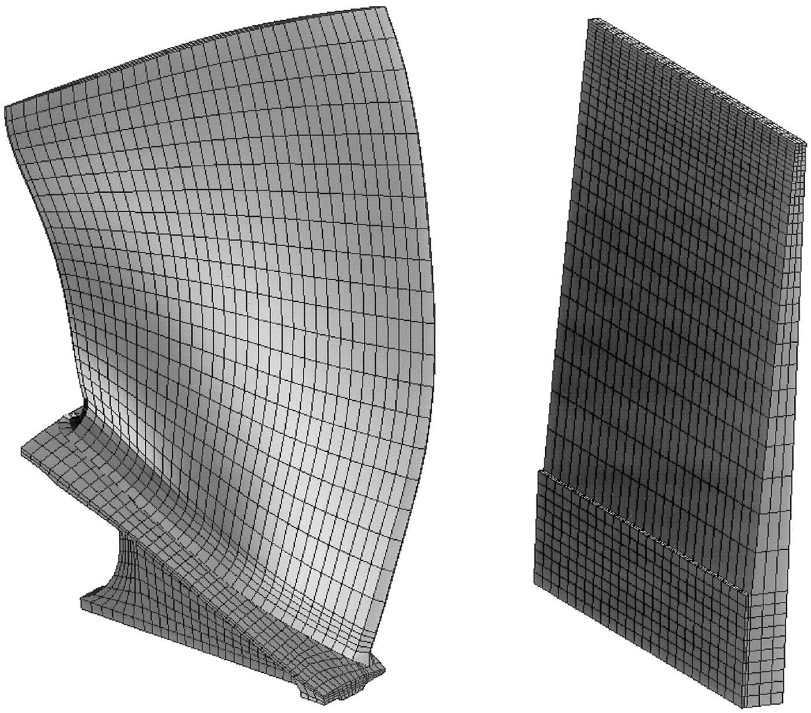

Finite element models. Left: Scaled fan blade. Right: Blade-simulating projectile.

bend and rotate about the tip region, resulting in a secondary impact between the heavy shank section and the specimen. Analyses predicted that this secondary impact would produce more damage than the initial impact at the tip. This is consistent with experimental results.

The test procedure has been used to evaluate a number of different fan containment concepts, including two metallic systems and two composite systems. Preparations are under way for tests of more composite and hybrid metal/composite systems.

Glenn contacts:
Dr. J. Michael Pereira, 216–433–6738,
J.M.Pereira@grc.nasa.gov;
Matthew E. Melis, 216–433–3322,
Matthew.E.Melis@grc.nasa.gov;
Duane M. Revilock, 216–433–3186,
Duane.M.Revilock@grc.nasa.gov; and
Dr. Gary D. Roberts, 216–433–3244,
Gary.D.Roberts@grc.nasa.gov

Acoustics

Low-Noise Potential of Advanced Fan Stage Stator Vane Designs Verified in NASA Lewis Wind Tunnel Test

With the advent of new, more stringent noise regulations in the next century, aircraft engine manufacturers are investigating new technologies to make the current generation of aircraft engines as well as the next generation of advanced engines quieter without sacrificing operating performance. A current NASA initiative called the Advanced Subsonic Technology (AST) Program has set as a goal a 6–EPNdB (effective perceived noise) reduction in aircraft engine noise relative to 1992 technology levels by the year 2000. As part of this noise program, and in cooperation with the Allison Engine Company, an advanced, low-noise, high-bypass-ratio fan stage design and several advanced technology stator vane designs were recently tested in NASA Lewis Research Center's 9- by 15-Foot Low-Speed Wind Tunnel (an anechoic facility). The project was called the NASA/Allison Low Noise Fan (see the figures).

A bypass fan stage consists of a fan and a stator vane assembly. The advanced technology bypass fan stage for this project was 22 in. in diameter and consisted of a low-pressure ratio, 18-bladed fan and an integral, 42-bladed stator vane assembly. The testing used an air turbine propulsion simulator to power the model fan stage across a wide range of operating conditions from idle to full takeoff power at a wind tunnel

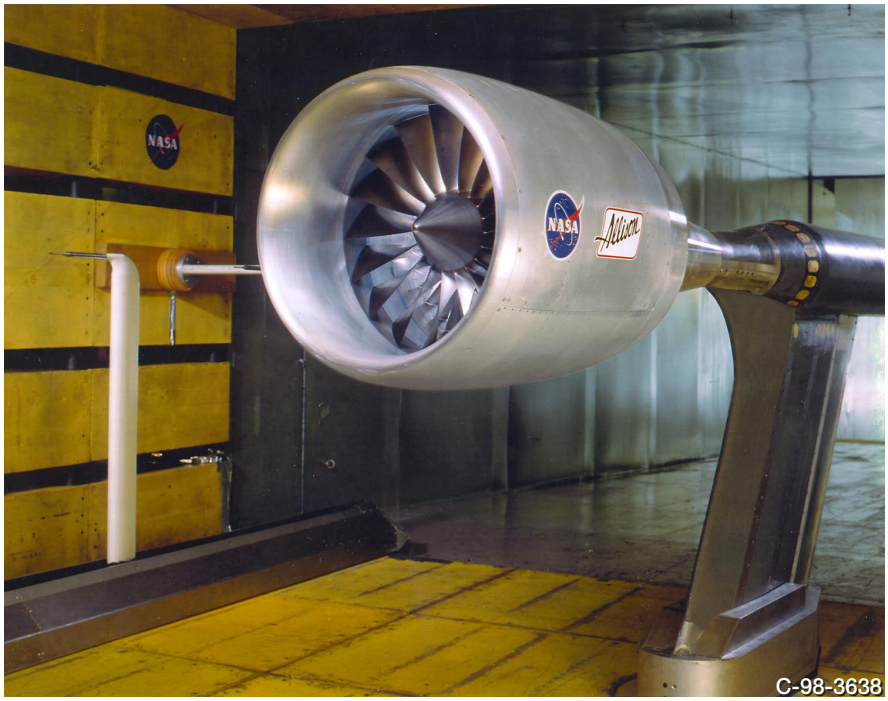

NASA/Allison Engine Company Low Noise Fan test in Lewis' 9- by 15-Foot Low-Speed Wind Tunnel.

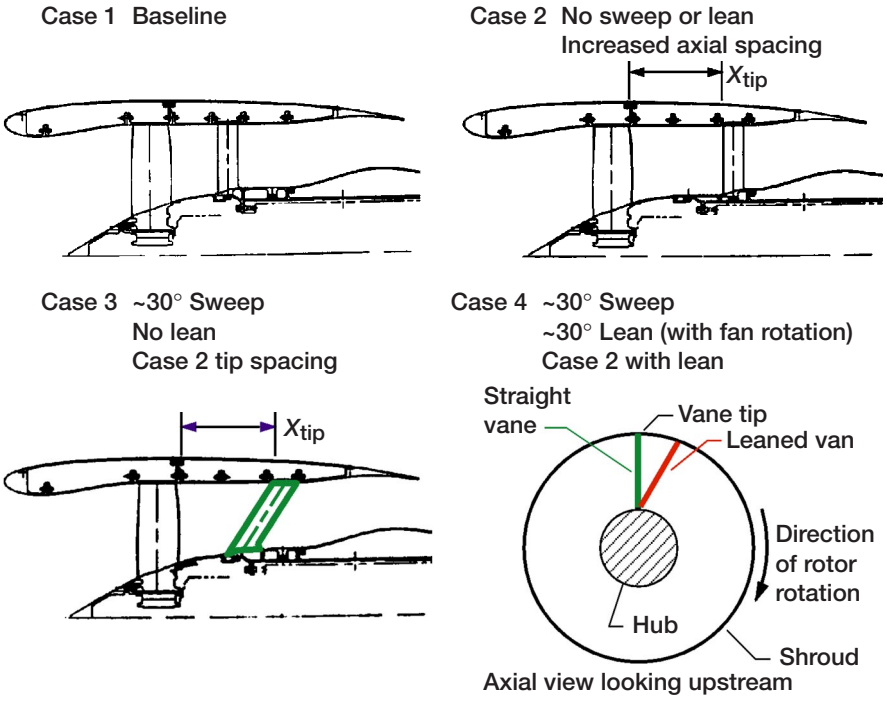

NASA/Allison Low Noise Fan test; stator vane sweep and lean.

velocity of Mach 0.10, or about 67 knots. The main objective of the project was to evaluate the noise reduction potential of a series of advanced stator vane designs. Variations in stator vane geometry that were introduced include increasing the spacing between the fan and the stator vanes, incorporating sweep into the stator vanes (similar to aircraft wing sweep), and finally leaning the swept stator vanes over in the fan direction of rotation. During testing, the acoustic characteristics of each fan and stator vane assembly combination were measured using fixed and traversing microphones inside the wind tunnel. The aerodynamic performance of each fan/stator vane combination was also measured using pressure/temperature rakes and force balances to determine what effect the new low-noise stator vanes would have on the fan stage efficiency.

The research results generated as part of this project allowed a major interim milestone, to demonstrate a 3–EPNdB reduction in noise by 1997**,** to be reached for the Advanced Subsonic Technology Program. Test results will be used to create a data base that engineers can draw upon for comparison with computer predictions of the effect of fan stage geometry on aircraft engine noise. In addition, aircraft manufacturers will be able to use these results to influence the design of the next generation of advanced technology aircraft engines or the next growth version of current technology engines.

Glenn contacts:
Christopher E. Hughes, 216–433–3924, Christopher.E.Hughes@grc.nasa.gov; and Richard P. Woodward, 216–433–3923, Richard.P.Woodward@grc.nasa.gov

Acoustics and Thrust of Separate Flow Exhaust Nozzles With Mixing Devices Investigated for High Bypass Ratio Engines

The jet noise from modern turbofan engines is a major contributor to the overall noise from commercial aircraft. Many of these engines use separate nozzles for exhausting core and fan streams. The illustration shows a typical exhaust nozzle system for a bypass ratio of about 5. As a part of NASA's Advanced Subsonic Technology (AST) program, the NASA Glenn Research Center at Lewis Field led an experimental investigation using model-scale nozzles in Glenn's Aero-Acoustic Propulsion Laboratory. The goal of the investigation was to develop technology for reducing the jet noise by 3 EPNdB.[1] Teams of engineers from Glenn, the NASA Langley Research Center, Pratt & Whitney, United Technologies Research Corporation, the Boeing Company, GE Aircraft Engines, Allison Engine Company, and Aero Systems Engineering contributed to the planning and implementation of the test.

New nozzles were designed to reduce the fully expanded jet velocity by mixing (1) core flow with fan flow only, (2) fan flow with ambient flow only, or (3) both flows simultaneously. Depending on the type of mixing attempted, these designs fell into two broad categories: tabs and chevrons. Tabs are severe protrusions into the flow at the nozzle exit plane. Chevrons are also protrusions, but of much less severity than tabs. The aggressive mixing produced by the tabs greatly reduced low-frequency

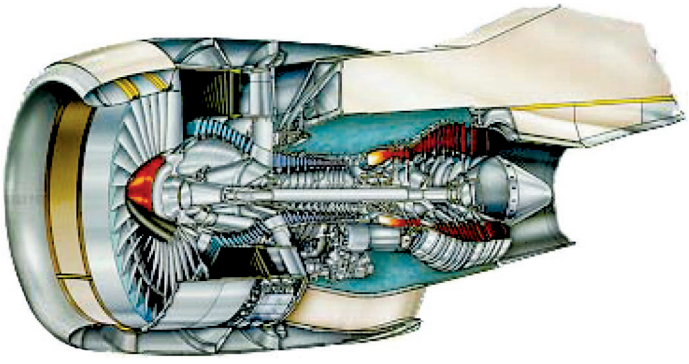

Typical installed separate-flow exhaust nozzle system.

[1]Effective perceived noise in decibels.

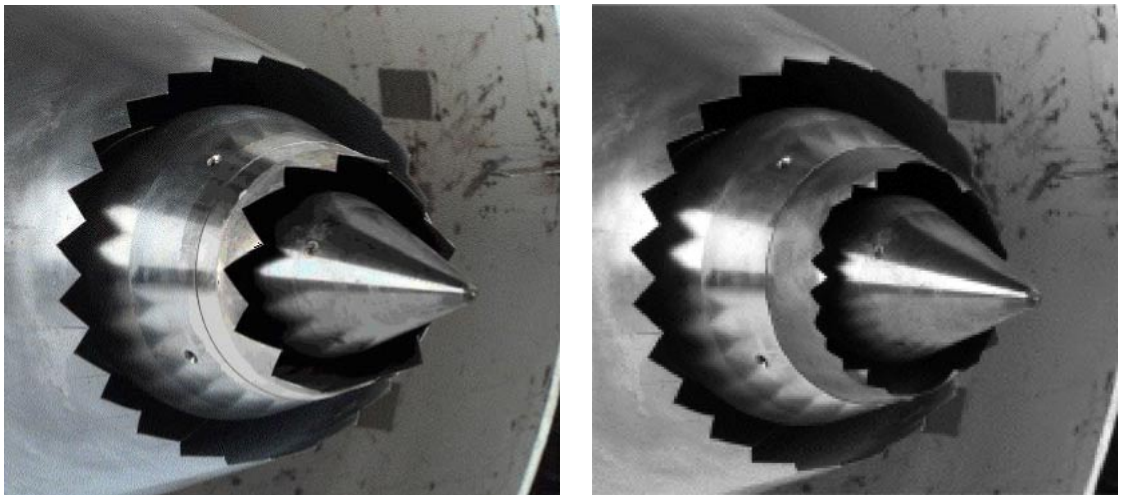

Left: Chevrons on both nozzles. Right: Chevrons on fan nozzle and tabs on core nozzle.

noise, but with the penalty of tab-induced high-frequency noise. Chevrons, which provided a more balanced approach to mixing, reduced low-frequency noise without significant chevron-induced high-frequency noise. Other nozzle designs attempted to shield the core flow by using a scarf fan nozzle and an offset fan nozzle.

A total of 54 exhaust nozzle systems were tested, including various combinations of nozzle designs within each category (tabs and chevrons) for each flow (core and fan). An extensive data base was generated on far-field acoustics, plume Schlieren images, exhaust plume pressures and temperatures, plume infrared signatures, jet noise source locations measured by one- and two-dimensional phased arrays, and thrust performance at a simulated cruise Mach of 0.8.

Several exhaust nozzle systems reduced jet noise by more than 2.5 EPNdB, calculated for a 1500-ft level flyover, without significant thrust loss either at takeoff or at cruise. The photos on the preceding page show two of the best exhaust nozzle systems.

Because of increasingly stringent restrictions near airports, the noise of an aircraft, much like its range and payload capability, has become a competitive factor. This investigation has generated great interest because of its timeliness and application to current exhaust nozzle systems. We expect the resultant technologies to be incorporated in future turbofan engines.

Glenn contacts:
Naseem H. Saiyed, 216–433–6736,
Naseem.Saiyed@grc.nasa.gov; and
Dr. James E. Bridges, 216–433–2693,
James.E.Bridges@grc.nasa.gov

Mechanical Components

New High-Temperature Turbine Seal Rig Fabricated

Current NASA program goals for aircraft engines and vehicle performance include reducing direct operating costs for commercial aircraft by 3 percent in large engines and 5 percent in regional engines, reducing engine fuel burn up to 10 percent, and reducing engine oxides of nitrogen emissions by more than 50 percent. Significant advancements in current gas turbine engines and engine components, such as seals, are required to meet these goals. Specifically, advanced seals have been identified as critical in meeting engine goals for specific fuel consumption, thrust-to-weight ratio, emissions, durability, and operating costs.

In a direct effort to address and make progress toward these goals, researchers at the NASA Glenn Research Center at Lewis Field have developed a unique high-temperature, high-speed engine seal test rig to evaluate seals under the temperature, speed, and pressure conditions anticipated for next generation turbine engines. This new seal test rig has capabilities beyond those of any existing seal rigs. It can test air seals (i.e., labyrinth, brush, and new seal concepts) at temperatures of up to 1500 °F and pressures up to 100 psid (even higher pressures are possible at lower temperatures), and at all surface speeds anticipated in future NASA (Ultra Efficient Engine Technology, UEET and Integrated High-Performance Turbine Engine Technology, IHPTET) engine programs. In addition, seals can be tested offset from the rotor centerline, in the rotor runout condition,[1] and with simulated mission profiles. Support for this new rig was provided by NASA Glenn, the U.S. Air Force, and the U.S. Army.

The turbine seal test facility is planned to be installed at Glenn by October of 2000. Installation will include upgrading airflow systems, heating systems, instrumentation and measurement systems, and data acquisition systems. The operational envelope of the test rig will be verified through its full operating capabilities prior to actual seal tests.

For more information about turbine seal work at Glenn, please visit the following web pages:
http://www.grc.nasa.gov/WWW/5900/5950/
http://www.grc.nasa.gov/WWW/TurbineSeal/TurbineSeal.html

U.S. Army Research Laboratory at Glenn contact:
Irebert R. Delgado, 216–433–3935,
Irebert.R.Delgado@grc.nasa.gov

Glenn contacts:
Margaret P. Proctor, 216–977–7526,
Margaret.P.Proctor@grc.nasa.gov; and
Dr. Bruce M. Steinetz, 216–433–3302,
Bruce.M.Steinetz@grc.nasa.gov

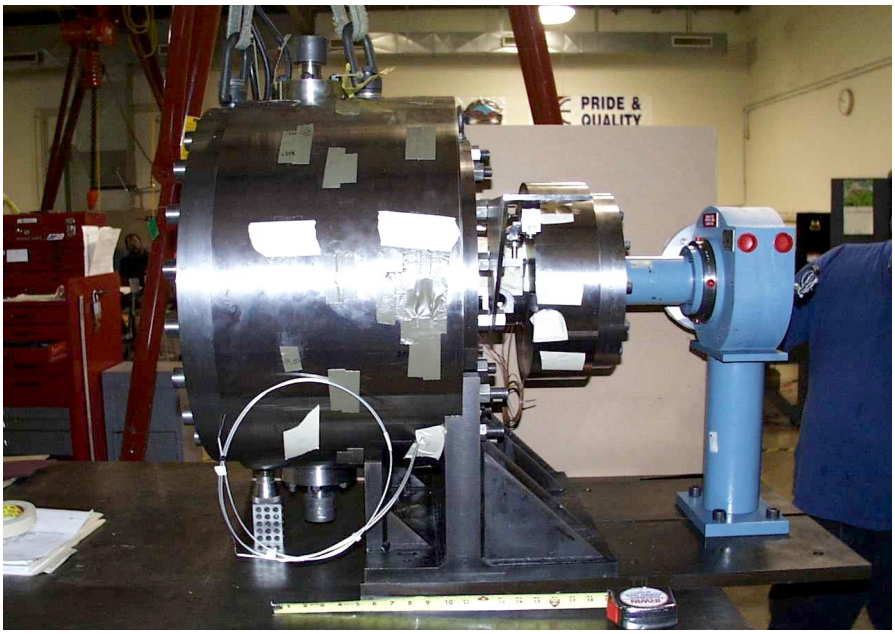

High-Temperature Seal Rig fabrication complete.

[1]With the rotor outer diameter eccentric to the rotor inner diameter.

NASA Space Mechanisms Handbook—Lessons Learned Documented

The need to improve space mechanism reliability is underscored by a long history of flight failures and anomalies caused by malfunctioning mechanisms on spacecraft and launch vehicles. Some examples of these failures are listed in the table. Mechanism anomalies continue to occur and to be a cause of catastrophic mission failures. Several factors cause problems for space system mechanisms. The space environment produces wide temperature ranges, thermal gradients, and rapid changes in temperature, which can bind the moving parts of mechanisms. Ultraviolet radiation and vacuum cause the properties of many materials to degrade to unacceptable levels or to behave differently in space than on Earth, making it difficult to simulate operation during ground tests. The lack of gravity in space causes mechanisms to operate differently than on the ground. Sometimes the effects of zero gravity can be simulated to some degree in ground testing, such as by offloading the weight of a deployable appendage. Other effects, such as lubricant migration, cannot be simulated and must be considered in the design. Finally, the launch environment imposes severe dynamic loads on mechanisms and can cause structural damage, loosen fasteners, and damage delicate surfaces.

Given these complexities, it is not surprising that it is not always possible to uncover and correct all the hidden problems with mechanisms prior to launch. Fortunately, there are ways to reduce the number of failures involving mechanisms and/or mitigate the effects of a failure of a component. In many cases, failures were caused by design problems that have caused similar failures in the past, and thus could have been avoided had the designers been aware of the past mistakes. Because much experience has been gained over the years, many specialized design practices have evolved and many unsatisfactory design approaches have been

SUMMARY OF SPACECRAFT MECHANISM FAILURES

Program	Date	Problem	Cause
Program 461	1964	Solar array failed to deploy fully	Mishandling during stowage
STP 67–2 (OV2–5)	1968	Solar array booms failed to deploy fully	Field modification problem
777	1970	Omni antenna latch broke during spin-up	Attitude control instability
Program A	1971	Antenna failed to deploy fully	Wire harness binding
Program B	1971	Solar array deployed late	Silicon rubber sticking
STP 71–5	1972	Boom failed to deploy	Dynamic clearance problem
Skylab	1973	Solar array failed to deploy	Interference with cabling or thermal blankets
Transit	1975	Solar array failed to deploy fully; cable hung up	Anomalous flat trajectory caused high heating rates
Viking	1975	Sampling arm failed to deploy	Debris in gear train
STP 74–1 (Solrad)	1976	Solar panel failed to deploy	Release mechanism binding
DMSP F–1	1976	Solar array failed to deploy fully	Excessive wire harness stiffness
DMSP F–2	1977	Solar array delayed release	Friction welding
		Science boom failed to deploy fully	Microswitch failed
Voyager	1977	Science boom failed to deploy fully	Microswitch failed
		Scan platform gearbox seized	Lubricant failed
		Magnetometer boom misaligned	Unknown
Seasat	1978	Spacecraft power failed	Slip ring debris between power and ground rings
Apple	1981	Solar array failed to deploy	Failure of deployment device
DE	1981	Sensing antenna failed to deploy	Unknown
Insat 1	1982	Solar sail failed to deploy	Unknown
ERBS	1982	Solar array failed to deploy	Unknown
GLOMR	1985	Spacecraft failed to separate from orbiter	Canister door did not open fully
VUE	1988	Telescope failed to rotate about azimuth	Inadequate torque margin on azimuth caging arm
Galileo	1989	High-gain antenna failed to deploy	Cold welding in ball and socket joint
		Instrument cover jettisoned late	Thermal binding
Magellan	1989	Solar array failed to latch at end of travel	Microswitch misadjusted
Macsat	1990	Gravity gradient boom failed to deploy	Inadequate force margin
CRRES	1990	Magnetometer boom failed to orient fully	Interference between thermal blanket Velcro and wiring harness
Ulysses	1990	Spin-stabilized spacecraft wobbled	Antenna boom thermal distortion caused spacecraft center-of-gravity offset
Hubble	1990	Solar array booms jittered as telescope went between sun and shade	Thermal gradient across boom diameter
ANIK E2	1991	C-band antenna failed to fully deploy	Thermal blanket interference
Unknown		Sampling arm failed to deploy	Screw backed out and wedged against housing
Tether Satellite System	1993	Reel-out mechanism jammed	Screw added for structural margin interfered with reel-out mechanism
GOES 10	1997	Solar Array Drive malfunctioned	Under investigation

identified. In many cases, however, this knowledge has remained with the individual mechanism designer and has not been widely shared.

To alleviate this situation, NASA and the NASA Lewis Research Center conducted a Lessons Learned Study (Shapiro et al., 1995a and 1995b) and wrote a handbook to document what has been learned in the past. The primary goals of the handbook were to identify desirable and undesirable design practices for space mechanisms and to reduce the number of failures caused by the repetition of past design errors. Another goal was to identify a variety of design approaches for specific applications and to provide the associated considerations and caveats for each approach in an effort to help designers choose the approach most suitable for each application. The handbook also provides some design principles. These principles, which can be applied to any mechanism to avoid common failure modes, can be particularly useful for the esoteric mechanism configurations that dwell on topics that are not unique to space applications, it does cite references, where appropriate, for additional information or more indepth discussion of specific topics.

The handbook is divided into six parts. Part I, *Introduction to Space Mechanisms*, starts with an overview of various types of spacecraft mechanisms. It then discusses the requirements that are typically imposed on space mechanisms, their implications, and what steps can be taken to ensure that the requirements are met. The discussion concludes with a description of a typical mechanism design process and addresses how the design evolves from concept to fabrication. Part II, *Design Considerations for Space Mechanisms*, provides guidelines for recommended design practices for most spacecraft mechanisms. It also contains subsequent chapters that are devoted to guidelines applicable to specific types of mechanisms. Part III, *Space Mechanism Components*, proceeds to the next level of detail and discusses design considerations for mechanisms. This part is divided into general design guidelines that are applicable to the various components of spacecraft mechanisms. Part IV delves into two areas of testing, environmental testing and tribological testing of space mechanisms. Part V lists expert areas and the names and addresses of individuals who are experts in those areas of testing. Finally, Part VI lists testing laboratories and the individuals involved in the testing programs.

We anticipate that this handbook will be useful to a variety of readers. By studying the numerous guidelines presented in this handbook, entry-level design engineers will be able to quickly gather practical information on how to avoid common pitfalls. Experienced mechanical design engineers who are new to space mechanism applications will benefit from learning the unique requirements created by the space and launch environments. Also, users who need to evaluate their suppliers' products, but have little personal experience in the design of mechanisms, can find useful information on identifying key performance, risk, and cost drivers for most space mechanisms and components. The Space Mechanisms Handbook is available from Glenn's Mechanical Components Branch.

Glenn contact: Robert L. Fusaro, 216–433–6080, Robert.L.Fusaro@grc.nasa.gov

Experimental and Analytical Determinations of Spiral Bevel Gear-Tooth Bending Stress Compared

Spiral bevel gears are currently used in all main-rotor drive systems for rotorcraft produced in the United States. Applications such as these need spiral bevel gears to turn the corner from the horizontal gas turbine engine to the vertical rotor shaft. These gears must typically operate at extremely high rotational speeds and carry high power levels. With these difficult operating conditions, an improved analytical capability is paramount to increasing aircraft safety and reliability. Also, literature on the analysis and testing of spiral bevel gears has been very sparse in comparison to that for parallel axis gears. This is due to the complex geometry of this type of gear and to the specialized test equipment necessary to test these components.

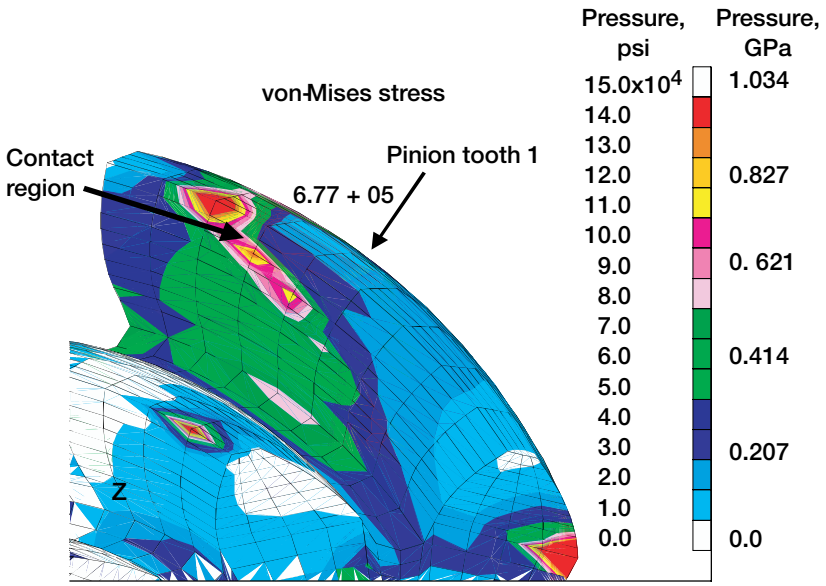

Example of stress output produced by the model.

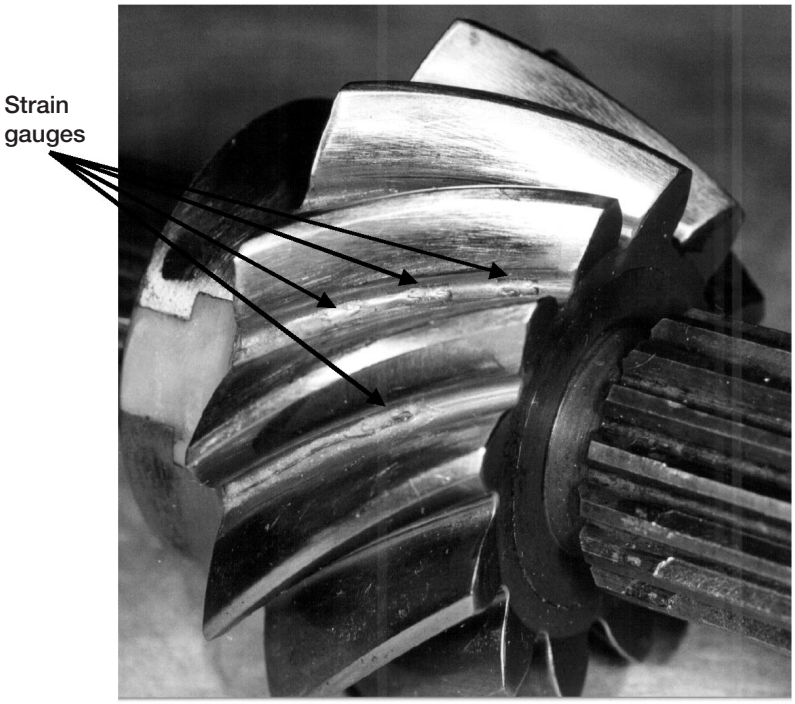

Instrumented spiral bevel pinion used in the tests.

To develop an analytical model of spiral bevel gears, researchers use differential geometry methods to model the manufacturing kinematics. A three-dimensional spiral bevel gear modeling method was developed that uses finite elements for the structural analysis. This method was used to analyze the three-dimensional contact pattern between the test pinion and gear used in the Spiral Bevel Gear Test Facility at the NASA Glenn Research Center at Lewis Field. Results of this analysis are illustrated in the top figure. The development of the analytical method was a joint endeavor between NASA Glenn, the U.S. Army Research Laboratory, and the University of North Dakota.

To validate the predictions made by the newly developed numerical method, experimental tests were conducted on Glenn's Spiral Bevel Gear Test Facility. The bottom figure shows the instrumented spiral bevel pinion that was used in the test. The instrumented spiral bevel gears were tested from static to high rotational speeds (14,400 rpm) at various levels of load (up to 539 kW (720 hp)).

Results from the experiments were compared with those produced analytically by the newly developed

model. As seen in the final figure, the experimental and analytical results are in good agreement with each other. In addition, both sets of results indicate that the peak gear-tooth bending stresses occur in the fillet radius near the midface of the tooth.

Find out more about this research on the World Wide Web: http://www.grc.nasa.gov/WWW/5900/5950/

**Glenn/U.S. Army Research Laboratory contact:
Dr. Robert F. Handschuh,
216–433–3969,
Robert.F.Handschuh@grc.nasa.gov**

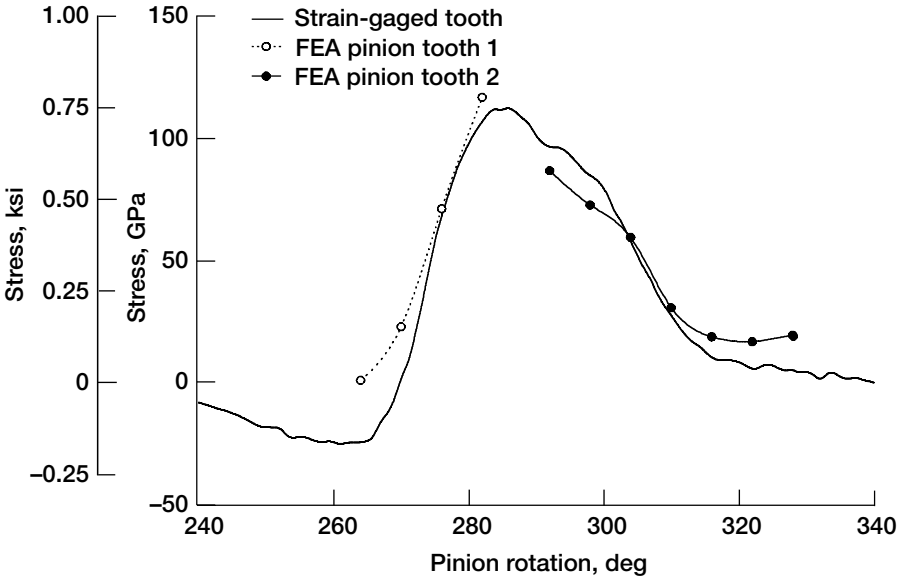

Comparison of experimental and analytical stresses at the pinion midface at 14,400 rpm and 539 kW (720 hp).

Metrology Evaluation of Superfinished Gears Completed

Gears, bearings, and similar mechanical elements transmit loads through the surfaces that are in contact with one another. Thus, the fatigue lives of gears can be improved by providing smoother tooth surfaces. At the NASA Lewis Research Center, we completed a metrology evaluation of one method for making gears with a highly polished, mirrorlike surface (see the photo). The polished gears were measured carefully. The measurement data showed that the polishing process did, indeed, reduce the surface roughness but did not change the overall tooth shape in any harmful way.

This work was done as a partnership of NASA, the U.S. Army, and the University of Wales. NASA provided conventionally ground gear specimens and has begun testing to determine the fatigue lives of the superfinished gears. Under contract, the University of Wales superfinished the gears and inspected them before and after the superfinishing operation. The U.S. Army European Research Office provided the funds and procured the contract with the University of Wales.

For gears, the rate of fatigue is greatly affected by the ratio of the oil film thickness to the roughness of the contacting surfaces. In this work we are seeking to improve fatigue lives by reducing the surface roughness. Conventionally ground,

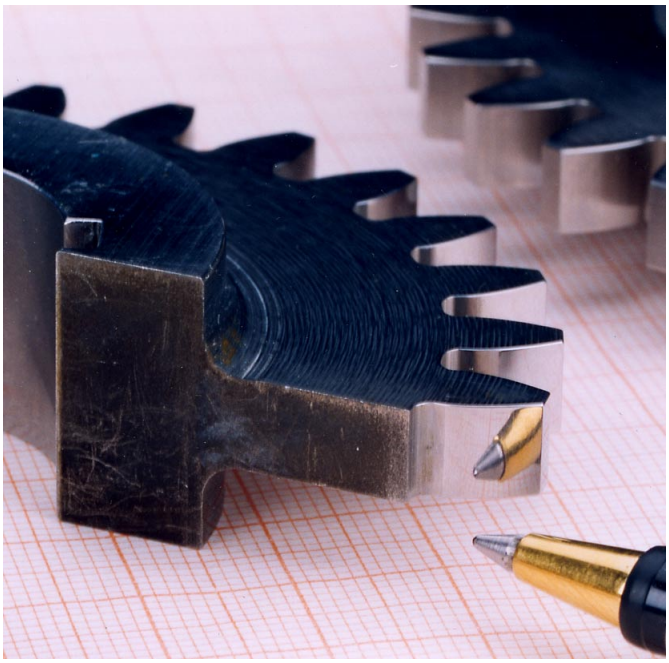

Highly polished surface of superfinished gears.

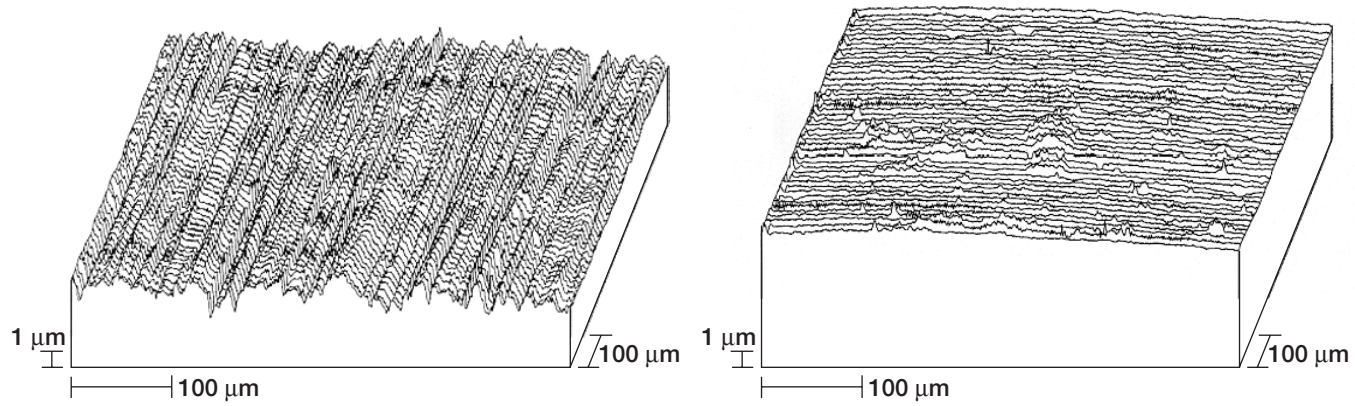

Profile of tooth surfaces. Left: Ground. Right: Superfinished.

aerospace quality gears were manufactured, and their geometry was inspected. Next, the gears were superfinished by placing them in a vibrating bath consisting of water, detergent, abrasive powder, and small pieces of zinc. Upon removal from the bath, the surfaces were highly polished (see the preceding photo). The gears were then again inspected, and the measurements of the gears before and after the superfinishing operation were compared. Typical inspection data are provided in the plots above. The grinding marks are clearly evident in the figure on the left. Superfinishing removed the peaks of the grinding marks and left a much smoother surface as is evident in the figure on the right. Profile and spacing checks proved that the overall gear tooth shape was not affected in any harmful way. Superfinishing uniformly removed approximately 2.5 μm from each surface. See Snidle, Evans, and Alanou (1997) for a complete report.

Glenn contact:
Timothy L. Krantz, 216–433–3580,
Timothy.L.Krantz@grc.nasa.gov

Gear Durability Shown To Be Improved by Superfinishing

Gears, bearings, and similar mechanical elements transmit loads through contacting surfaces. At the NASA Glenn Research Center at Lewis Field, we postulated that the fatigue lives of gears could be improved by providing smoother tooth surfaces. A superfinishing process was applied to a set of conventionally ground, aerospace-quality gears. This process produced a highly polished, mirrorlike surface as shown in the photograph on page 73. The surface fatigue lives of both superfinished and conventionally ground gears were measured by experiments. The superfinished gears survived about four times longer than the conventionally ground gears.

These superfinished gears were produced from conventionally ground, aerospace-quality gears whose geometry had been inspected. The gears were superfinished by placing them in a vibrating bath consisting of water, detergent, abrasive powder, and small pieces of zinc. Upon removal from the bath, the surfaces were highly polished, as depicted in the following photograph. The gears were again inspected, and dimensional measurements made before and after the superfinishing operation were compared. Superfinishing removed the peaks of the grinding marks and left a much smoother surface. Profile and spacing checks proved that the overall gear tooth shape was not affected in any harmful way. Superfinishing uniformly removed approximately 2.5 μm from each surface. See Snidle, Evans, and Alanou (1997) for a complete report.

Superfinished 28-tooth, 8-pitch gears made from AISI 9310 steel were tested at Glenn at a hertzian contact stress of 1.71 GPa (248 ksi) for 300 million cycles or until surface failure occurred on any one tooth as illustrated in the photograph on the next page. The fatigue data, shown on Weibull coordinates in the graph, were analyzed using the method of Johnson (1964). The lives shown are the lives of gear pairs in terms of stress cycles or revolutions. The lives of the superfinished gears

Typical surface fatigue failure.

were about four times longer than those of conventionally ground gears. The confidence number that the 10 percent life of the superfinished gears is greater than the 10 percent life of the conventionally ground gears is more than 90 percent, a statistically significant result.

This work was done as a partnership between NASA, the U.S. Army (Army Research Laboratory and The Army European Research Office), and the University of Wales.

Find out more about this research on the World Wide Web: http://www.grc.nasa.gov/WWW/5900/5950/

U.S. Army Research Laboratory at Glenn contact:
Timothy L. Krantz, 216–433–3580,
Timothy.L.Krantz@grc.nasa.gov

Glenn contact:
James J. Zakrajsek, 216–433–3968,
James.J.Zakrajsek@grc.nasa.gov

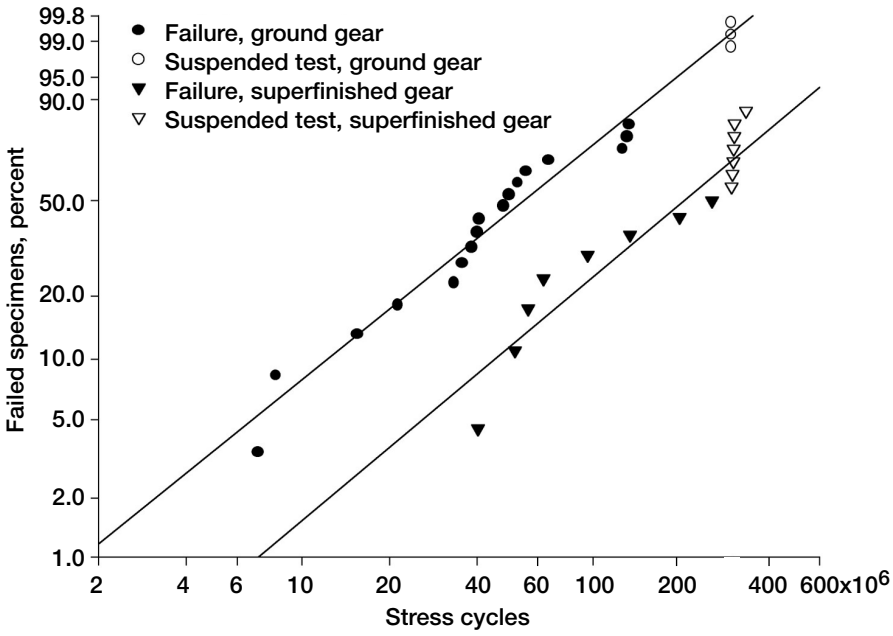

Weibull plot of gear fatigue experiments.

Three-Dimensional Gear Crack Propagation Studied

Gears used in current helicopters and turboprops are designed for light weight, high margins of safety, and high reliability. However, unexpected gear failures may occur even with adequate tooth design. To design an extremely safe system, the designer must ask and address the question, "What happens when a failure occurs?" With gear-tooth bending fatigue, tooth or rim fractures may occur. A crack that propagates through a rim will be catastrophic, leading to disengagement of the rotor or propeller, loss of an aircraft, and possible fatalities. This failure mode should be avoided. A crack that propagates through a tooth may or may not be catastrophic, depending on the design and operating conditions. Also, early warning of this failure mode may be possible because of advances in modern diagnostic systems.

One concept proposed to address bending fatigue fracture from a safety aspect is a split-tooth gear design (Drago, Sane, and Brown, 1997). The prime objective of this design would be to control crack propagation in a desired direction such that at least half of the tooth would remain operational should a bending failure occur. A study at the NASA Lewis Research Center analytically validated the crack-propagation failsafe characteristics of a split-tooth gear (Lewicki et al., 1999). It used a specially developed three-dimensional crack analysis program that was based on boundary element modeling and principles of linear elastic fracture mechanics. Crack shapes as well as the crack-propagation life were predicted on the basis of the calculated stress intensity factors, mixed-mode crack-propagation trajectory theories, and fatigue crack-growth theories.

The following figures show the effect of the location of initial cracks on crack propagation. Initial cracks in the fillet of the teeth produced stress intensity factors of greater magnitude (and thus, greater crack growth rates) than those in the root or groove areas of the teeth. Crack growth was simulated in a case study to evaluate crack-propagation paths (see the figure on the next page). Tooth fracture was predicted from the crack-growth simulation for an initial crack in the tooth fillet region. This was the desired failure mode for an ultrasafe design. Lastly, tooth loads on the uncracked mesh of the split-tooth design were up to five times greater than those on the cracked mesh if equal deflections of the cracked and uncracked teeth were considered. This effect needs to be considered in the design of a split-tooth configuration.

This work was done in-house at Lewis in support of the National Rotorcraft Technology Center project, Ultra-Safe Gear Design, with the Boeing Defense

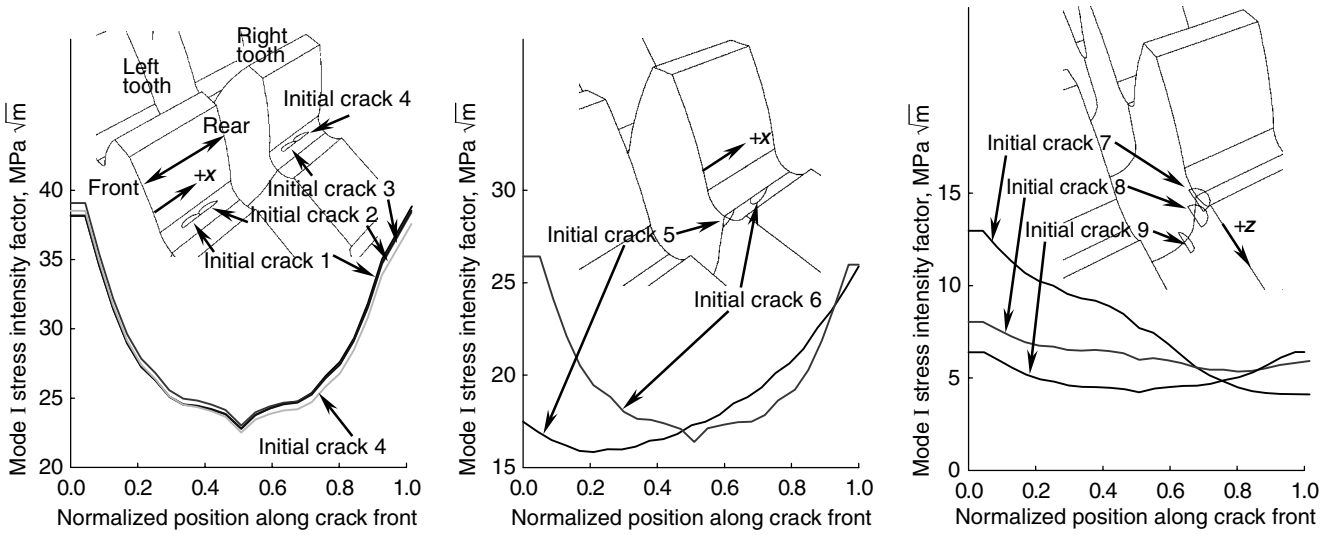

Effect of initial crack location on mode I stress intensity factors. Left: Tooth fillet locations. Center: Tooth foot locations. Right: Tooth groove locations.

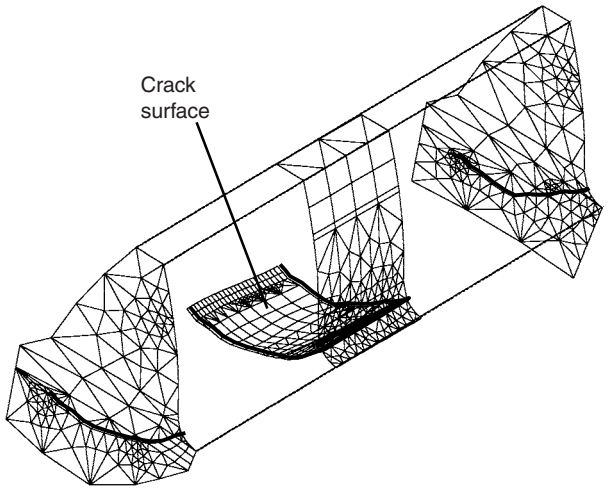

Exploded gear tooth view of predicted crack growth after 15 steps.

and Space Group. The crack-propagation package was developed by the Cornell Fracture Group at Cornell University. The reported results, which are the initial findings of Lewis' gear-crack-propagation research for the Rotorcraft Base Program, will be further investigated to develop generalized gear design guidelines.

Glenn contact:
Dr. David G. Lewicki, 216–433–3970,
David.G.Lewicki@grc.nasa.gov

Pressure-Balanced, Low-Hysteresis Finger Seal Developed and Tested

The "finger seal" is a revolutionary new technology in air-to-air sealing for secondary flow control and gas path sealing in gas turbine engines. Although this seal was developed for gas turbines, it can be

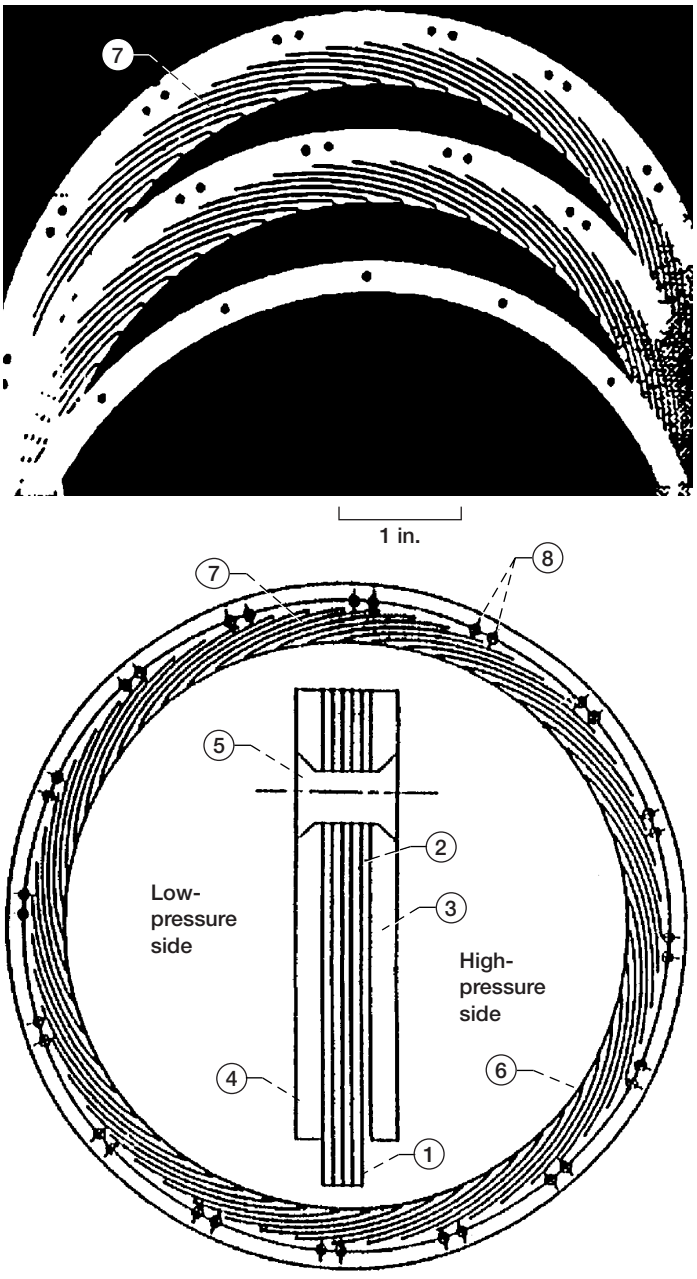

1. Finger element
2. Spacer
3. Forward cover plate
4. Aft cover plate
5. Rivet
6. Finger contact pad
7. Finger
8. Indexing and rivet holes

Baseline finger seal and its nomenclature.

used in any machinery where a high-pressure air cavity has to be sealed from a low-pressure air cavity, for both static and rotating applications. Recently patented (Johnson and Medlin, 1992) by AlliedSignal Engines, the finger seal has demonstrated considerably less air leakage than a conventional labyrinth seal, and it costs considerably less than a brush seal.

The availability of a long-life, low-leakage finger seal has many benefits for propulsion gas turbine engines. The most direct benefit would be to replace labyrinth seals at locations where very high pressures drop directly to the ambient pressure, typically main engine and thrust balance seals. This could save 1 to 2 percent of the engine flow, directly reducing specific fuel consumption by 0.7 to 1.4 percent and operating costs by 0.35 to 0.7 percent. Finger seals are made by photoetching finger shapes around the inner diameter of thin metal laminate rings, stacking the laminates so that the fingers of one laminate overlap the fingers of the adjacent laminates, sandwiching the stack of laminates between two sideplates, and riveting the whole stack together. Some final machining is required. The cost to produce finger seals is estimated to be 40 to 50 percent of the cost to produce brush seals.

A low-hysteresis finger seal designed by AlliedSignal Engines under a NASA contract was successfully developed and tested in a turbine seal rig at the NASA Glenn Research Center at Lewis Field. Finger seal air leakage measured 20 to 70 percent less than for a typical four-knife labyrinth seal with a 0.005-in. radial clearance. Finger seal operation was demonstrated at two extreme turbine operating conditions: (1) a tip speed of 778 ft/sec, a pressure differential of 60 psi, and an operating temperature of 1000 °F and (2) a tip speed of 945 ft/sec, a pressure differential of 80 psi, and an operating temperature of 800 °F. A total of 13 finger seal configurations were tested to achieve the low-hysteresis design. The best design is a pressure-balanced finger seal with higher stiffness fingers. This design demonstrated very low hysteresis in repeated rig testing. The low-hysteresis seal design has undergone extensive rig testing to assess its hysteresis, leakage performance, and life capabilities. On the basis of this extensive testing, we have determined that the finger seal is ready for testing in an engine (see Arora et al., 1999 for more details).

For more information about turbine seal work at Glenn, refer to our Web pages:
Mechanical Components Branch:
http://www.grc.nasa.gov/WWW/5900/5950/

Turbine Seals:
http://www.grc.nasa.gov/WWW/TurbineSeal/TurbineSeal.html

Glenn contacts:
Margaret P. Proctor, 216–977–7526, Margaret.P.Proctor@grc.nasa.gov; and
Dr. Bruce M. Steinetz, 216–433–3302, Bruce.M.Steinetz@grc.nasa.gov

Lewis-Developed Seal Is a Key Technology for High-Performance Engines

Ultrahot, pressurized combustion gases within the National Aerospace Plane (NASP) engine needed to be sealed to prevent them from leaking past the movable engine panels to rear engine cavities and causing the engine or entire aircraft to fail. The need to seal the hot gases and distortion of the engine's sidewalls required the development of a device nearly as flexible as a rubber O-ring yet able to operate at over 2000 °F. The advanced, High-Temperature, Flexible Fiber Preform Seal is one very important step in that direction.

This seal is braided of emerging high-temperature ceramic fibers or superalloy wires into a flexible, flow-resistant seal. It has been used for numerous NASA applications since it was patented in 1992. The patented technology was used by GE in the joint NASA/Department of Defense/GE Integrated High Performance Turbine Engine Technology (IHPTET) program. This hybrid rope seal successfully sealed the perimeter of advanced nickel-aluminide turbine vane airfoils, allowing the vanes to grow relative to the supporting structure, thus overcoming the thermal shock failure experienced with the conventional sealing approach. In a successful full-scale Joint Turbine Advanced Gas Generator (JTAGG) engine test, the high-temperature turbine vane/seals, in combination with several other advanced technologies, contributed to meeting the program goals of reducing specific fuel consumption by 20 percent and increasing the engine power-to-weight ratio by 40 percent.

Seal Requirements

- Operate hot—
  Seal/metal temperature, 1200 °F
  Gas stream temperature, last stage vane
- Exhibit low leakage; minimize cooling requirements
- Permit relative vane-to-shroud thermal growths
- Seal complex turbine airfoil geometries
- Resist abrasion in high acoustic environment
- Maintain structural integrity

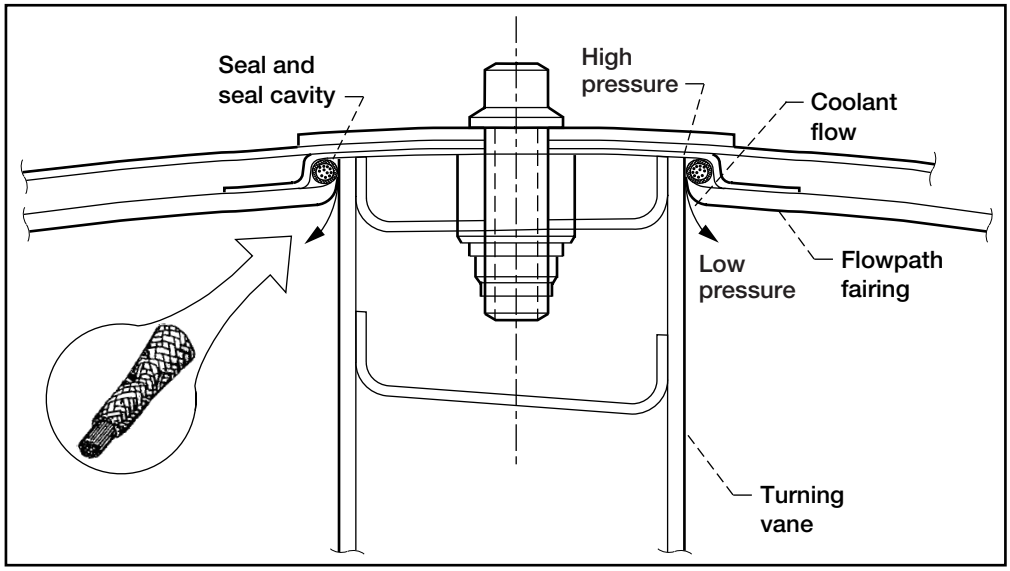

Pratt & Whitney turbine vane seal for the F22 fighter engine.

The invention is being evaluated by Pratt & Whitney as a potential replacement for sealing interfaces between large nozzle turning vanes and flow-path fairing elements (see the figure) for the F119 engine that will be used in the F22 fighter, the country's next-generation premier fighter. Pratt & Whitney tested the seal in a full-scale engine (Fall 1997), and after 24 hr of testing the seals showed no signs of degradation.

In addition, Williams International is evaluating the seal for an advanced turbine engine, and AlliedSignal Inc. is considering using the seal as part of an industrial gas turbine generator for auxiliary electric power. Lewis researchers helped qualify the seals for subsequent engine and industrial system tests.

NASA is developing a future replacement for the space shuttle and will be testing many of the technologies on an experimental vehicle, the X–33. The X–33 contractor team is exploring possible use of the NASA rope seals for sealing the joints between the aerospike engine nozzles and the joints between the vehicle's heat-resistant thermal tiles.

Although the seal was developed for aerospace uses, it is being evaluated for industrial applications as well. Under a reimbursable Space Act Agreement, NASA Lewis is working with Praxair, a major U.S. producer of industrial gases, to adapt the seal technology for use in the company's high-temperature, proprietary industrial gas systems. Other potential future applications include sealing furnace doors, heat exchangers, and continuous-casting and glass-processing equipment.

The seal is able to bend around sharp radii (about equal to the seal's diameter) conforming to and sealing complex components. In addition, the seal exhibits low leakage, retains resilience after high-temperature cycling, and can support structural loads.

For more information, be sure to check our web site: http://www.grc.nasa.gov/WWW/TU/InventYr/1996Inv_Yr.htm

Glenn contact: Dr. Bruce M. Steinetz, 216–433–3302, Bruce.M.Steinetz@grc.nasa.gov

Special recognition: The 1996 Government Invention of the Year was awarded to Dr. Bruce Steinetz and Mr. Paul Sirocky (retired) for co-developing the advanced, High-Temperature, Flexible Fiber Preform Seal. This is the first time Lewis has won this NASA-wide competition since 1988 when Harold Sliney won the award for his high-temperature solid-film lubricants.

NASA Lewis Thermal Barrier Feasibility Investigated for Use in Space Shuttle Solid-Rocket Motor Nozzle-to-Case Joints

Assembly joints of modern solid-rocket motor cases are usually sealed with conventional O-ring seals. The 5500 °F combustion gases produced by rocket motors are kept a safe distance away from the seals by thick layers of insulation and by special compounds that fill assembly splitlines in the insulation. On limited occasions, NASA has observed charring of the primary O-rings of the space shuttle solid-rocket nozzle-assembly joints due to parasitic leakage paths opening up in the gap-fill compounds during rocket operation. Thus, solid-rocket motor manufacturer Thiokol approached the NASA Lewis Research Center about the possibility of applying Lewis' braided-fiber preform seal as a thermal barrier to protect the O-ring seals. This thermal barrier would be placed upstream of the primary O-rings in the nozzle-to-case joints to prevent hot gases from impinging on the O-ring seals (see the following illustration). The illustration also shows joints 1 through 5, which are potential sites where the thermal barrier could be used.

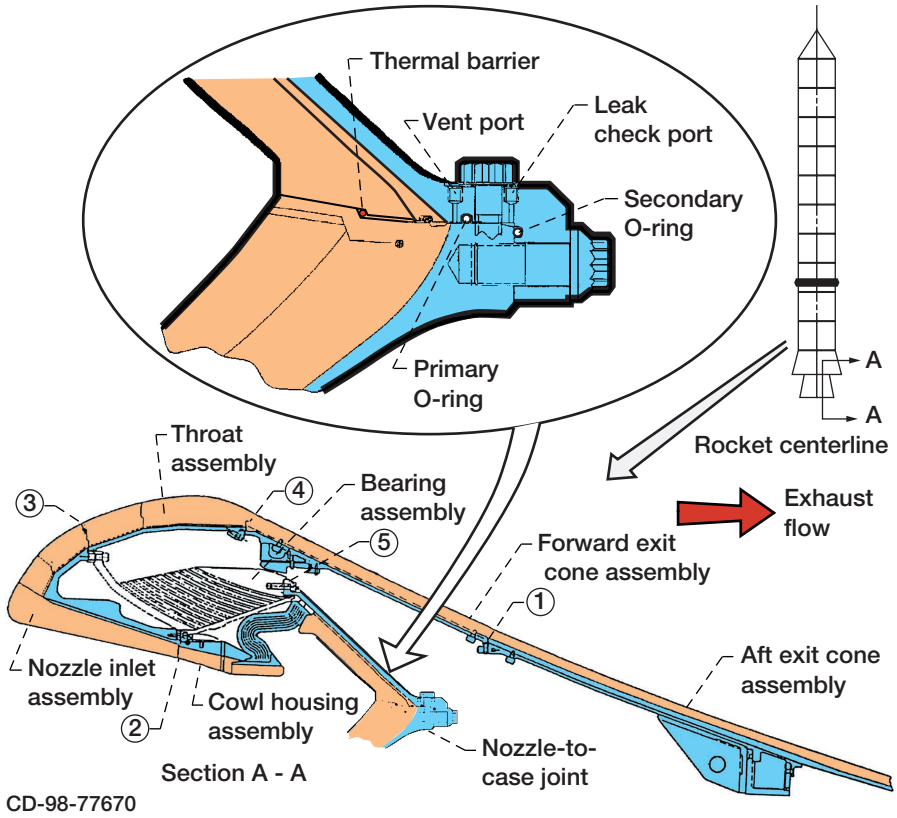

Potential shuttle solid-rocket motor joint locations (circled numbers) for candidate thermal barrier. Top: Enlarged view of nozzle-to-case joint showing primary and secondary pressure O-rings, leak-check part, and proposed thermal barrier location. Bottom: Overall nozzle cross section (half view).

Burn tests at temperatures representative of the rocket thermal environment were used to evaluate the thermal resistance of braided rope thermal barriers made of different materials. Thermal barriers were placed in the hottest part of the flame of an oxyacetylene torch at 5500 °F, and the amount of time to completely cut through them was measured. A 0.125-in.-diameter stainless steel rod was cut through in 5 sec, whereas 0.125-in.-diameter thermal barriers of braided ceramic and superalloy materials lasted less than 15 sec. In contrast, 0.125-in.-diameter thermal barriers of braided carbon fibers lasted over 2 min. Carbon-fiber thermal barriers with diameters of 0.200 and 0.260 in. lasted over 6.5 and 8.5 min., respectively, before they were cut through (see the photo on the following page). As a point of reference, the solid-rocket motors of the space shuttle only burn for 2 and 4 sec, much shorter than the burn-through times of the carbon-fiber thermal barriers. On the basis of these results, the decision was made to use carbon fibers to braid the thermal barriers.

Flow tests performed on the thermal barriers showed that they blocked hot gas flow but were permeable enough to allow leak checks of the primary/secondary O-ring system. The barriers also were resilient enough to accommodate flange movements in the solid-rocket motor. To simulate a rocket environment, Thiokol performed subscale rocket "char" motor tests in which the thermal barrier was subjected to hot gases that flowed through an intentional 0.060-in. circumferential gap defect both upstream and downstream of the thermal barrier. During the 11-sec rocket firing, temperatures over 3200 °F were measured on the hot side of the 0.260-in.-diameter thermal barrier, whereas temperatures on

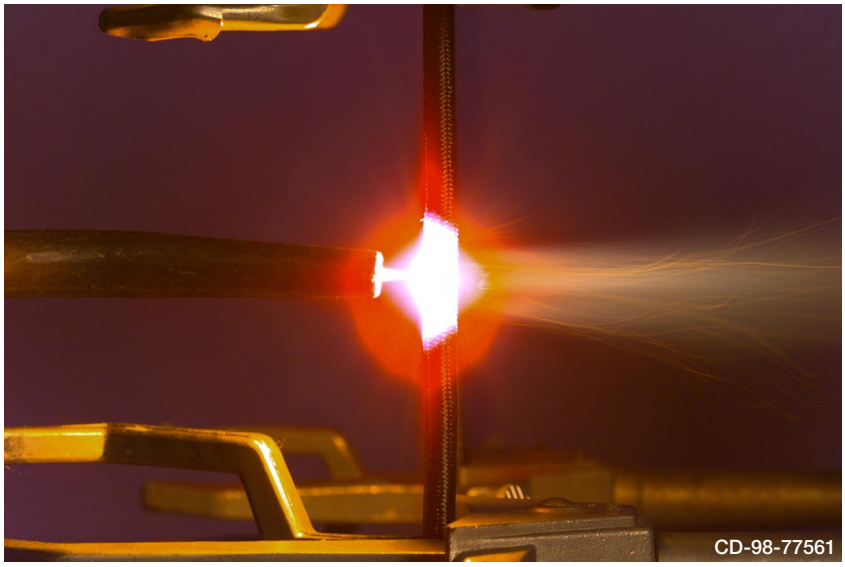

Candidate thermal barrier (0.2-in. diameter) for shuttle solid-rocket motor in 5500 °F oxyacetylene burn test. Time for burn through, 6.5 min.

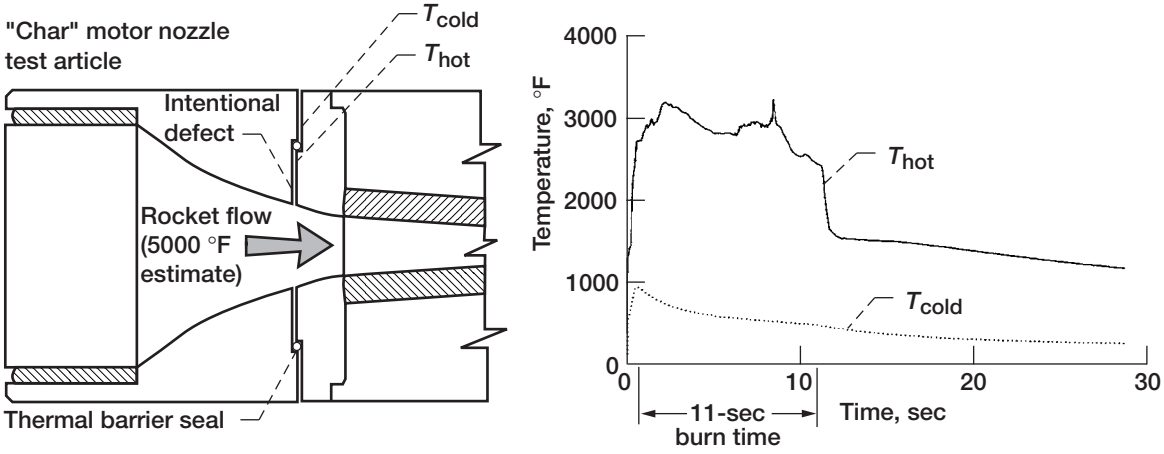

Preliminary subscale (70-lbf thrust) "char" motor tests examining thermal barrier effectiveness. Left: Test configuration: thermal barrier (0.125-in. diameter) filling an intentional joint defect. Right: Temperature data: upstream (T_{hot}) and downstream (T_{cold}) sides of thermal barrier. (Copyright Thiokol Corp.; used with permission.)

the cold side were about 950 °F, for a temperature drop of over 2200 °F across the thermal barrier (see the graphs).

On the basis of these results, additional mechanical and thermal testing is planned at Lewis to help further characterize the thermal barrier. Thiokol is planning to test the thermal barrier in a subscale solid-rocket motor, where it would be installed first in its undamaged state and then with an intentional defect (Spring and Fall 1999). If all planned tests show success, the Lewis-developed thermal barrier would be prepared for Full Scale RSRM static tests in November 2000 (no-joint defect) and May 2002 (with joint defect); it would be subsequently qualified for flight.

Find out more on the World Wide Web: http://www.grc.nasa.gov/WWW/TU/InventYr/1996Inv_Yr.htm

Glenn contact:
Dr. Bruce M. Steinetz, 216–433–3302,
Bruce.M.Steinetz@grc.nasa.gov

Modern Technologies Corp. contact:
Patrick H. Dunlap, Jr., 216–433–6374,
Patrick.H.Dunlap@grc.nasa.gov

Special recognition: 1996 NASA Invention of the Year awarded to the fiber preform seal, precursor to the thermal barrier seal

Thermal Barriers Developed for Solid Rocket Motor Nozzle Joints

Space shuttle solid rocket motor case assembly joints are sealed with conventional O-ring seals that are shielded from 5500 °F combustion gases by thick layers of insulation and by special joint-fill compounds that fill assembly splitlines in the insulation. On a number of occasions, NASA has observed hot gas penetration through defects in the joint-fill compound of several of the rocket nozzle assembly joints. In the current nozzle-to-case joint, NASA has observed penetration of hot combustion gases through the joint-fill compound to the inboard wiper O-ring in one out of seven motors. Although this condition does not threaten motor safety, evidence of hot gas penetration to the wiper O-ring results in extensive reviews before resuming flight. The solid rocket motor manufacturer (Thiokol) approached the NASA Glenn Research Center at Lewis Field about the possibility of applying Glenn's braided fiber preform seal as a thermal barrier to protect the O-ring seals. Glenn and Thiokol are working to improve the nozzle-to-case joint design by implementing a more reliable J-leg design and by using a braided carbon fiber thermal barrier that would resist any hot gases that the J-leg does not block. The proposed new seal arrangement is shown in the illustration on page 78. This illustration also shows joints 1 through 5, which are other sites where the thermal barrier could be used.

The thermal resistance of Glenn's braided carbon fiber thermal barriers was assessed by exposing them to burn tests at temperatures representative of the rocket thermal environment. The thermal barriers were placed in the hottest part of the flame of an oxyacetylene torch at 5500 °F, and the amount of time needed to completely cut through them was measured. Thermal barrier designs with diameters of 0.20 and 0.26 in. resisted the flame for over 6 minutes before they were completely cut through, more than three times longer than the burn time for the shuttle's solid rocket motors.

A test fixture was developed that allows the temperature drop to be measured across and along a thermal barrier when the barrier is in a compressed state and subjected to rocket-simulating narrow jets of hot gas at upstream temperatures of 3000 °F (see the photograph). Tests performed on the 0.20- and 0.26-in.-diameter thermal barriers showed that they are excellent insulators, causing temperature drops of 2500 to 2800 °F through their diameters. Gas temperatures measured only one seal diameter downstream from the thermal barrier were within the Viton[1] O-ring temperature limit of 600 °F. The test fixture also measured the jet-spreading feature of the rope seal. Results show that the 0.082-in. hot incoming jet was spread over a wide section of the braid (>1 in.), as measured by multiple cold-side thermocouples.

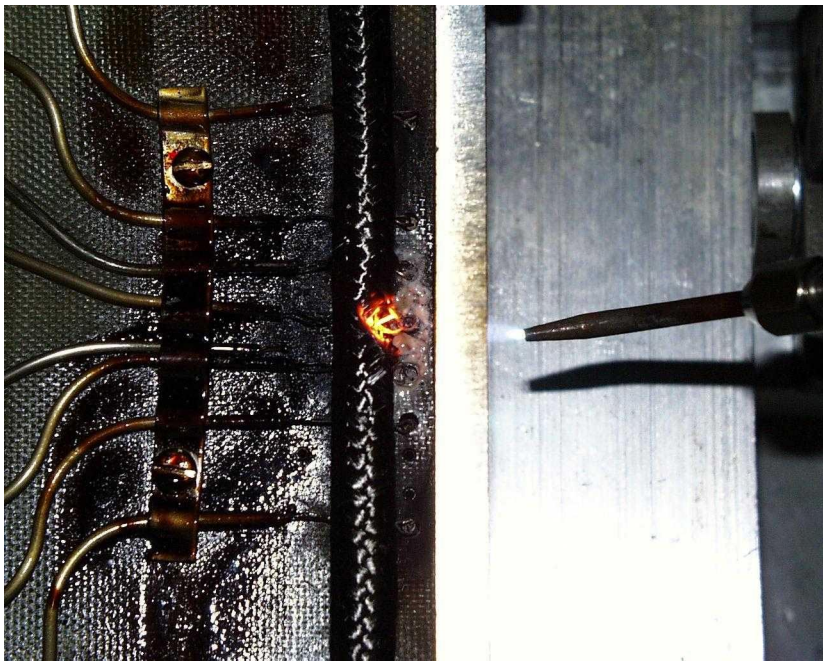

Temperature-drop fixture showing a flame on the thermal barrier.

To simulate a rocket environment, Thiokol performed subscale rocket "char" motor tests in which the 0.26-in.-diameter thermal barrier was subjected to hot gas at 3200 °F for an 11-sec rocket firing, simulating the maximum downstream joint-cavity fill time. The thermal barrier reduced the incoming hot gas temperature by 2200 °F in an intentionally oversized gap defect, spread the incoming jet flow, and blocked hot slag, thereby offering protection to the downstream O-rings. These results were consistent with those from the temperature-drop tests performed at Glenn.

[1]Viton is a registered trademark of DuPont.

NASA Glenn thermal barrier feasibility proven in MNASA–10 RSRM. (Specimen was removed from the nozzle-to-case joint for this photo.)

A Glenn-developed braided carbon fiber thermal barrier was successfully evaluated at NASA Marshall in an MNASA–10 rocket, a one-fifth-scale version of the reusable solid rocket motor (RSRM) used to launch the space shuttle. The specimen was tested in the redesigned nozzle-to-case joint configuration. During the 29-sec rocket firing, an intentional flaw in the nozzle insulation allowed hot combustion gases to reach the thermal barrier as evidenced by soot observed on hardware upstream of the thermal barrier 5 in. on each side of the flaw (see the final photo). Posttest inspection revealed no soot downstream of the thermal barrier and no damage or erosion to either the thermal barrier or to downstream O-rings that the thermal barrier is designed to protect.

The Glenn-developed carbon thermal barrier is the primary candidate being considered by Thiokol for the space shuttle RSRM nozzle-to-case joint redesign to prevent Viton O-ring damage. Thiokol is continuing to perform qualification tests of the Glenn-developed thermal barrier for the nozzle-to-case joint and has expressed interest in using the thermal barrier in joints 1 through 5 of the solid rocket motor nozzle. Thiokol is planning to perform full-scale RSRM static tests using the thermal barrier in January 2001 (no joint defect) and in May 2002 (with joint defect) to qualify the new design for its first shuttle flight in September 2002.

Find out more about this research on the World Wide Web:
http://www.grc.nasa.gov/WWW/5900/5950/
http://www.grc.nasa.gov/WWW/TU/InventYr/1996Inv_Yr.htm

Glenn contacts:
Dr. Bruce M. Steinetz, 216–433–3302, Bruce.M.Steinetz@grc.nasa.gov; and Patrick H. Dunlap, Jr., 216–433–6374, Patrick.H.Dunlap@grc.nasa.gov

Special recognition:
1996 NASA Invention of the Year awarded to the fiber preform seal, precursor to the thermal barrier

Bibliography

Achenbach, J.D.; and Rajapakse, Y., eds.: Solid Mechanics Research and Qualitative Non-Destructive Evaluation, Martinus Nijhoff Publishers, Dordrecht, The Netherlands, 1987.

Arnold, S.M.; Saleeb, A.F.; and Castelli, M.G.: A General Reversible Hereditary Constitutive Model: Part II—Application to a Titanium Alloy. NASA TM–107494, 1997.

Arnold, S.M.; and Wilt, T.E.: Deformation and Life Prediction of Circumferentially Reinforced SCS–6/Ti–15–3 Ring. MMC Life System Development (Phase I)—A NASA/Pratt & Whitney Life Prediction Cooperative Program. E.V. Zaretsky, ed., NASA RP–1361, 1996, pp. 51–60.

Arora, G.K., et al.: Pressure Balanced, Low Hysteresis, Finger Seal Test Results. NASA/TM—1999-209191, 1999. http://gltrs.grc.nasa.gov/GLTRS

Ashley, S.: Flywheels Put a New Spin on Electric Vehicles. Mech. Engrg., vol. 115, no. 10, Oct. 1993, pp. 44–51.

Baaklini, G.Y., et al.: Nondestructive Evaluation of Titanium Alloy MMC Rings for Gas Turbine Engines. MMC Life System Development (Phase I)—A NASA/Pratt & Whitney Life Prediction Cooperative Program. E.V. Zaretsky, ed., NASA RP–1361, 1996, pp. 61–73.

Baaklini, G.Y., et al.: Structural Characterization of Metal Matrix Composites Using NDE Data. HITEMP Review 1997, NASA CP–10192, Vol. II, 1997, paper no. 41, pp. 1–15. (Available from NASA Glenn's Subsonic Systems Office.)

Bakhle, M.A., et al.: Aeroelastic Calculations Based on Three-Dimensional Euler Analysis. AIAA Paper 98–3295, July 1998.

Bibel, G.D.; and Handschuh, R.F.: Meshing of a Spiral Bevel Gearset With 3-D Finite Element Analysis. NASA TM–107336, 1996.

Bishop, J.E.; and Kinra, V.K.: Some Improvement in the Flexural Damping Measurement Technique. M^3D: Mechanics and Mechanisms of Material Damping. ASTM STP 1169, V.K. Kinra and A. Wolfenden, eds., ASTM, Philadelphia, PA, 1992, pp. 457–470.

Brockmeyer, J.W.; and Schnittgrund, G.D.: Fiber-Reinforced Ceramic Composites for Earth-to-Orbit Rocket Engine Turbines. NASA CR–185264, 1990.

Castelli, M.G.: Mechanical Characterization of the Thermomechanical Matrix Residual Stresses Incurred During MMC Processing. HITEMP Review 1997. NASA CP–10192, 1997, paper 29, pp. 1–12. (Available from NASA Glenn's Subsonic Systems Office.)

Castelli, M.G.; Sutter, J.K.; and Benson, D.: Durability and Damage Tolerance of a Polyimide/Chopped Fiber Composite Subjected to Thermomechanical Fatigue Missions and Creep Loadings. Time Dependent and Nonlinear Effects in Polymers and Composites. ASTM STP–1357, R.A. Schapery and C.T. Sun, eds., American Society for Testing and Materials, 1999.

Chamis, C.C.; Murthy, P.L.N.; and Minnetyan, L.: Progressive Fracture of Polymer Matrix Composite Structures. Theoret. Appl. Fracture Mech., vol. 25, no. 1, 1996, pp. 1–15.

Choi, S.R.; and Gyekenyesi, J.P.: Elevated-Temperature, 'Ultra'-Fast Fracture Strength of Advanced Ceramics: An Approach to Elevated-Temperature Inert Strength. ASME Paper 98–GT–479, 1998.

Choi, S.R.; and Gyekenyesi, J.P.: Elevated Temperature 'Ultra'-Fast Fracture Strength Behavior of Advanced Structural Ceramics. Ceramic Materials and Components for Engines, K. Niihara, et al., eds., Technoplaza Co., Japan, 1998, pp. 689–694.

Choi, S.R.; and Gyekenyesi, J.P.: Fatigue Strength as a Function of Preloading in Dynamic Fatigue Testing of Glass and Ceramics. J. Eng. Gas Turbines Power, vol. 119, no. 3, 1997, pp. 493–499.

Choi, S.R.; and Salem, J.A.: Effect of Preloading on Fatigue Strength in Dynamic Fatigue Testing of Ceramic Materials at Elevated Temperatures. Ceram. Eng. Sci. Proc., vol. 16, no. 4, 1995, pp. 87–94.

Choi, S.R.; and Salem, J.A.: Preloading Technique in Dynamic Fatigue Testing of Glass and Ceramics With an Indentation Flaw System. J. Am. Ceram. Soc., vol. 79, no. 5, 1996, pp. 1228–1232.

Choi, S.R.; and Salem, J.A.: Preloading Technique in Dynamic Fatigue Testing of Ceramics: Effect of Preloading on Strength Variation. J. Mater. Sci. Lett., vol. 15, 1996, pp. 1963–1965.

Choi, S.R.; and Salem, J.A.: 'Ultra'-Fast Fracture Strength of Advanced Ceramics at Elevated Temperature. Mater. Sci. Eng., A242, 1998, pp. 129–136.

Coppa. A.P.: Flywheel Containment and Safety Considerations. An Assessment of Integrated Flywheel System Technology. NASA CP–2346, 1984, pp. 243–264.

Dhadwal, H.S.; and Kurkov, A.P.: Dual-Laser Probe Measurements of Blade-Tip Clearance. ASME Paper 98–GT–183, 1998.

Drago, R.J.; Sane, A.D.; and Brown, F.W.: UltraSafe Gear Systems for Critical Applications—Initial Development. AGMA TP–97FTM10, 1997.

Draper, S.L.: Pereira, J.M.; and Nathal, M.V.: Impact Resistance of γ-Ti-48Al-2Nb-2Cr. HITEMP Review 1997, NASA CP–10192, Vol. II, 1997, paper no. 25, pp. 1–13. (Available from NASA Glenn's Subsonic Systems Office.)

Effinger, M.R.; Koenig, J.R.; and Halbig, M.C.: C/SiC Mechanical and Thermal Design Data for a Turbopump Blisk. Proceedings of the Composites, Materials and Structures Conference, Cocoa Beach, FL, Jan. 1997.

Genge, G.G., et al.: Development of a Ceramic Matrix Composite Integrally Bladed Disk for Use in the SIMPLEX Turbopump. The 1996 JANNAF Propulsion Meeting, Vol. 2, 1996, pp. 587–598.

Gil, C.M.; Lissenden, C.J.; and Lerch, B.A.: Determination of Yield in Inconel 718 for Axial-Torsional Loading at Temperatures up to 649 °C. NASA/TM—1998-208658, 1998. http://gltrs.grc.nasa.gov/GLTRS

Gil, C.M.; Lissenden, C.J.; and Lerch, B.A.: Investigation of Anomalous Behavior in Metallic-Based Materials Under Compressive Loading. NASA/TM—1998-206640, 1998. http://gltrs.grc.nasa.gov/GLTRS

GENOA Progressive Failure Analysis Program: Computational Simulation of Three-Dimensional Fiber Reinforced Composites. Volume 1—Theoretical Manual, Prepared by Dade Huang, Alpha STAR Corporation, Long Beach, CA, Sept. 1998.

GENOA: Progressive Failure Analysis Module for 2D/3D Laminate/Woven/Braided/Stitched Polymer Matrix Composites, USER's Manual, Version 7.0, Alpha STAR Corporation, Long Beach, CA, Jan. 1999.

Gyekenyesi, A.L.; and Baaklini G.Y.: Quantifying Residual Stresses by Means of Thermoelastic Stress Analysis. SPIE: Conference on the NDE of Aging Materials and Composites, Newport Beach, CA, March 5–9, 2000.

Gyekenyesi, A.L.; and Baaklini G.Y.: Thermoelastic Stress Analysis: The Mean Stress Effect in Metallic Alloys. NASA/TM—1999-209376, 1999. http://gltrs.grc.nasa.gov/GLTRS

Handschuh, R.F.; and Bibel, G.D.: Comparison of Experimental and Analytical Tooth Bending Stress of Aerospace Spiral Bevel Gears. NASA/TM—1999-208903,1999. http://gltrs.grc.nasa.gov/GLTRS

HITEMP Review 1988, 1989, 1990, 1991, and 1992. NASA CP–10025, CP–10039, CP–10051, CP–10082, and CP–10104, 1988–1992. (Available from NASA Glenn's Subsonic Systems Office.)

Huber, R.D.; and Green, R.E.: Acousto-Ultrasonic Nondestructive Evaluation of Materials Using Laser Beam Generation and Detection. NASA CR–186694, 1994.

Jadaan, O.M.; Powers, L.M.; and Gyekenyesi, J.P.: Creep Life Prediction of Ceramic Components Subjected to Transient Tensile and Compressive Stress States. ASME Paper 97–GT–319, 1997.

Janosik, L.A.; and Duffy, S.F.: A Viscoplastic Constitutive Theory for Monolithic Ceramics—I. ASME Paper 96–GT–368, 1996.

Janosik, L.A.; and Duffy, S.F.: A Viscoplastic Constitutive Theory for Monolithic Ceramics—I. J. Engrg. Gas Turb. Power (ASME Paper 96–GT–368) vol. 120, no. 1, Jan. 1998, pp. 155–161.

Johnson, L.G.: The Statistical Treatment of Fatigue Experiments. Elsevier Pub. Co., New York, NY, 1964.

Johnson, M.D.; and Medlin, E.G.: Laminated Finger Seal With Logarithmic Curvature. U.S. Patent 5,108,116, Apr. 1992.

Kautz, H.E.: Non-Contact Determination of Antisymmetric Plate Wave Velocity in Ceramic Matrix Composites. NASA TM–107125, 1996.

Kautz, H.E.: Detecting Lamb Waves With Broadband Acousto-Ultrasonic Signals in Composite Structures. Res. Nondestr. Eval., vol. 4, no. 3, 1992, pp. 151–164.

Kurkov, A.P.; and Dhadwal, H.S.: Simultaneous Optical Measurements of Axial and Tangential Steady-State Blade Deflections. NASA/TM—1999-209051, March 1999. http://gltrs.grc.nasa.gov/GLTRS

Lee, H.-J.; and Saravanos, D.A.: The Effect of Temperature Induced Material Property Variations on Piezoelectric Composite Plates. AIAA Paper 97–1355, 1997.

Lee, H.-J.; and Saravanos, D.A.: A Review of Smart Structures Modeling Activities. HITEMP Review 1997. NASA CP–10192, 1997, paper 37, pp. 1–10. (Permission to cite this material was granted by Carol A. Ginty, February 19, 1998.)

Lee, H.-J.; and Saravanos, D.A.: Thermal Shape Control of Active and Sensory Piezoelectric Composite Plates. Analysis and Design Issues for Modern Aerospace Vehicles 1997. ASME AD–Vol. 55, 1997.

Lee, H.-J.; and Saravanos, D.A.: A Mixed Multi-Field Finite Element Formulation for Thermopiezoelectric Composite Shells. Smart Structures and Materials 1999: Mathematics and Control in Smart Structures. V.V. Varadan, ed., SPIE Proceedings, vol. 3667, Bellingham, WA, 1999, pp. 449–460.

Lerch, B.A., et al.: Effect of Defects on the Fatigue Life of γ-TiAl. NASA/CP—1999-208915, Vol. II, HITEMP Review 1999, paper no. 30, pp. 1–11. (Available from NASA Glenn's Subsonic Systems Office.)

Lewicki, D.G., et al.: Three-Dimensional Gear Crack Propagation Studies. NASA/TM—1999-208827, 1999. http://gltrs.grc.nasa.gov/GLTRS

Lissenden, C.J., et al.: Robinson: Experimental Determination of Yield and Flow Surfaces Under Axial-Torsional Loading. Multiaxial Fatigue and Deformation Testing Techniques. ASTM STP–1280, S. Kalluri and P.J. Bonacuse, eds., 1997, pp. 92–112.

Lissenden, C.J., et al.: Experimental Determination of Yield and Flow Surfaces Under Axial-Torsional Loading. S. Kalluri and P.J. Bonacuse, eds., Am. Soc. Test. Mater. Spec. Tech. Publ. 1280, 1997, pp. 92–112.

Lissenden, C.J., et al.: Verification of Experimental Techniques for Flow Surface Determination. NASA TM–107053, 1996.

The MacNeal-Schwendler Corporation: MSC/PATRAN Graphics and Finite Element Package. Vols. I and II, MacNeal-Schwendler, Costa Mesa, CA, 1997.

MARC Analysis Research Corporation: MARC General Purposes Finite Element Analysis program. Vol. A: User Information manual, and Vol. F: Theoretical Manual. MARC Analysis Research Corporation, Palo Alto, CA, 1996.

Mital, S.K., et al.: Micromechanics-Based Modeling of Thermal and Mechanical Properties of an Advanced SiC/SiC Composite Material. NASA TM–206295, 1998. (Available from Glenn's HSR or UEET Project Office.)

Monchalin, J.P.: Optical Detection of Ultrasound. IEEE Trans. UFFC, vol. 33, no. 5, Sept. 1986, pp. 485–499.

Murthy, P.L.N.; Mital, S.K.; and Dicarlo, J.A.: Characterizing the Properties of a Woven SiC/SiC Composite Using W–CEMCAN Computer Code. NASA/TM—1999-209173, 1999. http://gltrs.grc.nasa.gov/GLTRS

Nemeth, N.N., et al.: Designing Ceramic Components for Durability. Advanced Ceramic Matrix Composites—Design Approaches, Testing and Life Prediction Methods, E.R. Generazio, ed., Technomic Publishing Company, Lancaster, PA, 1996, pp. 3–16.

Nemeth, N.N., et al.: Durability Evaluation of Ceramic Components Using CARES/*LIFE*. J. Eng. Gas Turbines Power, vol. 118, Jan. 1996, pp. 150–158.

Olszewski, M.; et al.: On the Fly or Under Pressure. Mech. Engrg., vol. 110, no. 6, Jun. 1988, pp. 50–58.

Patnaik, S.N., et al.: Cascade Optimization Strategy for Aircraft and Airbreathing Propulsion System Concepts. J. Aircraft, vol. 34, no. 1, pp. 136–139, 1997.

Patnaik, S.N., et al.: Neural Network and Regression Approximations in High Speed Civil Transport Aircraft Design Optimization. NASA TM–206316, 1998. http://gltrs.grc.nasa.gov/GLTRS

Pereira, J.M., et al.: Fan Containment Impact Testing and Analysis at NASA Lewis Research Center. HITEMP Review 1997. NASA CP–10192, 1997, paper 13, pp. 1–12. (Available from NASA Glenn's Subsonic Systems Office.)

Powers, L.M.; Jadaan, O.M.; and Gyekenyesi, J.P.: Creep Life of Ceramic Components Using a Finite Element Based Integrated Design Program (CARES/*CREEP*). ASME Paper 96–GT–369, 1996.

Rahman, S.; Nemeth, N.N.; and Gyekenyesi, J.P.: Life Prediction and Reliability Analysis of Ceramic Structures Under Combined Static and Cyclic Fatigue. ASME Paper 98–GT–569, 1998.

Roth, D.J.: Single Transducer Ultrasonic Imaging Method That Eliminates the Effect of Plate Thickness Variation in the Image. NASA TM–107184, 1996. http://gltrs.grc.nasa.gov/GLTRS

Roth, D.J., et al.: Commercial Implementation of Ultrasonic Velocity Imaging Methods via Cooperative Agreement Between NASA Lewis Research Center and Sonix, Inc. NASA TM–107138, 1996. http://gltrs.grc.nasa.gov/GLTRS

Roth, D.J., et al.: Commercial Implementation of NASA-Developed Ultrasonic Imaging Methods via Technology Transfer. Mater. Eval., vol. 54, no. 11, 1996, pp. 1305–1309.

Roth, D.J.: Using a Single Transducer Ultrasonic Imaging Method to Eliminate the Effect of Thickness Variation in the Images of Ceramic and Composite Plates. J. Nondestr. Eval., vol. 16, no. 2, June 1997.

Roth, D.J., et al.: 3–D Surface Depression Profiling Using High-Frequency Focused Air-Coupled Ultrasonic Pulses. NASA/TM—1999-209053, 1999. http://gltrs.grc.nasa.gov/GLTRS

Safaeinili, A.; Lobkis, O.I.; and Chimenti, D.E.: Air-Coupled Ultrasonic Characterization of Composite Plates. Materials Eval., vol. 53, 1995, pp. 1186–1190.

Saleeb, A.F.; and Arnold, S.M.: A General Reversible Hereditary Constitutive Model: Part I—Theoretical Developments. NASA TM–107493, 1997.

Sanders, W.A.; and Baaklini, G.Y.: Correlation of Processing and Sintering Variables With the Strength and Radiography of Silicon Nitride. Adv. Ceram. Mater., vol. 3, no. 1, 1988, pp. 88–94.

Scruby, C.B.; and Drain, L.E.: Laser Ultrasonics. Adam Hilger, New York, 1990.

Shapiro, W., et al.: Space Mechanisms Lessons Learned Study, Volume I—Summary. NASA TM–107046, 1995.

Shapiro, W., et al.: Space Mechanisms Lessons Learned Study, Volume II—Literature Review. NASA TM–107047, 1995.

Snidle, R.W.; Evans, H.P.; and Alanou, M.P.: The Effect of Superfinishing on Gear Tooth Profile. Report AD–A327916, June 1997. Available from the Defense Technical Information Center (DTIC, http://www.dtic.mil/) or the National Technical Information Service (NTIS, http://www.ntis.gov/), or the Center for AeroSpace Information (CASI, http://www.sti.nasa.gov/rselect/FAQ.html#docorder).

Srivastava, R., et al.: Application of Time-Shifted Boundary Conditions to a 3D Euler/Navier-Stokes Aeroelastic Code. ASME Paper 98–GT–42, 1998.

Steinetz, B.M.; and Dunlap, P.H.: Feasibility Assessment of Thermal Barrier Seals for Extreme Transient Temperatures. AIAA Paper 98–3288 (NASA/TM—1998-208484) 1998. http://gltrs.grc.nasa.gov/GLTRS

Steinetz, B.M.; Hendricks, R.C.; and Munson, J.: Advanced Seal Technology Role in Meeting Next Generation Turbine Engine Goals. NASA/TM—1998-206961, 1998. http://gltrs.grc.nasa.gov/GLTRS

Steinetz, B.M.; and Dunlap, P.H., Jr.: Development of Thermal Barriers for Solid Rocket Motor Nozzle Joints. NASA/TM—1999-209278 (AIAA Paper 99–2823), 1999. http://gltrs.grc.nasa.gov/GLTRS

Tang, B.; and Henneke II, E.G.: Long Wavelength Approximation for Lamb Wave Characterization of Composite Laminates. Res. Nondestr. Eval., vol. 1, no. 1, 1989, pp. 51–64.

Ting, J.M.; and Crawley, E.F.: Characterization of Damping of Materials and Structures From Nanostrain Levels to One Thousand Microstrain. AIAA J., vol. 30, no. 7, 1992, pp. 1856–1863.

Vary, A.; and Snyder, J., eds.: Proceedings of the Nondestructive Testing of High-Performance Ceramics Conference, The American Ceramics Society, Westerville, OH, 1987.

Vary, A.; and Klima, S.J.: Nondestructive Techniques for Characterizing Mechanical Properties of Structural Materials—An Overview. ASME Paper 86–GT–75, 1986.

Vary, A.: NDE Standards for High Temperature Materials. NASA TM–103761, 1991.

Velocity^2 Technical Reference Manual Version 2.1, Velocity™ From 3D Imaging to 3D Reality. IMAGE3, LLC, South Salt Lake City, UT, 1996–1999.

Wilt, T.E.: Arnold, S.M.; and Goldberg, R.: Micromechanics Analysis Code, MAC Features and Applications. HITEMP Review 1997, NASA CP–10192, Vol. II, 1997, paper no. 30, pp. 1–13. (Available from NASA Glenn's Subsonic Systems Office.)

REPORT DOCUMENTATION PAGE

Form Approved
OMB No. 0704-0188

1. AGENCY USE ONLY (*Leave blank*)	2. REPORT DATE	3. REPORT TYPE AND DATES COVERED
	March 2001	Technical Memorandum

4. TITLE AND SUBTITLE

Structures and Acoustics Division Annual Report for 1997 to 1999

5. FUNDING NUMBERS

WU–910–30–11–00

6. AUTHOR(S)

Cynthia S. Acquaviva

7. PERFORMING ORGANIZATION NAME(S) AND ADDRESS(ES)

National Aeronautics and Space Administration
John H. Glenn Research Center at Lewis Field
Cleveland, Ohio 44135–3191

8. PERFORMING ORGANIZATION REPORT NUMBER

E–12415

9. SPONSORING/MONITORING AGENCY NAME(S) AND ADDRESS(ES)

National Aeronautics and Space Administration
Washington, DC 20546–0001

10. SPONSORING/MONITORING AGENCY REPORT NUMBER

NASA TM—2001-210366

11. SUPPLEMENTARY NOTES

Responsible person, Cynthia Acquaviva, organization code 5900, 216–433–3306.

12a. DISTRIBUTION/AVAILABILITY STATEMENT

Unclassified - Unlimited
Subject Category: 39 Distribution: Nonstandard

Available electronically at http://gltrs.grc.nasa.gov/GLTRS

This publication is available from the NASA Center for AeroSpace Information, 301–621–0390.

12b. DISTRIBUTION CODE

13. ABSTRACT ***(Maximum 200 words)***

The Structures and Acoustics Division of the NASA Glenn Research Center is an international leader in rotating structures, mechanical components, fatigue and fracture, and structural aeroacoustics. Included in this report are disciplines related to life prediction and reliability, nondestructive evaluation, and mechanical drive systems. Reported is a synopsis of the work and accomplishments completed by the Division during the l997, l998, and l999 calendar years. A bibliography containing 93 citations is provided.

14. SUBJECT TERMS

Structural mechanics; Acoustics; Structural dynamics; Life prediction; Machine dynamics; Fatigue; Fracture; Vibration

15. NUMBER OF PAGES

97

16. PRICE CODE

A05

17. SECURITY CLASSIFICATION OF REPORT	18. SECURITY CLASSIFICATION OF THIS PAGE	19. SECURITY CLASSIFICATION OF ABSTRACT	20. LIMITATION OF ABSTRACT
Unclassified	Unclassified	Unclassified	